แบบจำลองเชิงพลวัตของการถ่ายเทมวลของออกซิเจน
ในถังสัมผัสแบบอากาศยก

นาย วิเชียร สุขสร้อย

สถาบันวิทยบริการ
จุฬาลงกรณ์มหาวิทยาลัย

วิทยานิพนธ์นี้เป็นส่วนหนึ่งของการศึกษาตามหลักสูตรปริญญาวิศวกรรมศาสตรมหาบัณฑิต
สาขาวิชา วิศวกรรมเคมี ภาควิชา วิศวกรรมเคมี
คณะวิศวกรรมศาสตร์ จุฬาลงกรณ์มหาวิทยาลัย
ปีการศึกษา 2543
ISBN 974-347-259-2
ลิขสิทธิ์ของจุฬาลงกรณ์มหาวิทยาลัย

TRANSIENT MODELS FOR OXYGEN MASS TRANSFER IN AIRLIFT CONTACTORS

Mr. Vichian Suksoir

สถาบันวิทยบริการ
จุฬาลงกรณ์มหาวิทยาลัย

A Thesis Submitted in Partial Fulfillment of the Requirements
for the Degree of Master of Engineering in Chemical Engineering
Department of Chemical Engineering
Faculty of Engineering
Chulalongkorn University
Academic Year 2000
ISBN 974-347-259-2

Thesis Title	Transient Models for Oxygen Mass Transfer in Airlift Contactors
By	Vichian Suksoir
Field of Study	Chemical Engineering
Thesis Advisor	Assistant Professor Prasert Pavasant, Ph.D.

Accepted by the Faculty of Engineering, Chulalongkorn University in Partial Fulfillment of the Requirements for the Master's Degree

…….Dean of Faculty of Engineering
(Professor Somsak Panyakeow, Dr.Eng.)

THESIS COMMITTEE

…….Chairman
(Associate Professor Tawatchai Charinpanitkul, Dr.Eng.)

…….Thesis Advisor
(Assistant Professor Prasert Pavasant, Ph.D.)

…….Member
(Assistant Professor Tharathon Mongkonsi, Ph.D.)

…….Member
(Assistant Professor Seeroong Prichanont, Ph.D.)

สถาบันวิทยบริการ
จุฬาลงกรณ์มหาวิทยาลัย

วิเชียร สุขสร้อย: แบบจำลองเชิงพลวัตของการถ่ายเทมวลของออกซิเจนในถังสัมผัสแบบอากาศยก (TRANSIENT MODELS FOR OXYGEN MASS TRANSFER IN AIRLIFT CONTACTORS) อาจารย์ที่ปรึกษาวิทยานิพนธ์: ผู้ช่วยศาสตราจารย์ ดร. ประเสริฐ ภวสันต์, 124 หน้า. ISBN 974-347-259-2

งานวิจัยนี้มีจุดมุ่งหมายเพื่อพัฒนาแบบจำลองทางคณิตศาสตร์ที่ใช้ในการทำนายพฤติกรรมการถ่ายเทมวลของออกซิเจนระหว่างวัฏภาคของของเหลวและก๊าซในถังสัมผัสแบบอากาศยก (Airlift Contactor) โดยที่แบบจำลองทางคณิตศาสตร์ที่ได้พัฒนาขึ้นสามารถจำแนกได้เป็นหลายประเภท ได้แก่ ถังกวนแบบต่อเนื่อง (CSTR model), อนุกรมของถังกวนแบบต่อเนื่อง (CSTRs-in-Series model), เครื่องปฏิกรณ์แบบท่อไหล (PFR model), เครื่องปฏิกรณ์แบบท่อไหลที่มีการกระจายตัวในแนวการไหล (Dispersion model) ซึ่งการหาคำตอบของแบบจำลองทางคณิตศาสตร์ด้วยวิธีการประมาณค่าต่าง ๆ กัน เช่น วิธีการแก้สมการแบบ Crank Nicholson และวิธีการอินทิเกรตสมการแบบ Runge-Kutta ทำให้ทราบว่าผลการคำนวณจากแบบจำลองต่างๆ มีความถูกต้องน่าเชื่อถือ และเมื่อเปรียบเทียบระหว่างผลที่ได้จากการคำนวณโดยแบบจำลองและผลที่ได้จากการทดลอง พบว่าแบบจำลองแบบระบบท่อที่มีการกระจายตัวในแนวการไหลสามารถทำนายพฤติกรรมการถ่ายเทมวลของออกซิเจนระหว่าง 2 วัฏภาคได้แม่นยำที่สุด โดยที่แบบจำลองแบบนี้จะพิจารณาส่วนของ riser และ downcomer ว่ามีพฤติกรรมการไหลเป็นแบบการไหลในท่อที่มีการกระจายตัวในแนวการไหล ขณะที่ในส่วนของ gas separator นั้น พิจารณาได้ด้วยการไหลแบบผสมผสานสมบูรณ์ งานวิจัยนี้ยังได้ทำการศึกษาถึงผลของ ค่าสัมประสิทธิ์การถ่ายเทมวลรวม (K_La) และค่าการกระจายตัวในแนวการไหลในวัฏภาคของก๊าซ ($D_{G,r}$) ที่มีผลต่อแบบจำลอง และพบว่าเมื่อเพิ่มค่า K_La และ $D_{G,r}$ จะเพิ่มอัตราการถ่ายเทมวลของออกซิเจนจากวัฏภาคก๊าซไปยังของเหลว นอกจากนี้การศึกษายังพบอีกว่าแบบจำลองที่ได้สามารถใช้ทำนายพฤติกรรมการถ่ายเทมวลของออกซิเจนในถังสัมผัสแบบอากาศยกในกรณีที่มีการเปลี่ยนแปลงค่าของอัตราส่วนของพื้นที่หน้าตัดระหว่าง downcomer และ riser (A_d/A_r) และอัตราการป้อนอากาศที่เข้าสู่ระบบ ($Q_{G,in}$) แบบจำลองยังสามารถใช้ได้ดีกับการทำนายพฤติกรรมการถ่ายเทมวลในถังสัมผัสแบบอากาศยกในกรณีที่มีการป้อนของเหลวด้วยอัตราคงที่ ($Q_{L,F}$) เข้าสู่ระบบ แต่แบบจำลองที่ได้ยังไม่สามารถอธิบายพฤติกรรมการถ่ายเทมวลของออกซิเจนที่เกิดขึ้นในระบบที่มีท่อทรงกระบอกภายใน (Draft tube) ขนาดสูง ๆ ได้ ซึ่งสาเหตุของความคลาดเคลื่อนที่เกิดขึ้นยังไม่ทราบแน่ชัด

ภาควิชา วิศวกรรมเคมี ลายมือชื่อนิสิต……..…

สาขาวิชา วิศวกรรมเคมี ลายมือชื่ออาจารย์ที่ปรึกษา……...

ปีการศึกษา 2543

4270533021 : MAJOR CHEMICAL ENGINEERING
KEY WORD: AIRLIFT CONTACTOR / DISPERSION MODEL/ OXYGEN MASS TRANSFER / DISPERSION COEFFICIENT / OVERALL MASS TRANSFER COEFFICIENT
VICHIAN SUKSOIR: TRANSIENT MODELS FOR OXYGEN MASS TRANSFER IN AIRLIFT CONTACTORS. THESIS ADVISOR: ASSIST. PROF. PRASERT PAVASANT, Ph.D. 124 PP. ISBN 974-347-259-2

The mathematical model was developed and verified for the prediction of gas-liquid oxygen mass transfer behavior in the airlift contactors (ALCs). Many types of unsteady state models were formulated, i.e. continuous stirred tank reactors (CSTR), CSTRs-in-series, plug flow reactor (PFR) and Dispersion models. Comparison between simulation results and experimental data concluded that the Dispersion model was most suitable for the prediction of gas-liquid oxygen mass transfer in the ALC. In the Dispersion model, both riser and downcomer were considered as a plug flow region with dispersion, whereas the gas separator was modeled as a region of completely mixed. The model predictions were satisfactory not only for their numerical accuracy, but also for their ability to agree well with the actual reported experimental data. The effect of the overall mass transfer coefficient (K_La) and gas phase dispersion coefficient ($D_{G,r}$) on the modeling results were investigated. The results showed that increasing either K_La and $D_{G,r}$ would result in a faster rate of mass transfer from gas bubble to liquid. In addition, the model was successfully verified over a range of operating parameters e.g. the ratio between downcomer and riser cross sectional areas (A_d/A_r) and the inlet gas flowrate ($Q_{G,in}$). The model was then used to predict the performance of the ALC with a constant liquid feed flowrate ($Q_{L,F}$). Lastly, it was found that the model was not able to correctly predict the behavior of the high draft tube ALC. The reason for this discrepancy was still unknown.

ศูนย์วิทยทรัพยากร
จุฬาลงกรณ์มหาวิทยาลัย

Department Chemical Engineering Student's signature…….
Field of study Chemical Engineering Advisor's signature……
Academic year 2000

Acknowledgement

Firstly, I would like to express my sincere gratitude to my advisor, Assistant Professor Dr. Prasert Pavasant, for his invaluable support, continuous guidance and kind suggestion. This thesis would not have been accomplished without his excellent supervision. I am grateful to Associate Professor Dr. Tawatchai Charinpanitkul, Chairman of the committee, Assistant Professor Dr. Tharathon Mongkonsi and Assistant Professor Dr. Seeroong Prichanont, members of thesis committee, for many valuable comments.

I have learnt so much during the past two years and every bit of warm help from friends has always been appreciated. Sincere thanks are made to all members of Biochemical Engineering Research for their warm support, particularly Sontaya who has always provided imperative helps and encouragement, Komgrit for being my roommate and assistant when I did my work at night, Phimchanok, Narong, Nuntiya, Geerati and everyone in Bio-Laboratary for good suggestions and encouragement. All members of Enviromental laboratory for enjoyable all time and Particle technology & Material processing for a little help e.g. food and coffee. My life would not be completed if Sahat, Kunawut, Chaiyanun and Methee did not introduce me to joy to their group, thank you indeed. Special thanks are also to Juntanee, Ratchat and Supa for their kind support and warm encouragement.

Most of all, I would like to express my utmost gratitude to my parents and everyone in my family for their inspiration and invaluable supports at all times.

สถาบันวิทยบริการ
จุฬาลงกรณ์มหาวิทยาลัย

CONTENTS

PAGE

CONTENTS(Cont.)

PAGE

CONTENTS(Cont.)

PAGE

สถาบันวิทยบริการ
จุฬาลงกรณ์มหาวิทยาลัย

LIST OF TABLES

สถาบันวิทยบริการ
จุฬาลงกรณ์มหาวิทยาลัย

LIST OF FIGURES

สถาบันวิทยบริการ
จุฬาลงกรณ์มหาวิทยาลัย

Nomenclature

A	cross-sectional area	[m^2]
A_{dc}	apparent contracted cross sectional area at downcomer entrance	[m^2]
A_{rc}	apparent contracted cross sectional area at riser entrance	[m^2]
D	axial dispersion coefficient	[$m^2.s^{-1}$]
d	diameter	[m]
d_B	bubble diameter	[m]
d_c	diameter of column	[m]
Fr	Froude number = $U_G / \sqrt{gD_r}$	
g	gravitation acceleration	[$m.s^{-2}$]
H	height	[m]
H_D	dispersion height	[m]
k_D	acceleration coefficient at downcomer entrance	
K_f	total friction coefficient	
k_La	volumetric mass transfer coefficient based on the liquid phase concentration driving force	[s^{-1}]
k_R	acceleration coefficient at riser entrance	
M	number of mixing state in riser	
Mo	Morton number	
M_W	molecular weight	
N	number of mixing state in circulation loop	
O	oxygen concentration	[mg $O_2.L^{-1}$]
P	total pressure	[atm]
P_{O_2}	oxygen partial pressure	[atm]
Q	flowrate	[$m^3.s^{-1}$]
R	gas constant	[$L.atm.(mg\ O_2)^{-1}.K^{-1}$]
Re	Reynold number	
S_ϕ	source term	
T	temperature	[K]
t	time	[s]
U	superficial velocity	[$m.s^{-1}$]
U_{BT}	terminal bubble rise velocity	[$m.s^{-1}$]
V	volume	[m^3]
v	velocity	[$m.s^{-1}$]
V_B	bubble volume	[m^3]
$V_{b\infty}$	bubble rise velocity in infinite medium	[$m.s^{-1}$]
V_D	dispersion volume	[m^3]
v_L	linear liquid velocity	[$m.s^{-1}$]
v_{Lr}	linear (interstitial) liquid velocity in riser	[$m.s^{-1}$]
v_M	velocity of total phase (gas+liquid)	[$m.s^{-1}$]
V_s	slip velocity	[$m.s^{-1}$]
Y_{O_2}	mole fraction of oxygen in gas phase	
z	axial coordinate	[m]
Z	dimensionless axial coordinate	

Greek symbols

ε	gas hold-up	
ρ	density	[kg.m^{-3}]
ξ_B	frictional loss coefficient at the bottom	
ξ_T	frictional loss coefficient at the top	
ϕ	total circulation path flow resistance in the flow circuit or parameter in Eq·2·1·4·1	
σ	surface tension	[kg.m^{-2}]
μ	viscosity	[kg.m^{-1}.s^{-1}]
μ_{eff}	effective viscosity	[kg.m^{-1}.s^{-1}]
γ	ratio of the number of liquid states to the number of gas states	

Superscripts

*	at equilibrium
—	average

Subscripts

0	ungassed
1	at the top
2	at the bottom
c	in the core region of a BC
d	downcomer
DT	draft tube
e	entrance
F	feed
G	gas
i	ith stage
in	inlet
K	phase K
L	liquid
m	at the conditions for which J_G was measured
out	outlet
p	in the middle point of the riser or column
r	riser
tc	top connection
top	gas seperator
z	axial direction

สถาบันวิทยบริการ
จุฬาลงกรณ์มหาวิทยาลัย

CHAPTER 1

Introduction

1.1 General Ideas

Various types of reactors have been used in biotechnological processes such as conventional stirred-tank reactors and bubble columns. Among these, an airlift reactor (ALR) has emerged as a potential alternative. Apart from the simple design and control, the main advantage of the ALRs over the counterpart bubble columns lays at the hydrodynamic performance because a rather high liquid circulation can be obtained in the ALR, but not in the bubble column. And when compared to the stirred tank, the ALRs provide an attractive good mixing without producing too high shear force, which could be detrimental to living cells in the system. In addition, the maintenance of the ALR is much simpler and easier than the effort necessary to maintain the integrity for the stirred tank because no mechanical components are used in the ALR. This is not to mention that the only power input to the ALR is derived from the power needed to overcome the hydrostatic pressure in the column, whilst an extra power is needed in the stirred tank to move the agitator. The use of ALRs have increased drastically in the biotechnological areas such as the bio-treatment of wastewater and other aerobic fermentation processes particularly the three phase systems.

In the development of the ALR, it is important that we understand the transport mechanism in the system. This can be done in two ways: (i) experimentally, and (ii) mathematically. A mathematical model is significant as it helps us simulate what is going to happen without having to do tedious experiments. Also it is an important tool if one needs to design a system for particular purposes such as a system with a high rate of gas-liquid mass transfer or a system with a high liquid circulation velocity.

Mathematical models can generally be categorized into two major forms. The first form is developed from the statistical analysis of experimental results which

is usually known in terms of a correlation between various parameters. This is significant as it facilitates in the determination of various parameters (at steady state) in the system, such as the gas holdup, liquid velocity and volumetric mass transfer coefficient. However, this type of model lacks the ability to predict the dynamic behavior of the system. In such circumstances, one needs to develop a second form of mathematical model which is based on mass and energy balances of the system. This model is time-dependent and can be used to predict the transient behavior of the system. The combination between the first and second types of models will enable us to describe the overall performance of the system.

Most of the models reported in the literature often were derived based on the assumptions of ideal conditions. (Dhaouadi et al. 1996) This can be a major flaw and it might be the reason why there were times that model predictions were inaccurate. (Choi 1999) The aims of this work are to develop a mathematical model for the airlift contactor system that is capable of explaining the non-ideality of the system, and to carry out experiment needed for the verification of the model.

1.2 Objectives

This work is set out to develop a suitable mathematical model capable of explaining the oxygen mass transfer behavior of an airlift contactors (ALCs).

1.3 Working Scopes

Equipment limitations

- The ALC employed in this work has dimensions as shown in Table 3.1.
- The gas superficial velocity in this work ranges from 0.00367 to 0.0381 $m \cdot s^{-1}$ (limited by the air compressor).
- The liquid phase dispersion coefficient is estimated from the residence time distribution of the acid pulse tracer in the ALC.

CHAPTER 2

Backgrounds and Literature Review

2.1 Backgrounds: Airlift Contactor

2.1.1 Classification of airlift contactors

Airlift contactors (ALCs) can be classified into two major types, the external loop and internal loop as shown diagrammatically in Figure 2.1.

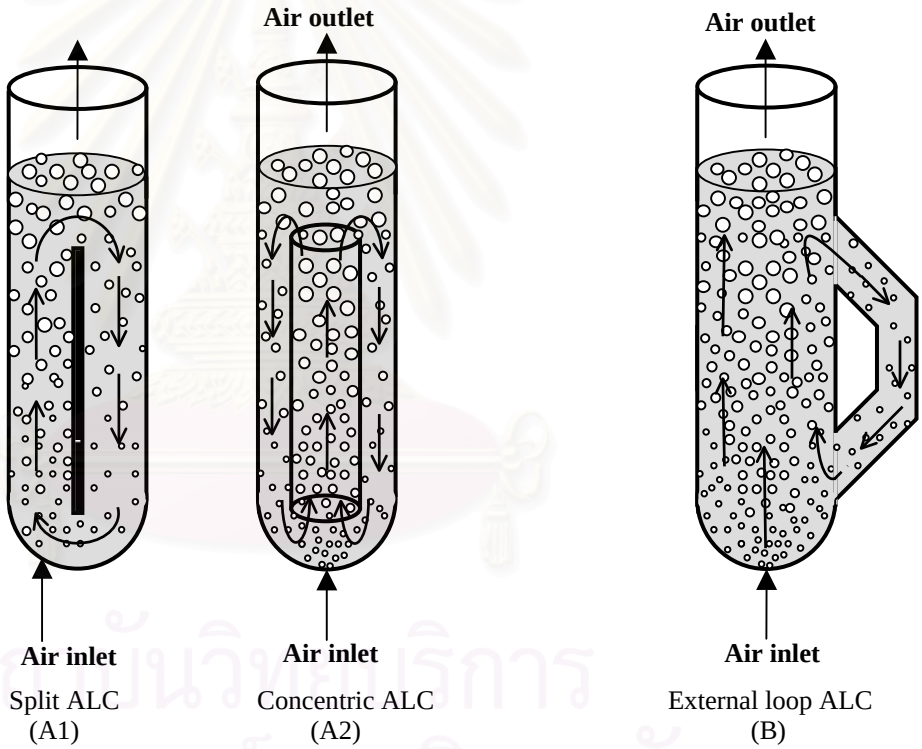

Figure 2.1. Airlift contactors: (A1) and (A2) are internal-loop airlift contactors and (B) is external-loop airlift contactor.

The internal loop ALC is simply a conventional bubble column that is separated into two sections by a baffle plate (split-type ALC, Figure 2.1(A1)) or a cylindrical tube (concentric ALC, Figure 2.1(A2)).

The external loop type is the ALC of which riser and downcomer are physically separated as two columns interconnected at the top and bottom for liquid flow as depicted in Figure 2.1(B).

2.1.2 Transport mechanism in ALCs

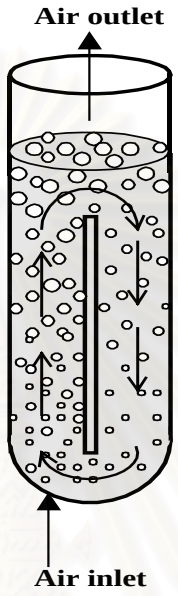

Figure 2.2. Basic structures of airlift contactor

The ALCs comprise three connecting zones: riser, downcomer and gas separator. The split-type ALC is chosen to illustrate the major components of ALCs, each of which is described as follows:

1. Riser is the section through which gas is sparged, creating a net upward flow of fluid. This upflow of fluid is replaced by the recirculating fluid from downcomer.
2. Fluid from riser enters the gas separator from which a large portion of gas disengages out at the top surface. The flow pattern in this section is similar to that found in CSTRs where the highly turbulence exists.
3. After the disengagement of gas bubbles, liquid and the remaining gas bubbles enter the downcomer. As the fluid in this section contains less proportion of gas, the density of the fluid becomes greater than that in other sections of the ALC. This creates a downward movement of the fluid

which leaves the downcomer at the bottom and enters the riser together with the supplied gas.

The movement of the fluid in the ALC is primarily caused from the momentum transfer of gas bubbles to the liquid. However, as the majority of gas bubbles passes through the riser and leaves at the gas separator, this creates the three distinct zones each of which contains different proportion of gas bubbles as described above. Hence, a fluid circulation pattern is induced in the system as “lighter” fluid (in the riser) moves upwards and “heavier” liquid moves downwards.

2.1.3 Hydrodynamic behavior in the ALCs

Investigations of hydrodynamic behavior of ALCs have been numerous as will be described in detailed in Section 2.2. It is surprising to learn that various hydrodynamic parameters can be mathematically correlated. Many investigators had developed a number of correlations to describe the relationships between various hydrodynamic parameters in the ALC. Those correlations developed for the external loop ALC are summarized in Table 2.1 whilst Table 2.2 is for the internal loop ALC. Table 2.3 summarizes most of the correlations that have been reported for both types of ALCs.

สถาบันวิทยบริการ
จุฬาลงกรณ์มหาวิทยาลัย

Table 2.1. Correlations between various hydrodynamic parameters for external loop ALCs.

Author	Equation	Remark
Merchuk et al, 1981	$\frac{U_G}{\varepsilon_G} = 1.03(U_G + U_L) - 0.33$	$d_r = d_d = 0.14$ m.
Bello et al, 1984	$U_{Lr} = 1.55(A_d/A_r)^{0.74} U_{Gr}^{1/3}$ $t_m t_c = 3.5(A_d/A_r)^{0.5}$ $(K_L a)_r = 2.28(U_{Gr}/U_{Lr})^{0.9}(1+A_d/A_r)^{-1}$	Media: water and 0.15 kmol/m^3 NaCl $A_d/A_r = 0.11$-0.69 $d_r = 0.152$ m $d_d = 0.05$ - 0.102 m $H_D = 1.8$m
Calvo and Leton, 1991	mean liquid velocity in the central core $\overline{U}_{Lc} = \frac{\overline{U}_{L0}}{2(1-\varepsilon)}$ Energy balance: $P_m U_{Gm} \ln\left(1+\frac{\rho_L g H}{P_1}\right) = \frac{1}{2} K_f \frac{A_d}{A_r} \rho_L v_{Lc}^3 + 0.2\frac{\rho_L H}{d} v_{L0}^3 + v_s \rho_L g H \varepsilon$ gas hold-up $\varepsilon = \frac{U_{Gp}}{v_s + 0.5 v_{Lc} + v_{Lp}}$	$A_d = 0.1$ m $A_r = 0.1$ m $H_0 = 2.15$ m
Kemblowski et al, 1993	$\varepsilon_r = 0.203 \frac{Fr^{0.31}}{M_0^{0.012}} \left[\frac{U_{Gr} A_r}{U_{Lr} A_d}\right]^{0.78}$	Media: water, water with surfactant, glycol solutions, sugar syrup, CMC solution $U_{Gr} = 0.001$- 0.5 m·s^{-1} $U_{Lr} = 0.07$-1.3 m·s^{-1} $U_{Lr} / U_{Gr} = 1$-153 $Fr = 0.0005$ - 14.1 $Mo = 0.247$ - 0.39 $A_d/A_r = 0.11$-1 $H/d_r = 10.2$-228 $A_d/A_r = (5.6$ –$360)\times10^{-5}$ $Re_{Lr} = 40$-$130{,}000$

สถาบันวิทยบริการ
จุฬาลงกรณ์มหาวิทยาลัย

Table 2.2. Correlations between various hydrodynamic parameters for internal loop ALCs.

Author	Equation	Remark
Bello et al, 1984	$U_{Lr} = 0.66(A_d/A_r)^{0.74}\, U_{Gr}^{1/3}$	A_d/A_r = 0.13, 0.35 and 0.56, d_r = 0.152 m d_d = 0.05 - 0.102 m H_D= 1.8 m
Zhao et al, 1994	When H≥ 0.8 m $K_L a d_c = 9.33\times10^{-5}(d_c U_G \rho/\mu)^{0.56}(U_G \mu/\sigma)^{0.09}(U_G/\sqrt{g d_c})^{-0.86}$ When H< 0.8 m. $K_L a d_c = 2.95\times10^{-3}(d_c U_G \rho/\mu)^{0.29}(U_G^2 d_c \rho/3)^{-0.13}(U_G/\sqrt{g d_c})^{-0.31} * (\frac{H}{d_c})^{-0.5}$	Media: Newtonian and non-Newtonian liquids d_c = 0.14 m U_G = 0.007 - 0.6 m · s^{-1} μ = 0.001 - 1.26 Pa · s σ = 0.03 - 0.07 N · m
Gavrilescu and Tudose, 1998	Linear liquid velocities in riser and downcomer: $U_{L,r} = V_{Lr}(1-\varepsilon_{Gr})$ $U_{L,d} = V_{Ld}(1-\varepsilon_{Gd})$ an acceleration coefficient: $k_R = \frac{A_{rc}}{A_r}$ $k_D = \frac{A_{dc}}{A_d}$ $U_{L,r} = \left[\frac{2gH_D(\varepsilon_{G,r}-\varepsilon_{G,d})}{\left(\frac{1}{k_R^2}-1\right)\frac{1}{(1-\varepsilon_{G,r})^2}+\left(\frac{1}{k_D^2}-1\right)\frac{A_r^2}{A_d^2}\frac{1}{(1-\varepsilon_{G,d})^2}}\right]^{0.5}$	$0.05<U_{Gr}<0.12$ m · s^{-1}
Shamlou et al, 1995	$K_L a = 12(\frac{D_L}{\pi})^{0.5}\left[\frac{U_{BT}+C_0(U_{G,r}+U_{L,r})}{d_B^3}\right]^{0.5}\left[\frac{\varepsilon_G}{(1-\varepsilon_G)^3}\right]$	Medium: Fermentation broth of *Saccharovisiae cerevisiae*

Table 2.3. Correlations between various hydrodynamic parameters for both external and internal loop ALCs.

Author	Equation	Remark
Bello et al, 1985b	Liquid velocity effects: $k_L a_D H_D = 2.28(U_{Gr}/U_{Lr})^{0.9}(1+A_d/A_r)^{-1}$ $\varepsilon_{Gr} = 0.16(U_{Gr}/U_{Lr})^{0.57}(1+A_d/A_r)$ for external loops: $\varepsilon_{Gd} = 0.79\,\varepsilon_{Gr} - 0.057$ for internal loops: $\varepsilon_{Gd} = 0.89\,\varepsilon_{Gr}$	for external loop: A_d/A_r = 0.11-0.69 for internal loop: A_d/A_r = 0.13,0.35 and 0.56 d_r = 0.152 m d_d = 0.05 - 0.102 m H_D= 1.8m U_{Gr} = 0.0137-0.086 m·s^{-1} Sparger: perforated stainless plate with 52 holes of 1.02 mm
Chisti et al, 1988	$U_{L,r} = \left[\frac{2gH_D(\varepsilon_{G,r}-\varepsilon_{G,d})}{\frac{\varsigma_T}{(1-\varepsilon_{G,r})^2}+\frac{\varsigma_B}{(1-\varepsilon_{G,d})^2}\times\frac{A_r}{A_d}}\right]^{0.5}$	H= 3.21 m. Reactor volume 1.46 m^3 d_r = 0.142 m. A_d/A_r = 0.11- 1
Calvo , 1988	Energy balance: $P_1 U_{G1} \ln\frac{P_1+\rho_L g H_0}{P_1} = \frac{1}{2}K_f\frac{A_d}{A_r}\rho_L V_{Ld}^3 + \varepsilon V_s \rho_L g H_0$ Mean gas hold-up equation $\varepsilon = \frac{U_G}{v_{L,r}+v_s}$	0.01<U_G<0.06 m·s^{-1}
Chisti et al, 1988b	$\varepsilon = 2.47U_G^{0.97}$ $\varepsilon = 0.49U_G^{0.46}$	For U_G < 0.05 m·s^{-1} For U_G > 0.05 m·s^{-1}

2.1.4 Transient models in ALCs

When compared to the hydrodynamic models, far fewer investigations were carried out on the development of a mathematical model that was based on mass and energy balances of the system. This type of model is useful in predicting the transient behavior of the ALC particularly at the start up, shut down, or when there is changes in operating conditions. Some of these models are summarized as follows:

Dhaouadi et al, 1996: In an airlift system

Navier-stokes equation was applied (for all sections) to explain the behavior of the system:

$$\frac{\partial(\rho\varepsilon\Phi)_k}{\partial t} = -\frac{\partial}{\partial z}(\rho\varepsilon U\Phi)_k + \frac{\partial}{\partial z}(\frac{\mu_{eff}}{\sigma}\varepsilon\frac{\partial\Phi}{\partial z})_k + S_\Phi \qquad (2.1.4.1)$$

Dhaouadi et al, 1997: In an external loop airlift reactor

The ALC was divided into several sections, and equations for both liquid and gas phases were developed:

Liquid phase:

- riser : None

- gas-liquid separator : subsection 1 (originally called PMR1)

$$\frac{dO_L}{dt} = \frac{Q_1}{(1-\varepsilon_g)V}(O_{Le} - O_L) + \frac{K_L a}{(1-\varepsilon_g)}(O^* - O_L) \qquad (2.1.4.2)$$

- gas-liquid separator : subsection 2 (originally called PMR2)

$$\frac{dO_L}{dt} = \frac{Q_1}{V_{PMR2}}(O_{L,e} - O_L) \qquad (2.1.4.3)$$

- dowmcomer :

$$\frac{dO_L}{dt} = -u_L\frac{\partial O_L}{\partial z} \qquad (2.1.4.4)$$

- bottom junction : (originally called PMR3)

$$\frac{dO_L}{dt} = \frac{Q_1}{V_{PMR3}}(O_{Le} - O_L) \qquad (2.1.4.5)$$

Gas phase:

- riser :

$$\frac{dO_G}{dt} = -u_G \frac{\partial y}{\partial z} - u_G y \frac{1\partial P}{P\partial z} - K_L a(O_L^* - O_L)\frac{M_w}{\rho_L} y \qquad (2.1.4.6)$$

- gas-liquid separator : PMR1

$$\frac{dO_G}{dt} = \frac{Q_G}{\varepsilon_G V}(O_{Ge} - O_G) - \frac{K_L a}{\varepsilon_G}(O^* - O_L) \qquad (2.1.4.7)$$

- gas-liquid separator : PMR2 Neglected

- downcomer Neglected

- bottom junction Neglected

Choi, 1999: In an External-Loop Airlift Reactor

Oxygen balance equations at various sections of the ALC were derived from the mass balance condition:

- For the *1st* stage of the gas phase in riser:

$$\frac{dO_{G,1}}{dt} = \frac{\gamma_r (Q_{G,in} + Q_{G,d} O_{G,M_G+N_G} - Q_{G,r} O_{G,1})}{\varepsilon_r V_{r,i}} - K_L a \frac{(1-\varepsilon_r)}{\varepsilon_r}(O_{L,1}^* - O_{L,1}) \qquad (2.1.4.8)$$

- For the *1st* stage of the liquid phase in riser:

$$\frac{dO_{L,1}}{dt} = \frac{Q_L (O_{L,M_L+N_L} - O_{L,1})}{V_{r,i}(1-\varepsilon_r)} + K_L a(\overline{O}_{L,1}^* - O_{L,1}) \qquad (2.1.4.9)$$

- For the *i th* stage of the gas phase in riser:

$$\frac{dO_{G,i}}{dt} = \frac{\gamma_r Q_{Gr} (O_{G,i-1} - O_{G,i})}{\varepsilon_r V_{r,i}} - K_L a \frac{(1-\varepsilon_r)}{\varepsilon_r}(O_{L,i}^* - O_{L,i}) \qquad (2.1.4.10)$$

- For the *i th* stage of the liquid phase in riser:

$$\frac{dO_{L,i}}{dt} = \frac{Q_L (O_{L,i-1} - O_{L,i})}{V_{r,i}(1-\varepsilon_r)} + K_L a(\overline{O}_{L,i}^* - O_{L,i}) \qquad (2.1.4.11)$$

- For the gas phase in the top section above the riser:

$$\frac{dO_{G,M_G+N_G+1}}{dt} = \frac{(Q_{G,r} - Q_{G,tc})(O_{G,M_G} - O_{G,M_G+N_G+1})}{\varepsilon_{r,i} V_{tr}} - K_L a \frac{(1-\varepsilon_{tr})}{\varepsilon_{tr}}(O_{G,M_G+N_G+1}^* - O_{L,M_L+N_L+1}) \qquad (2.1.4.12)$$

- For the liquid phase in the top section above the riser:

$$\frac{dO_{L,M_L+N_L+1}}{dt} = K_L a(O_{L,M_G+N_G+1}^* - O_{L,M_L+N_L+1}) \qquad (2.1.4.13)$$

- For the gas phase in the downcomer and bottom conection:

$$\frac{dO_{G,i}}{dt} = \frac{\gamma_c Q_{Gd}(O_{G,i-1} - O_{G,i})}{\varepsilon_d V_{ci}} - K_L a \frac{(1-\varepsilon_d)}{\varepsilon_d}(O^*_{L,i} - O_{L,i}) \qquad (2.1.4.14)$$

- For the liquid phase in the downcomer and bottom conection:

$$\frac{dO_{L,i}}{dt} = \frac{Q_L(O_{L,i-1} - O_{L,i})}{V_{c,i}(1-\varepsilon_d)} + K_L a(\overline{O}^*_{L,i} - O_{L,i}) \qquad (2.1.4.15)$$

2.2 Literature Review: Hydrodynamic and Time Independent Models of ALCs

The behavior of bioreactors is determined not only by the reactor geometry but also by its hydrodynamic properties. Therefore knowledge of liquid velocities and (local) gas hold-up is essential for a reliable prediction of mixing and mass transfer characteristics.

Several models have been proposed in order to describe flow behavior in an ALC. In most cases, the models were based on experimental data in some forms of empirical correlations specific to a particular ALC. Verlann et al,1986 for instance, applied the drift-flux model of Zuber et al, 1965, supplemented with an empirical correlation for two different pilot scale ALCs with a working volume of 0.165 m^3 and 0.6 m^3 respectively. The model was adapted for non-isobaric conditions and took into account non-uniform flow profiles and gas hold-up distributions across the duct. The model was able to accurately predict liquid velocities and (local) gas hold-up in the ALC (with approx. 10% error). Calvo, 1989 studied and modeled hydrodynamic behaviors in three different airlift contactors and with three different draft tube diameters. The simple model based on an energy balance in airlift reactors was shown to predict liquid circulation and gas hold-up in each device. Calvo et al, 1991 later applied this simple model to the prediction of gas hold-up in the bubble column (BC) over a broad range of geometrical configurations and experimental conditions, and compared the results with the ALC performance. In this model, it was assumed that the energy input due to isothermal gas expansion in the riser of each contactor was dissipated to counterbalance the friction at the gas-liquid interface which caused the liquid motion. The liquid circulation model for draft-tube sparged concentric-tube

airlift reactors was developed using an energy balance over the circulation loop by Gavrilescu and Tudose, 1997. In this work, an energy balance of concentric tube airlift reactors was developed to explain liquid circulation velocities, taking into account the energy losses along the total circulation loop, especially at the bottom and top sections. Such losses are caused by apparent contraction of the cross-sectional area, and quantified by the acceleration coefficients that were estimated using measurements of static pressure profiles. Sáez et al, 1998 suggested the new mathematical model capable of predicting accurately hydrodynamic parameters of a gas-lift reactor. The information on gas hold-up profiles in the riser section, and liquid circulation velocities was included in the model. The model was based on macroscopic balances for gas-liquid separator and external downcomer, and spatially-averaged, one-dimensional mass and momentum balances in the riser.

2.3 Literature Review: Dynamic Model of ALCs

Mass transfer was one of the most important designed parameters of gas-liquid reactors for either chemical or biochemical applications. Various methods for the mass transfer calculations on the basis of the dynamic method have been published. Almost all the previous works took into account the effects of pressure on gas solubility, especially for tall columns; few of them took into account the axial dispersion of the liquid phase. Nearly all of the reported models neglected the oxygen depletion in the gas phase. Hence, neither the oxygen profiles in the liquid phase nor in the gas phase was considered.

Andre et al, 1983 developed a simple criterion that represented the well-mixed conditions both in the liquid and gas phases. A tank-in-series model for both the riser and the downcomer was also employed to represent the deviation from the ideal case. However, the system was assumed to work with very low gas throughput so that the circulation of the gas phase in the downcomer did not have to be considered.

Dhaouadi et al, 1996, 1997 proposed that the model of the airlift reactor system could be formulated by dividing the reactor into four sections: riser, gas-liquid separator, downcomer, and bottom junction. In this model it was found that the riser could well be interpreted as a bubble column, the downcomer as a plug flow with

axial dispersion, and the remaining two sections, gas-liquid separator and bottom junction, as CSTRs with and without bubbles, respectively. All the model equations were derived principally from the Navier-Stokes equation which considered only one dimension (usually ignored the radial effects), and this system of differential equations was solved in the real time domain.

Choi, 1999 developed a mathematical model for the external-loop airlift reactor. In this study, the model considered both the effect of the gas circulation rate and the role of the downcomer in oxygen transfer. It was reported that the oxygen concentrations in the contactor varied with time and position. Hence, he used a tank-in-series model to explain the behavior of the riser, and in each tank the fluid was separated into the liquid and gas regimes with the mass transfer between them. The tank-in-series model was also applied to the gas separator and downcomer sections. All of these models were based on mass balance of oxygen in both liquid and gas phases.

It can be seen that there have been attempts to develop mathematical models for the various types of ALC, most of which were based on their assumptions of ideal reactors or at most a reactors-in-series model. However, several experimental works revealed that there existed the “non-ideality” of the ALC systems. (Andre et al, 1983 and Choi, 1999) Therefore this work aims at the development of the mathematical model which is capable of describing the non-ideal behavior of the “split-type” ALC (Figure 2.1(A1)). This includes mainly the effect of axial dispersion and the interaction between the gas and liquid phases.

สถาบันวิทยบริการ
จุฬาลงกรณ์มหาวิทยาลัย

CHAPTER 3

Experiment

3.1 Experimental Apparatus

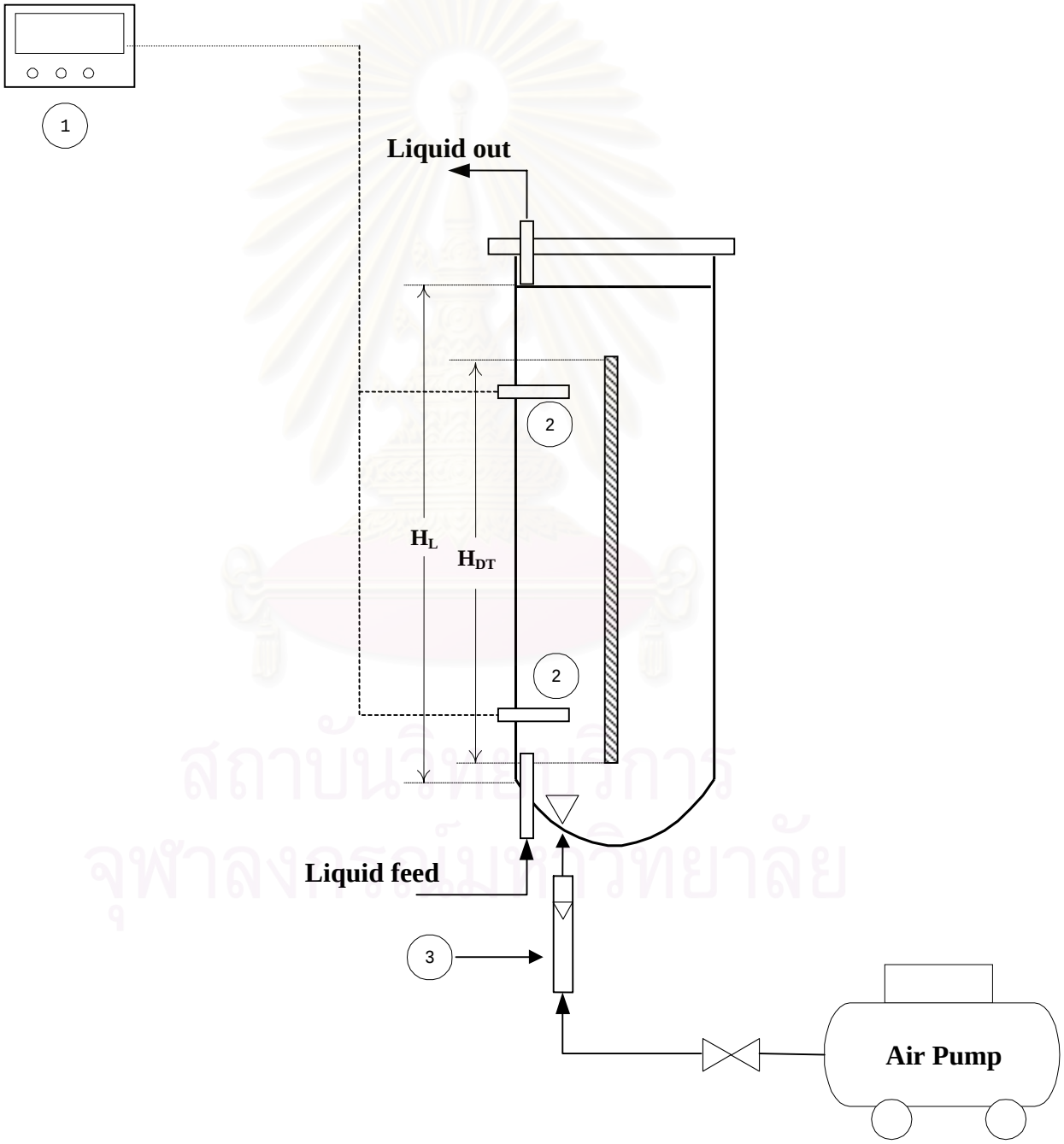

Figure 3.1 Schematic diagram of the Split-type Airlift Contactor (Split ALC).
1. pH meter, 2.pH probe, 3.Rotameter

สถาบันวิทยบริการ
จุฬาลงกรณ์มหาวิทยาลัย

Figure 3.1 shows a schematic diagram with detailed design of the airlift contactor (ALC) used in this study. The airlift vessel is made of acrylic plastic with 5 mm wall thickness. A split-type ALC is employed where the vessel is divided into two sections by a rectangular plastic plate. The ratio between the riser to downcomer cross-section areas (A_d/A_r) can be adjusted by changing the location of this plastic plate (A_d/A_r = 1 where the plastic plate is installed in the middle of the vessel). The plate is located 0.1 m above the base of the contactor. A series of measuring ports are attached along the column height with 0.1 m spacing between each port for pressure measurement. Also these ports are used as a tracer injection point to measure liquid velocity and to determine the residence time distribution (RTD) in the ALC. The height of the vessel is 1.2 m which makes the nominal volume of 15 litres, but the unaerated liquid height in the vessel is controlled at 1.08 m. which corresponds to a working liquid volume of 13.5 litres.

Compressed air is injected at the bottom of the airlift contactor through a porous sparger. Air flow rates are measured by a calibrated gas rotameter and controlled by a valve attached to a gas compressor. Gas superficial velocity in the riser varies from 0.00367 to 0.0381 $m \cdot s^{-1}$. Tap water is used as liquid phase and it is continuously added into the downcomer with liquid feed rate ranging between (6.853 to 10.769)x10^{-6} $m^3 \cdot s^{-1}$, and the total volume is controlled by the drain located at the top of the gas separator. The location of the drain is not fixed, but variable to ensure that the total volume of liquid in the contactor is 13.5 litres. The airlift contactor works in a continuous fashion for both liquid and gas phases, at atmospheric pressure and a constant temperature of 23^{o}C.

Experimental conditions and the dimensions of the experiment equipment are summarized in Table 3.1.

สถาบันวิทยบริการ
จุฬาลงกรณ์มหาวิทยาลัย

3.2 Experimental Methods

3.2.1 Experiment Preparation

All experiments described below are subject to the preparation described in this section.

1. Calibrate the rotameter. This is accomplished using the technique of replacement of air in water.
2. Fill column with tap water up to the level of 1.08 m, this level is called “unaerated liquid height” (0.05 m above acrylic plastic plate).
3. Sparge air through a porous sparger on the contactor base. A precalibrated rotameter is used for the adjustment of air volumetric flow rate (which is fixed constant at a decided value, e.g. 0.0381 $m^3 \cdot s^{-1}$).
4. Wait for a few seconds until no further changes in bubble distribution in the dispersed volume are observed.
5. Add tap water continuously into the riser entrance with a liquid feed rate ranging between (6.853 to 10.769)x10^{-6} $m^3 \cdot s^{-1}$. The total volume is controlled by the drain located at the gas separator.

3.2.2 Measurement and Calculation of Residence Time Distributions

Derivation of equations used to determine the residence time distribution

The residence time distribution (RTD) of the liquid phase are determined experimentally by using the tracer response technique where an inert chemical tracer is injected into the contactor at a certain time (*t=0*) and then its concentration in the effluent stream is measured as a function of time. This input is treated as a perfect pulse input, although in practice it is impossible to obtain a perfect pulse. However, a rapid, turbulent injection of the tracer may be approximated as a perfect pulse, i.e. the

injection takes place over a very short period compared to residence time in the various segments of the contactor. It is also assumed that the amount of dispersion between the point of injection and the entrance of the contactor is so small that the system can be treated as an open system.

The volume of tracer is kept small in relation to the total volume within the contactor and injection is carried out as quickly and smoothly as possible. The effluent concentration-time curve is referred to as the C curve in the RTD analysis. The curve *C(t)* allows us to determine the residence time function (or the exit-age distribution function), that describes in a quantitative manner how much time different fluid elements spend in the contactor.

To obtain the *E(t)* curve from the *C(t)* curve, we divide *C(t)* by the integral: $\int_0^\infty C(t)dt$ which is the area under the C curve. This area can be found using the graphical integration:

$$E(t_i) = \frac{C(t_i)}{\sum_{i=1}^{n} C(t_i)\Delta t_i} \qquad (3.2.1)$$

$E(t)$ is the most frequently used of the distribution functions which are related to contactor analysis.

Since the functions of distribution are obtained as discrete values of the concentration at the time, i.e. $C(\Delta t_i)$, the value of the residence time (t_s) and its variance (σ^2) are obtained from the following relationships:

$$t_s \cong \frac{\sum t_i C(t_i)\Delta t_i}{\sum C(t_i)\Delta t_i} \qquad (3.2.2)$$

$$\sigma^2 \cong \frac{\sum (t_i - t_s)^2 C(t_i)\Delta t_i}{\sum C(t_i)\Delta t_i} \qquad (3.2.3)$$

These values, t_s and σ^2, are directly linked by theory to $\frac{D}{uL}$. For cases where nonsymmetrical E curves exist, a large deviation from plug flow condition is implied and $\frac{D}{uL}$ can be evaluated from: (Levenspiel and Smith, 1957)

$$\frac{\sigma^2}{t_s^2} = 2\frac{D}{uL} + 8\left[\frac{D}{uL}\right]^2 \qquad (3.2.4)$$

Residence time measurement

1. Inject 40ml of hydrochloric solution (2N) as a pulse tracer into the port at the downcomer entrance.
2. Analyze the concentration of acid at the detection points (located in the middle of downcomer just under the injection point, middle of riser, and at the gas separator) using a pH meter (EYELA model FC-2000).
3. Plot C curve and determine the residence time distribution and its variance using Eqs. 3.2.1-3.2.3.
4. Determine the dispersion coefficient using Eq. 3.2.4.

3.2.3 Experimental Repetition

All the experiments are repeated at various gas superficial velocities, i.e, 0.00367, 0.0153, 0.0230, 0.0305, 0.0381 $m \cdot s^{-1}$ and also various liquid feed rates, i.e, (6.85, 7.83, 8.81, 9.79, 10.769)x10^{-6} $m^3 \cdot s^{-1}$.

3.3 Mathematical Models: Derivation

Basically, an airlift contactor consists of three distinct sections; riser, downcomer, and gas separator (Figure 2.2). Each section exhibits different hydrodynamic behavior and mixing performance. It is necessary to understand both hydrodynamics and mixing characteristics of the system when designing a reactor. Many researchers paid attention on different methods in developing a mathematical model of the unsteady state oxygen transfer in the ALCs. Verlann et al., (1989) who studied the mixing behavior in individual sections of an external loop airlift contactor by time domain analysis found that the gas separator could be fairly described as a well mixed region, while the riser and downcomer by plug flow condition. Similarly, Merchuk and Siegal (1988) investigated a simple model for split airlift contactors which represented by two plug flow zones for the riser and downcomer whilst completely mixed zone for the gas separating section. The model was found

reasonable in describing the well-mixed behavior in the top section but it neglected the effect of axial dispersion both in riser and downcomer.

For the sake of generality of the model, this work will concentrate mostly on the dynamic models that are capable of describing the mass transfer performance in various sections of the ALC. The following derivations lead to various types of mathematical models for the ALC. These models include:

1. The CSTR model
2. The PFR model
3. The CSTRs-in-series model
4. The Dispersion model

Note that, in the riser of the ALC, liquid flows in a similar fashion to a plug-flow but the gas bubbles cause mixing in this region. Therefore it is not certain on the types of model that are suitable for describing the behavior of the riser. The gas separator, on the other hand, can be regarded as a completely mixed section as the liquid and gas bubbles from the riser enter and change their flow direction instantaneously. This results in a high level of back mixing. Therefore this section will only be described by a CSTR model. The behavior of the fluid in the downcomer is closer to the plug flow condition as only a few portion of gas bubbles enters this section which means that the level of mixing in this region is rather low. Hence, the downcomer should be described using either the PFR or CSTRs-in-Series models. However, in the following, we will divide the detailed derivation of the mathematical models for the ALC into three categories: (i) the CSTR model, (ii) the CSTRs-in-Series model, and (iii) the Dispersion model. Firstly, in the CSTR model, all regions (riser, gas separator, and downcomer) will be modeled by the CSTR. Next, in the CSTRs-in-Series model, the riser and downcomer will be represented by CSTRs in series, whilst the CSTR will be used to represent the gas separator. Lastly, the Dispersion model will consider both riser and downcomer as a plug flow region with dispersion, whereas the gas separator will still be modeled as a region of completely mixed. To obtain the PFR model, one can simply fix the values of all dispersion coefficient in the Dispersion model to be zero.

Note that in the actual simulation, other combinations of these various types of mathematical model is possible, for instance, the riser can be represented by the Dispersion, whereas the downcomer is explained by the CSTRs-in-Series model.

The model will include the interaction between the liquid and gas phases as the oxygen from gas bubble will be transferred into the liquid. The non-ideal behavior of the system will be included in terms of the axial dispersion of the liquid in the riser and downcomer. All the model derivation will start from the mass balance equation Eq. 3.3.1.

$$\left\{\begin{array}{c}\text{Accumulation}\\ \text{within the system}\end{array}\right\} = \left\{\begin{array}{c}\text{Input into system}\\ \text{boundaries}\end{array}\right\} - \left\{\begin{array}{c}\text{Output from}\\ \text{system boundaries}\end{array}\right\} + \left\{\begin{array}{c}\text{Generation within}\\ \text{the system}\end{array}\right\} - \left\{\begin{array}{c}\text{Consumption}\\ \text{within the system}\end{array}\right\} \quad (3.3.1)$$

The assumptions for the derivation of the model are summarized here.

1. The system is isothermal.
2. There is no radial effect in the ALC.
3. Oxygen is sparingly soluble in water and Henry's law can be applied to explain the solubility of oxygen in the contactor.
4. The behavior of the gas in the system is ideal.
5. The operating parameters, e.g. gas holdups, liquid circulation flow rate, are not a function of time and space.
6. The volumetric mass transfer coefficient(K_La) is constant and identical for all sections in the contactor.

The last assumption is considered suitable for small to medium scale ALCs which should be able to apply to case studies in this work.

3.3.1 The CSTR Model

As described earlier, the model of airlift contactor system is formulated based on the concept that the airlift contactor is divided into three sections: riser, gas separator and downcomer (see Figure 2.2). To develop a CSTR model to describe the ALC, it is assumed that all of the elements of ALC behave like a completely mixed tank (see Figure 3.2), after which, each component in Eq. 3.3.1 can be formulated. The development of the model for each section of the ALC follows:

Riser

1. The accumulation of oxygen in the CSTR:

Accumulation of O_2 in the gas phase = $\varepsilon_r V_r \frac{d}{dt} O_{G,r}$ (3.3.1.1)

Accumulation of O_2 in the liquid phase = $(1-\varepsilon_r) V_r \frac{d}{dt} O_{L,r}$ (3.3.1.2)

2. Input to CSTR.

in gas phase:

1. O_2 into the volume element with air inlet flow = $\varepsilon_r A_r v_{G,in} O_{G,in}$ (3.3.1.3)

2. O_2 into the volume element with the recycled gas bubbles from downcomer section = $\varepsilon_d A_d v_{G,d} O_{G,d}$ (3.3.1.4)

in liquid phase:

1. O_2 into the volume element with the recycled liquid from downcomer section = $(1-\varepsilon_d) A_d v_{L,d} O_{L,d}$ (3.3.1.5)

2. O_2 into the volume element with mass transfer

$= (1-\varepsilon_r) K_L a V_r (O^*_{G,r} - O_{L,r})$ (3.3.1.6)

Note: O_2 into the volume element with feed flow rate ($Q_{L,F} O_{L,F}$) = 0 as it is assumed that O_2 in the liquid feed is very dilute.

3. Output from CSTR

in gas phase:

1. O_2 out from the volume element with gas flow = $\varepsilon_r A_r v_{G,r} O_{G,r}$ (3.3.1.7)

2. O_2 out from the volume element with mass transfer

$$= (1-\varepsilon_r) K_L a V_r (O^*_{G,r} - O_{L,r}) \quad (3.3.1.8)$$

in liquid phase:

O_2 out from the volume element with liquid flow

$$= (1-\varepsilon_r) A_r v_{L,r} O_{L,r} \quad (3.3.1.9)$$

Gas separator

1. The accumulation of oxygen in the CSTR:

Accumulation of O_2 in the gas phase = $\varepsilon_{top} V_{top} \frac{d}{dt} O_{G,top}$ (3.3.1.10)

Accumulation of O_2 in the liquid phase = $(1-\varepsilon_{top}) V_{top} \frac{d}{dt} O_{L,top}$ (3.3.1.11)

2. Input to CSTR.

in gas phase:

O_2 into the volume element with gas flow

from riser section = $\varepsilon_r A_r v_{G,r} O_{G,r}$ (3.3.1.12)

in liquid phase:

1. O_2 into the volume element with liquid flow

from riser section = $(1-\varepsilon_r) A_r v_{L,r} O_{L,r}$ (3.3.1.13)

2. O_2 into the volume element with mass transfer

$$= (1-\varepsilon_{top}) K_L a V_{top} (O^*_{G,top} - O_{L,top}) \quad (3.3.1.14)$$

.

3. Output from CSTR

in gas phase:

1. O_2 out from the volume element with gas flow

$$= \varepsilon_{top} A_{top} v_{G,top} O_{G,top} \quad (3.3.1.15)$$

2. O_2 out from the volume element with mass transfer

$$= (1-\varepsilon_{top}) K_L a V_{top} (O^*_{G,top} - O_{L,top}) \quad (3.3.1.16)$$

3. O_2 out from the volume element with

$$\text{gas over flow} = \varepsilon_{top} A_{top} v_{G,out} O_{G,top} \quad (3.3.1.17)$$

in liquid phase:

1. O_2 out from the volume element with

$$\text{liquid flow} = (1-\varepsilon_{top}) A_{top} v_{L,top} O_{L,top} \quad (3.3.1.18)$$

2. O_2 out from the volume element with

$$\text{liquid overflow} = (1-\varepsilon_{top}) A_{top} v_{L,out} O_{L,top} \quad (3.3.1.19)$$

Downcomer

1. The accumulation of oxygen in the CSTR:

$$\text{Accumulation of } O_2 \text{ in the gas phase} = \varepsilon_d V_d \frac{d}{dt} O_{G,d} \quad (3.3.1.20)$$

$$\text{Accumulation of } O_2 \text{ in the liquid phase} = (1-\varepsilon_d) V_d \frac{d}{dt} O_{L,d} \quad (3.3.1.21)$$

2. Input to CSTR.

in gas phase:

O_2 into the volume element with gas flow from

$$\text{gas separator section} = \varepsilon_{top} A_{top} v_{G,top} O_{G,top} \quad (3.3.1.22)$$

in liquid phase:

1. O_2 into the volume element with liquid flow from

$$\text{gas separator section} = (1-\varepsilon_{top}) A_{top} v_{L,top} O_{L,top} \quad (3.3.1.23)$$

สถาบันวิทยบริการ
จุฬาลงกรณ์มหาวิทยาลัย

2. O_2 into the volume element with mass transfer

$$= (1-\varepsilon_d)K_L a V_d (O^*_{G,d} - O_{L,d}) \qquad (3.3.1.24)$$

3. Output from CSTR

in gas phase:

1. O_2 out from the volume element with gas flow = $\varepsilon_d A_d v_{G,d} O_{G,d}$ (3.3.1.25)

2. O_2 out from the volume element with mass transfer

$$= (1-\varepsilon_d)K_L a V_d (O^*_{G,d} - O_{L,d}) \qquad (3.3.1.26)$$

in liquid phase:

O_2 out from the volume element with liquid flow

$$= (1-\varepsilon_d)A_d v_{L,d} O_{L,d} \qquad (3.3.1.27)$$

Combining Eqs. 3.3.1.1-3.3.1.27 gives the mass balance equation Eq.3.3.1 for O_2 in the ALC as follows:

Gas phase in the riser.

$$\varepsilon_r V_r \frac{d}{dt} O_{G,r} = \varepsilon_r A_r v_{G,in} O_{G,in} + \varepsilon_d A_d v_{G,d} O_{G,d} - \varepsilon_r A_r v_{G,r} O_{G,r} - (1-\varepsilon_d)K_L a V_r (O^*_{G,r} - O_{L,r}) \qquad (3.3.1.28)$$

Dividing Eq. 3.3.1.28 with $\varepsilon_r V_r$ gives:

$$\frac{d}{dt} O_{G,r} = \frac{(A_r v_{G,in} O_{G,in} - A_r v_{G,r} O_{G,r})}{V_r} + \frac{\varepsilon_d A_d v_{G,d} O_{G,d}}{\varepsilon_r V_r} - \frac{(1-\varepsilon_d)K_L a (O^*_{G,r} - O_{L,r})}{\varepsilon_r}$$

where

$$O_G = \frac{P Y_{O_2}}{RT} \qquad (3.3.1.30)$$

According to Henry's law, the partial pressure of oxygen in the gas phase at equilibrium is proportional to the concentration of oxygen in the liquid film.

$$O^*_G = \frac{P_{O_2}}{H} = \frac{O_G RT}{H} \qquad (3.3.1.31)$$

Liquid phase in the riser

$$(1-\varepsilon_r)V_r\frac{d}{dt}O_{L,r} = (1-\varepsilon_d)A_d v_{L,d}O_{L,d} - (1-\varepsilon_r)A_r v_{L,r}O_{L,r} + (1-\varepsilon_r)K_L aV_r(O^*_{G,r} - O_{L,r})$$

(3.3.1.32)

Dividing Eq. 3.3.1.32 with $(1-\varepsilon_r)V_r$ gives:

$$\frac{d}{dt}O_{L,r} = \frac{(1-\varepsilon_d)A_d v_{L,d}O_{L,d} - (1-\varepsilon_r)A_r v_{L,r}O_{L,r}}{(1-\varepsilon_r)V_r} + K_L a(O^*_{G,r} - O_{L,r})$$

(3.3.1.33)

Gas phase in the gas separator

$$V_{top}\varepsilon_{top}\frac{d}{dt}O_{G,top} = \varepsilon_r A_r v_{G,r}O_{G,r} - \varepsilon_{top}A_{top}v_{G,top}O_{G,top} - \varepsilon_{top}A_{top}v_{G,out}O_{G,top} - (1-\varepsilon_{top})K_L aV_{top}(O$$

Dividing Eq. 3.3.1.34 which $\varepsilon_{top}V_{top}$ gives:

$$\frac{d}{dt}O_{G,top} = \frac{\varepsilon_r A_r v_{G,r}O_{G,r}}{V_{top}\varepsilon_{top}} - \frac{(A_{top}v_{G,top}O_{G,top} + A_{top}v_{G,out}O_{G,top})}{V_{top}} - \frac{(1-\varepsilon_{top})K_L a(O^*_{G,top} - O_{L,top})}{\varepsilon_{top}}$$

(3.3.1.35)

Liquid phase in the gas separator

$$(1-\varepsilon_{top})V_{top}\frac{d}{dt}O_{L,top} = (1-\varepsilon_r)A_r v_{L,r}O_{L,r} - (1-\varepsilon_{top})A_{top}v_{L,top}O_{L,top}$$
$$- (1-\varepsilon_{top})A_{top}v_{L,out}O_{L,top} + (1-\varepsilon_{top})K_L aV_{top}(O^*_{G,top} - O_{L,top})$$

(3.3.1.36)

Dividing Eq. 3.3.1.36 which $(1-\varepsilon_{top})V_{top}$ gives:

$$\frac{d}{dt}O_{L,top} = \frac{(1-\varepsilon_r)A_r v_{L,r}O_{L,r}}{V_{top}(1-\varepsilon_{top})} - \frac{(A_{top}v_{L,top}O_{L,top} + A_{top}v_{L,out}O_{L,top})}{V_{top}}$$
$$+ K_L a(O^*_{G,top} - O_{L,top})$$

(3.3.1.37)

Gas phase in the downcomer

$$\varepsilon_d V_d\frac{d}{dt}O_{G,d} = \varepsilon_{top}A_{top}v_{G,top}O_{G,top} - \varepsilon_d A_d v_{G,d}O_{G,d} - (1-\varepsilon)_d K_L aV_d(O^*_{G,d} - O_{L,d})$$

Dividing Eq. 3.3.1.38 which $\varepsilon_d V_d$ gives:

$$\frac{d}{dt}O_{G,d} = \frac{\varepsilon_{top} A_{top} v_{G,top} O_{G,top} - \varepsilon_d A_d v_{G,d} O_{G,d}}{V_d \varepsilon_d} - \frac{(1-\varepsilon_d) K_L a (O^*_{G,d} - O_{L,d})}{\varepsilon_d} \tag{3.3.1.39}$$

Liquid phase in the downcomer

$$(1-\varepsilon_d)V_d \frac{d}{dt}O_{L,d} = (1-\varepsilon_{top})A_{top} v_{L,top} O_{L,top} - (1-\varepsilon_d)A_d v_{L,d} O_{L,d} + (1-\varepsilon_d)K_L a V_d (O^*_{G,d} - O_{L,d}) \tag{3.3.1.40}$$

Dividing Eq. 3.3.1.40 which $(1-\varepsilon_d)V_d$ gives:

$$\frac{d}{dt}O_{L,d} = \frac{(1-\varepsilon_{top})A_{top} v_{L,top} O_{L,top} - (1-\varepsilon_d)A_d v_{L,d} O_{L,d}}{(1-\varepsilon_d)V_d} + K_L a (O^*_{G,d} - O_{L,d}) \tag{3.3.1.41}$$

สถาบันวิทยบริการ
จุฬาลงกรณ์มหาวิทยาลัย

3.3.2 The CSTRs-in-Series model

In this model, the flow of the gas and liquid phases in both sections; riser and downcomer, are interpreted as CSTRs connected in series and the gas separator section is still treated as a CSTR.

A schematic diagram of a CSTRs-in-Series model is shown in Figure 3.3. It is assumed that the total numbers of CSTRs in riser and downcomer are equal to *N* and *M*, respectively. The model development follows.

Riser

1. The accumulation of oxygen in the CSTRs-in-Series at the i^{th} CSTR (*i = 1, 2,.. , N*):

   Accumulation of O_2 in the gas phase = $\varepsilon_r V_r \frac{d}{dt} O_{G,r,i}$ (3.3.2.1)

   Accumulation of O_2 in the liquid phase = $(1-\varepsilon_r) V_r \frac{d}{dt} O_{L,r,i}$ (3.3.2.2)

2. Input to CSTRs-in-Series

   In the CSTRs-in-Series at the first CSTR:

   in gas phase:

   1. O_2 into the first CSTR with air inlet flow = $\varepsilon_r A_r v_{G,in} O_{G,in}$ (3.3.2.3)

   2. O_2 into the first CSTR with the recycled gas bubble from downcomer section = $\varepsilon_d A_d v_{G,d} O_{G,d,M}$ (3.3.2.4)

   in liquid phase:

   1. O_2 into the first CSTR with the recycled liquid from downcomer section = $(1-\varepsilon_d) A_d v_{L,d} O_{L,d,M}$ (3.3.2.5)

   2. O_2 transfer from the gas bubbles into the liquid = $(1-\varepsilon_r) K_L a V_r (O^*_{G,r,1} - O_{L,r,1})$ (3.3.2.6)

   Note: O_2 into the volume element with feed flow rate ($Q_{L,F} O_{L,F}$) = 0 because O_2 in the liquid feed is very dilute.

   In the CSTRs-in-Series at the i^{th} CSTR:

   in gas phase:

   O_2 into the i^{th} CSTR from the gas flow (*i = 2, 3, …, N*)

$$= \varepsilon_r A_r v_{G,r} O_{G,r,i-1} \quad (3.3.2.7)$$

in liquid phase:

1. O_2 into the i^{th} CSTR from the liquid flow ($i = 2, 3, \ldots, N$)

2. O_2 transfer from the gas bubbles into the liquid

$$\text{for } i^{th} \text{ CSTR} = (1-\varepsilon_r) K_L a V_r (O^*_{G,r,i} - O_{L,r,i}) \quad (3.3.2.9)$$

3. Output from CSTRs-in-Series

In the CSTRs-in-Series at the i^{th} CSTR ($i = 1, 2, \ldots, N$):

In gas phase:

1. O_2 out from any i^{th} CSTR with gas flow

$$= \varepsilon_r A_r v_{G,r} O_{G,r,i} \quad (3.3.2.10)$$

2. O_2 out from any i^{th} CSTR with mass transfer to the liquid phase

$$= (1-\varepsilon_r) K_L a V_r (O^*_{G,r,i} - O_{L,r,i}) \quad (3.3.2.11)$$

in liquid phase:

O_2 out from any i^{th} CSTR with liquid flow

$$= (1-\varepsilon_r) A_r v_{L,r} O_{L,r,i} \quad (3.3.2.12)$$

Gas separator

1. The accumulation of oxygen in the CSTR:

$$\text{Accumulation of } O_2 \text{ in the gas phase} = \varepsilon_{top} V_{top} \frac{d}{dt} O_{G,top} \quad (3.3.2.13)$$

$$\text{Accumulation of } O_2 \text{ in the liquid phase} = (1-\varepsilon_{top}) V_{top} \frac{d}{dt} O_{L,top} \quad (3.3.2.14)$$

2. Input to CSTR.

in gas phase:

O_2 into the volume element with gas flow

$$\text{from riser section} = \varepsilon_r A_r v_{G,r} O_{G,r,N} \quad (3.3.2.15)$$

in liquid phase:

1. O_2 into the volume element with liquid flow

$$\text{from riser section} = (1-\varepsilon_r)A_r v_{L,r} O_{L,r,M} \quad (3.3.2.16)$$

2. O_2 into the volume element with mass transfer

$$= (1-\varepsilon_{top})K_L a V_{top}(O^*_{G,top} - O_{L,top}) \quad (3.3.2.17)$$

3. Output from CSTR

in gas phase:

1.O_2 out from the volume element with gas flow

$$= \varepsilon_{top} A_{top} v_{G,top} O_{G,top} \quad (3.3.2.18)$$

2.O_2 out from the volume element with mass transfer

$$= (1-\varepsilon_{top})K_L a V_{top}(O^*_{G,top} - O_{L,top}) \quad (3.3.2.19)$$

3.O_2 out from the volume element with

$$\text{gas over flow} = \varepsilon_{top} A_{top} v_{G,out} O_{G,top} \quad (3.3.2.20)$$

in liquid phase:

1.O_2 out from the volume element with

$$\text{liquid flow} = (1-\varepsilon_{top})A_{top} v_{L,top} O_{L,top} \quad (3.3.2.21)$$

2.O_2 out from the volume element with

$$\text{liquid overflow} = (1-\varepsilon_{top})A_{top} v_{L,out} O_{L,top} \quad (3.3.2.22)$$

สถาบันวิทยบริการ
จุฬาลงกรณ์มหาวิทยาลัย

Downcomer

1. The accumulation of oxygen in the CSTRs-in-Series at the i^{th} CSTR ($i = 1,2,..,M$):

Accumulation of O_2 in the gas phase = $\varepsilon_d V_d \frac{dO_{G,d,i}}{dt}$ (3.3.2.23)

Accumulation of O_2 in the liquid phase = $(1-\varepsilon_d)V_d \frac{dO_{L,d,i}}{dt}$ (3.3.2.24)

2. Input to CSTRs-in-Series

In the CSTRs-in-Series at the first CSTR:

in gas phase:

O_2 into the first CSTR with gas flow from gas separator section

$$= \varepsilon_{top} A_{top} v_{G,top} O_{G,top} \quad (3.3.2.25)$$

in liquid phase:

1.O_2 into the first CSTR with liquid flow from gas separator section

$$(1-\varepsilon_{top}) A_{top} v_{L,top} O_{L,top} \quad (3.3.2.26)$$

2.O_2 into volume element with mass transfer

$$(1-\varepsilon_d) K_L a V_d (O^*_{G,d,1} - O_{L,d,1}) \quad (3.3.2.27)$$

In the CSTRs-in-Series at the i^{th} CSTR ($i = 2, 3, \ldots, M$):

in gas phase:

O_2 into the i^{th} CSTR with gas flow

$$= \varepsilon_{top} A_{top} v_{G,d} O_{G,d,i} \quad (3.3.2.28)$$

in liquid phase:

1.O_2 into the i^{th} CSTR with liquid flow

$$= (1-\varepsilon_{top}) A_{top} v_{L,d} O_{L,d,i} \quad (3.3.2.29)$$

2.O_2 into volume element with mass transfer

$$= (1-\varepsilon_d) K_L a V_d (O^*_{G,d,i} - O_{L,d,i}) \quad (3.3.2.30)$$

3. Output from CSTRs-in-Series

In the CSTRs-in-Series at the i^{th} CSTR ($i = 1, 2, \ldots, M$):

in gas phase:

1.O_2 out from the i^{th} CSTR with gas flow = $\varepsilon_d A_d v_{G,d} O_{G,d,i}$ (3.3.2.31)

2.O_2 out from the i^{th} CSTR with mass transfer

$$= (1-\varepsilon_d) K_L a V_d (O^*_{G,d,i} - O_{L,d,i}) \quad (3.3.2.32)$$

in liquid phase:

O_2 out from the i^{th} CSTR with liquid flow

$$= (1-\varepsilon_d) A_d v_{L,d} O_{L,d,i} \quad (3.3.2.33)$$

Combining Eqs. 3.3.2.1-3.3.2.33 gives the mass balance equations for O_2 in the contactor as summarized below:

Gas phase in the riser

At the first CSTR(i=1):

$$\varepsilon_r V_r \frac{d}{dt} O_{G,r,i} = \varepsilon_r A_r v_{G,in} O_{G,in} + \varepsilon_d A_d v_{G,d} O_{G,d,M} - \varepsilon_r A_r v_{G,r} O_{G,r,1} - (1-\varepsilon_r) K_L a V_r (O^*_{G,r,1} - O_{L,r,1}) \quad (3.3.2.34)$$

Dividing Eq. 3.3.2.34 with $\varepsilon_r V_r$ gives:

$$\frac{d}{dt} O_{G,r,1} = \frac{(A_r v_{G,in} O_{G,in} - A_r v_{G,r} O_{G,r,1})}{V_r} + \frac{\varepsilon_d A_d v_{G,d} O_{G,d,M}}{\varepsilon_r V_r} - \frac{(1-\varepsilon_r) K_L a (O^*_{G,r,1} - O_{L,r,1})}{\varepsilon_r} \quad (3.3.2.35)$$

where

$$O_G = \frac{P Y_{O_2}}{RT} \quad (3.3.1.30)$$

According to Henry's law, the partial pressure of oxygen in the gas phase at equilibrium is proportional to the concentration of oxygen in the liquid film.

$$O^*_G = \frac{P_{O_2}}{H} = \frac{O_G RT}{H} \quad (3.3.1.31)$$

At 2<i<N:

$$\varepsilon_r V_r \frac{d}{dt} O_{G,r,i} = \varepsilon_r A_r v_{G,r} O_{G,r,i-1} - \varepsilon_r A_r v_{G,r} O_{G,r,i} - (1-\varepsilon_d) K_L a V_r (O^*_{G,r,i} - O_{L,r,i})$$

Dividing Eq. 3.3.2.36 with $\varepsilon_r V_r$ gives:

$$\frac{d}{dt}O_{G,r,i} = \frac{A_r v_{G,r}(O_{G,r,i-1} - O_{G,r,i})}{V_r} - \frac{(1-\varepsilon_d)K_L a(O^*_{G,r,i} - O_{L,r,i})}{\varepsilon_r} \quad (3.3.2.37)$$

Liquid phase in the riser

At the first CSTR(i=1):

$$(1-\varepsilon_r)V_r \frac{d}{dt}O_{L,r,1} = (1-\varepsilon_d)A_d v_{L,d} O_{L,d,M} - (1-\varepsilon_r)A_r v_{L,r} O_{L,r,1} + (1-\varepsilon_r)K_L a V_r (O^*_{G,r,1} - O_{L,r,1}) \quad (3.3.2.38)$$

Dividing Eq. 3.3.2.38 with $(1-\varepsilon_r)V_r$ gives:

$$\frac{dO_{L,r,1}}{dt} = \frac{(1-\varepsilon_d)A_d v_{L,d} O_{L,d,M} - (1-\varepsilon_r)A_r v_{L,r} O_{L,r,1}}{(1-\varepsilon_r)V_r} + K_L a(O^*_{G,r,1} - O_{L,r,1}) \quad (3.3.2.39)$$

At 2<i<N:

$$(1-\varepsilon_r)V_r \frac{d}{dt}O_{L,r,i} = (1-\varepsilon_r)A_r v_{L,r} O_{L,r,i-1} - (1-\varepsilon_r)A_r v_{L,r} O_{L,r,i} + (1-\varepsilon_r)K_L a V_r (O^*_{G,r,i} - O_{L,r,i}) \quad (3.3.2.40)$$

Dividing Eq. 3.3.2.40 with $(1-\varepsilon_r)V_r$ gives:

$$\frac{d}{dt}O_{L,r,i} = \frac{A_r v_{L,r}(O_{L,r,i-1} - O_{L,r,i})}{V_r} + K_L a(O^*_{G,r,i} - O_{L,r,i}) \quad (3.3.2.41)$$

Gas phase in the gas separator

$$\varepsilon_{top} V_{top} \frac{d}{dt}O_{G,top} = \varepsilon_r A_r v_{G,r} O_{G,r,N} - \varepsilon_{top} A_{top} v_{G,top} O_{G,top} - \varepsilon_{top} A_{top} v_{G,out} O_{G,top}$$

Dividing Eq. 3.3.2.42 with $\varepsilon_{top} V_{top}$ gives:

$$\frac{d}{dt}O_{G,top} = \frac{\varepsilon_r A_r v_{G,r} O_{G,r,N}}{V_{top}\varepsilon_{top}} - \frac{(A_{top} v_{G,top} O_{G,top} + A_{top} v_{G,out} O_{G,top})}{V_{top}} - \frac{(1-\varepsilon_{top})K_L a(O^*_{G,top} - O_{L,top})}{\varepsilon_{top}} \quad (3.3.2.43)$$

Liquid phase in the gas separator

$$(1-\varepsilon_{top})V_{top} \frac{d}{dt}O_{L,top} = (1-\varepsilon_r)A_r v_{L,r} O_{L,r,N} - (1-\varepsilon_{top})A_{top} v_{L,top} O_{L,top} - (1-\varepsilon_{top})A_{top} v_{L,out} O_{L,top} + (1-\varepsilon_{top})K_L a V_{top}(O^*_{G,top} - O_{L,top}) \quad (3.3.2.44)$$

Dividing Eq. 3.3.2.44 with $(1-\varepsilon_{top})V_{top}$ gives:

$$\frac{d}{dt}O_{L,top}=\frac{(1-\varepsilon_r)A_r v_{L,r}O_{L,r,i}}{(1-\varepsilon_{top})V_{top}}-\frac{(A_{top}v_{L,top}O_{L,top}+A_{top}v_{L,out}O_{L,top})}{V_{top}}+K_L a(O^*_{G,top}-O_{L,top})$$

(3.3.2.45)

Gas phase in the downcomer

At the first CSTR(i=1):

$$\varepsilon_d V_d\frac{d}{dt}O_{G,d,1}=\varepsilon_{top}A_{top}v_{G,top}O_{G,top}-\varepsilon_d A_d v_{G,d}O_{G,d,1}-(1-\varepsilon_d)K_L aV_d(O^*_{G,d,1}-O_{L,d,1})$$

(3.3

Dividing Eq. 3.3.2.46 with $\varepsilon_d V_d$ gives:

$$\frac{d}{dt}O_{G,d,1}=\frac{\varepsilon_{top}A_{top}v_{G,top}O_{G,top}-\varepsilon_d A_d v_{G,d}O_{G,d,1}}{\varepsilon_d V_d}-\frac{(1-\varepsilon_d)K_L a(O^*_{G,d,1}-O_{L,d,1})}{\varepsilon_d}$$

(3.3.2.47)

At 2<i<M:

$$\varepsilon_d V_d\frac{d}{dt}O_{G,d,i}=\varepsilon_d A_d v_{G,d}O_{G,d,i-1}-\varepsilon_d A_d v_{G,d}O_{G,d,i}-(1-\varepsilon_d)K_L aV_d(O^*_{G,d,i}-O_{L,d,i})$$

Dividing Eq. 3.3.2.48 with $\varepsilon_d V_d$ gives:

$$\frac{d}{dt}O_{G,d,i}=\frac{\varepsilon_d A_d v_{G,d}(O_{G,d,i-1}-O_{G,d,i})}{V_d}-\frac{(1-\varepsilon_d)K_L a(O^*_{G,d,i}-O_{L,d,i})}{\varepsilon_d}$$

(3.3.2.49)

Liquid phase in the downcomer

At the first CSTR(i=1):

$$(1-\varepsilon_d)V_d\frac{d}{dt}O_{L,d,1}=(1-\varepsilon_{top})A_{top}v_{L,top}O_{L,top}-(1-\varepsilon_d)A_d v_{L,d}O_{L,d,1}$$
$$+(1-\varepsilon_d)K_L aV_d(O^*_{G,d,1}-O_{L,d,1})$$

(3.3.2.50)

Dividing Eq. 3.3.2.50 with $(1-\varepsilon_d)V_d$ gives:

$$\frac{d}{dt}O_{L,d,1}=\frac{(1-\varepsilon_{top})A_{top}v_{L,top}O_{L,top}-(1-\varepsilon_d)A_d v_{L,d}O_{L,d,1}}{(1-\varepsilon_d)V_d}+K_L a(O^*_{G,d,1}-O_{L,d,1})$$

At 2<i<N:

$$(1-\varepsilon_d)V_d \frac{d}{dt}O_{L,d,i} = (1-\varepsilon_d)A_d v_{L,d} O_{L,d,i-1} - (1-\varepsilon_d)A_d v_{L,d} O_{L,d,i}$$

$$+ (1-\varepsilon_d)K_L a V_d (O^*_{G,d,i} - O_{L,d,i}) \qquad (3.3.2.52)$$

Dividing Eq. 3.3.2.52 with $(1-\varepsilon_d)V_d$ gives: $\frac{d}{dt}O_{L,d,i} = \frac{A_d v_{L,d}(O_{L,d,i-1} - O_{L,d,i})}{V_d} + K_L a(O^*_{G,d}$

3.3.3 The Dispersion Model

In this model, the plug flow with axial dispersion is used to describe the mixing mode of fluid in riser and downcomer of the contactor. The gas separator is still described by the CSTR model as the condition in this section cannot be resembled by the PFR mode. The development for the CSTR model for the gas separator is the same as the detail given in Section 3.3.1. Hence, for the sake of brevity, the development of this model will not be repeated here, and only the derivation of Dispersion models will be detailed.

The volume element used to develop the Dispersion model is shown in Figure 3.4. The unsteady state model is formulated around the volume element in a step by step method as follows:

Riser

1. The accumulation of oxygen in each volume element in the riser:

   Accumulation of oxygen in the gas phase at any *z* along the

$$\text{column height} = \varepsilon_r A_r \Delta z \frac{\partial}{\partial t} O_{G,r}(z) \qquad (3.3.3.1)$$

   Accumulation of oxygen in the liquid phase at any *z* along the

$$\text{column height} = (1-\varepsilon_r) A_r \Delta z \frac{\partial}{\partial t} O_{L,r}(z) \qquad (3.3.3.2)$$

2. Input to each volume element in the riser.

   in gas phase:

   1.O_2 diffused into the volume element at any *z (z>0)*

$$= -\varepsilon_r A_r D_{G,r} \frac{\partial}{\partial z} O_{G,r}\Big|_z \qquad (3.3.3.3)$$

   2.O_2 into the volume element at any *z (z>0)* with gas flow

$$= \varepsilon_r A_r v_{G,r} O_{G,r}\Big|_z \qquad (3.3.3.4)$$

   in liquid phase:

   1.O_2 dispersed into the volume element at any *z (z>0)*

$$= -(1-\varepsilon_r) A_r D_{L,r} \frac{\partial}{\partial z} O_{L,r}\Big|_z \qquad (3.3.3.5)$$

   2.O_2 into the volume element at any *z (z>0)* with liquid flow

$$= (1-\varepsilon_r) A_r v_{L,r} O_{L,r}\Big|_z \qquad (3.3.3.6)$$

   3.O_2 transferred from the gas bubbles into the liquid at any *z (z>0)*

$$= (1-\varepsilon_r) K_L a A_r \Delta z (O^*_{G,r}(z) - O_{L,r}(z)) \qquad (3.3.3.7)$$

   Note: O_2 into the volume element with feed flow rate ($Q_{L,F}O_{L,F}$) = 0

   because O_2 in the liquid feed is very dilute.

3. Output from each volume element in the riser

in gas phase:

1.O_2 dispersed out from the volume element at any *z (z>0)*

$$-\varepsilon_r A_r D_{G,r} \frac{\partial}{\partial z} O_{G,r}\Big|_{z+\Delta z} \qquad (3.3.3.8)$$

2. O_2 out from the volume element at any *z (z>0)* with gas flow

$$= \varepsilon_r A_r v_{G,r} O_{G,r}\Big|_{z+\Delta z} \qquad (3.3.3.9)$$

3. O_2 out from the volume element with mass transfer

$$= (1-\varepsilon_r) K_L a A_r \Delta z (O^*_{G,r}(z) - O_{L,r}(z)) \qquad (3.3.3.10)$$

in liquid phase:

1. O_2 dispersed out from the volume element at any *z (z>0)*

$$= -(1-\varepsilon_r) A_r D_{L,r} \frac{\partial}{\partial z} O_{L,r}\Big|_{z+\Delta z} \qquad (3.3.3.11)$$

2. O_2 out from the volume element at any *z (z>0)* with liquid flow

$$= (1-\varepsilon_r) A_r v_{L,r} O_{L,r}\Big|_{z} \qquad (3.3.3.12)$$

Downcomer

1. The accumulation of oxygen in each volume element in the downcomer:

Accumulation of oxygen in the gas phase at any *z* along the

$$\text{column height} = \varepsilon_d A_d \frac{\partial}{\partial t} O_{G,d}(z) \qquad (3.3.3.13)$$

Accumulation of oxygen in the liquid phase at any *z* along the

$$\text{column height} = (1-\varepsilon_d) A_d \frac{\partial}{\partial t} O_{L,d}(z) \qquad (3.3.3.14)$$

2. Input to each volume element in the downcomer:

in gas phase:

1. O_2 diffused into the volume element at any *z (z>0)*

$$= -\varepsilon_d A_d D_{G,d} \frac{\partial}{\partial z} O_{G,d}\Big|_z \qquad (3.3.3.15)$$

2. O_2 into the volume element at any *z (z>0)* with gas flow

$$= \varepsilon_d A_d v_{G,d} O_{G,d}\Big|_z \qquad (3.3.3.16)$$

in liquid phase:

1. O_2 diffused into the volume element at any *z (z>0)*

$$-(1-\varepsilon_d) A_d D_{L,d} \frac{\partial}{\partial z} O_{L,d}\Big|_z \qquad (3.3.3.17)$$

2. O_2 into the volume element at any *z (z>0)* with liquid flow

$$= (1-\varepsilon_d) A_d v_{G,d} O_{L,d}\Big|_z \qquad (3.3.3.18)$$

3. O_2 into the volume element with mass transfer

$$= (1-\varepsilon_d) K_L a A_d \Delta z (O^*_{G,d}(z) - O_{L,d}(z)) \qquad (3.3.3.19)$$

3. Output from each volume element in the downcomer

in gas phase:

1. O_2 diffused out from the volume element at any *z (z>0)*

$$= -\varepsilon_d A_d D_{G,d} \frac{\partial}{\partial z} O_{G,d}\Big|_{z+\Delta z} \qquad (3.3.3.20)$$

2. O_2 out from the volume element at any *z (z>0)* with gas flow

$$= \varepsilon_d A_d v_{G,d} O_{G,d}\Big|_{z+\Delta z} \qquad (3.3.3.21)$$

3. O_2 out from the volume element at any *z (z>0)* with mass transfer

$$= (1-\varepsilon_d) K_L a A_d \Delta z (O^*_{G,d}(z) - O_{L,d}(z)) \qquad (3.3.3.22)$$

in liquid phase:

1. O_2 diffused out from the volume element at any *z (z>0)*

$$= -(1-\varepsilon_d)A_d D_{L,d}\frac{\partial}{\partial z}O_{L,d}\Big|_{z+\Delta z} \quad (3.3.3.23)$$

2. O_2 out from the volume element at any *z (z>0)* with liquid flow

$$= (1-\varepsilon_d)A_d v_{L,d} O_{L,d}\Big|_{z+\Delta z} \quad (3.3.3.24)$$

The mass balance equation for O_2 in the contactor becomes:

Gas phase in the riser.

At 0<z<*L*:

$$\varepsilon_r A_r \Delta z \frac{\partial}{\partial t}O_{G,r}(z) = (\varepsilon_r A_r D_{G,r}\frac{\partial}{\partial z}O_{G,r}\Big|_{z+\Delta z} - \varepsilon_r A_r D_{G,r}\frac{\partial}{\partial z}O_{G,r}\Big|_z)$$

$$-(\varepsilon_r A_r v_{G,r} O_{G,r}\Big|_{z+\Delta z} + \varepsilon_r A_r v_{G,r} O_{G,r}\Big|_z) - (1-\varepsilon_r)K_L a A_r \Delta z (O^*_{G,r}(z) - O_{L,r}(z)) \quad (3.3.3.25)$$

Dividing Eq. 3.3.3.25 with $\varepsilon_r A_r \Delta z$ and take limit $\Delta z \to 0$ gives:

$$\frac{\partial}{\partial t}O_{G,r}(z) = -v_{G,r}\frac{\partial}{\partial z}O_{G,r}(z) + D_{G,r}\frac{\partial^2}{\partial z^2}O_{G,r}(z) - \frac{(1-\varepsilon_r)K_L a}{\varepsilon_r}(O^*_{G,r}(z) - O_{L,r}(z)) \quad (3.3.3.26)$$

where

$$O_G = \frac{PY_{O_2}}{RT} \quad (3.3.3.27)$$

According to Henry's law, the partial pressure of oxygen in the gas phase at equilibrium is proportional to the concentration of oxygen in the liquid film.

$$O^*_G = \frac{P_{O_2}}{H} = \frac{O_G RT}{H} \quad (3.3.3.28)$$

Liquid phase in the riser

At 0<z<*L*:

$$(1-\varepsilon_r)A_r \Delta z \frac{\partial}{\partial t}O_{L,r}(z) = ((1-\varepsilon_r)A_r D_{L,r}\frac{\partial}{\partial z}O_{L,d}\Big|_{z+\Delta z} - (1-\varepsilon_r)A_r D_{L,r}\frac{\partial}{\partial z}O_{L,r}\Big|_z)$$

$$-((1-\varepsilon_r)A_r v_{L,r} O_{L,r}\big|_{z+\Delta z} - (1-\varepsilon_r)A_r v_{L,r} O_{L,r}\big|_z) + (1-\varepsilon_r)K_L a A_r \Delta z (O^*_{G,r}(z) - O_{L,r}(z))$$

(3.3.3.29)

Dividing Eq. 3.3.3.29 with $(1-\varepsilon_r)A_r \Delta z$ and take limit $\Delta z \to 0$ gives:

$$\frac{\partial}{\partial t} O_{L,r}(z) = -v_{L,r} \frac{\partial}{\partial z} O_{L,r}(z) + D_{L,r} \frac{\partial^2}{\partial z^2} O_{L,r}(z) + K_L a (O^*_{G,r}(z) - O_{L,r}(z)) \qquad (3.3.3.30)$$

Gas phase in the gas separator.

$$V_{top}\varepsilon_{top}\frac{d}{dt}O_{G,top} = \varepsilon_r A_r v_{G,r} O_{G,r} - \varepsilon_{top} A_{top} v_{G,top} O_{G,top} - \varepsilon_{top} A_{top} v_{G,out} O_{G,top}$$
$$+ (1-\varepsilon_{top}) K_L a V_{top} (O^*_{G,top} - O_{L,top}) \qquad (3.3.3.31)$$

Dividing Eq. 3.3.3.31 with $\varepsilon_{top} V_{top}$ gives:

$$\frac{d}{dt}O_{G,top} = \frac{\varepsilon_r A_r v_{G,r} O_{G,r} - \varepsilon_r A_{top} v_{G,top} O_{G,top} - \varepsilon_{top} A_{top} v_{G,out} O_{G,top}}{\varepsilon_{top} V_{top}}$$
$$- \frac{(1-\varepsilon_{top}) K_L a (O^*_{G,top} - O_{L,top})}{\varepsilon_{top}} \qquad (3.3.3.32)$$

Liquid phase in the gas separator

$$(1-\varepsilon_{top})V_{top}\frac{d}{dt}O_{L,top} = (1-\varepsilon_r)A_r v_{L,r} O_{L,r} - (1-\varepsilon_{top})A_{top} v_{L,top} O_{L,top}$$
$$- (1-\varepsilon_{top})A_{top} v_{L,out} O_{L,top} + (1-\varepsilon_{top}) K_L a V_{top} (O^*_{G,top} - O_{L,top}) \qquad (3.3.3.33)$$

Dividing Eq. 3.3.3.33 with $(1-\varepsilon_{top})V_{top}$ gives:

$$\frac{d}{dt}O_{L,top} = \frac{(1-\varepsilon_r)A_r v_{L,r} O_{L,r} - (1-\varepsilon_{top})A_{top} v_{L,top} O_{L,top} - (1-\varepsilon_{top})A_{top} v_{L,out} O_{L,top}}{(1-\varepsilon_{top})V_{top}} + K_L a (O^*_{G,top} - O_{L,t}$$

Gas phase in the downcomer

$$\varepsilon_d A_d \Delta z \frac{\partial}{\partial t} O_{G,d}(z) = (\varepsilon_d A_d D_{G,d} \frac{\partial}{\partial z} O_{G,d}\Big|_{z+\Delta z} - \varepsilon_d A_d D_{G,d} \frac{\partial}{\partial z} O_{G,d}\Big|_z)$$

$$-(\varepsilon_d A_d v_{G,d} O_{G,d}\big|_{z+\Delta z} - \varepsilon_d A_d v_{G,d} O_{G,d}\big|_z) - (1-\varepsilon_d) K_L a A_d \Delta z (O^*_{G,d}(z) - O_{L,d}(z)) \quad (3.3.3.35)$$

Dividing Eq. 3.3.3.35 with $\varepsilon_d A_d \Delta z$ gives:

$$\frac{\partial}{\partial t} O_{G,d}(z) = -v_{G,d} \frac{\partial}{\partial z} O_{G,d}(z) + D_{G,d} \frac{\partial^2}{\partial z^2} O_{G,d}(z) - \frac{(1-\varepsilon_d) K_L a (O^*_{G,d}(z) - O_{L,d(z)})}{\varepsilon_d} \quad (3.3.3.36)$$

Liquid phase in the downcomer

$$(1-\varepsilon_d) A_d \Delta z \frac{\partial}{\partial t} O_{L,d}(z) = ((1-\varepsilon_d) A_d D_{L,d} \frac{\partial}{\partial z} O_{L,d}\Big|_{z+\Delta z} - (1-\varepsilon_d) A_d D_{L,d} \frac{\partial}{\partial z} O_{L,d}\Big|_z)$$

$$-((1-\varepsilon_d) A_d v_{G,d} O_{L,d}\big|_{z+\Delta z} - (1-\varepsilon_d) A_d v_{G,d} O_{L,d}\big|_z) + (1-\varepsilon_d) K_L a A_d \Delta z (O^*_{G,d}(z) - O_{L,d}(z)) \quad (3.3.3.37)$$

Dividing Eq. 3.3.3.37 with $(1-\varepsilon_d) A_d \Delta z$ gives:

$$\frac{\partial}{\partial t} O_{L,d}(z) = -v_{L,d} \frac{\partial}{\partial z} O_{L,d}(z) + D_{L,d} \frac{\partial^2}{\partial z^2} O_{L,d}(z) + K_L a (O^*_{G,d}(z) - O_{L,d}(z)) \quad (3.3.3.38)$$

สถาบันวิทยบริการ
จุฬาลงกรณ์มหาวิทยาลัย

The initial and boundary conditions for Eqs. 3.3.3.25 to 3.3.3.38 are therefore.

Riser

In the gas phase

At $t = 0$, and $0 \le z \le L$: (Initial condition)

$$O_{G,r}(z) = 0 \tag{3.3.3.39}$$

At $t > 0$, and $z = 0$: (Boundary condition #1)

$$O_{G,r}\big|_{Z=0} = \frac{(v_{G,d} A_d O_{G,d} + Q_{G,in} O_{G,in})}{v_{G,d} A_d + Q_{G,in}} \tag{3.3.3.40}$$

At $t > 0$, and $z = L$: (Boundary condition #2)

$$O_{G,r}\big|_{Z=L} = O_{G,top} \tag{3.3.3.41}$$

In the liquid phase

At $t = 0$, and $0 \le z \le L$: (Initial condition)

$$O_{L,r}(z) = 0 \tag{3.3.3.42}$$

At $t = 0$, and $z = 0$: (Boundary condition #1)

$$O_{L,r}\big|_{Z=0} = \frac{(v_{L,d} A_d O_{L,d} + Q_{L,F} O_{L,F})}{v_{L,d} A_d + Q_{L,F}} \tag{3.3.3.43}$$

At $t > 0$, and $z = L$: (Boundary condition #2)

$$O_{L,r}\big|_{Z=L} = O_{L,top} \tag{3.3.3.44}$$

สถาบันวิทยบริการ
จุฬาลงกรณ์มหาวิทยาลัย

Gas seperator

In the gas phase

At $t = 0$: (Initial condition)

$$O_{G,top} = 0 \qquad (3.3.3.45)$$

In the liquid phase

At $t = 0$: (Initial condition)

$$O_{L,top}(z) = 0 \qquad (3.3.3.46)$$

Downcomer

In the gas phase

At $t = 0$, and $0 \le z \le L$: (Initial condition)

$$O_{G,d}(z) = 0 \qquad (3.3.3.47)$$

At $t > 0$, and $z = 0$: (Boundary condition #1)

$$O_{G,d}\big|_{Z=0} = O_{G,top} \qquad (3.3.3.48)$$

At $t > 0$, and z = L : (Boundary condition #2)

$$O_{G,d}\big|_{Z=L} = O_{G,d}\big|_{Z=L-\Delta L} \qquad (3.3.3.49)$$

In the liquid phase

At $t = 0$, and $0 \le z \le L$: (Initial condition)

$$O_{L,d}(z) = 0 \qquad (3.3.3.50)$$

At $t > 0$, and $z = 0$: (Boundary condition #1)

$$O_{L,d}\big|_{Z=0} = O_{L,top} \qquad (3.3.3.51)$$

At $t > 0$, and $z = L$: (Boundary condition #2)

$$O_{L,d}\big|_{Z=L} = O_{L,d}\big|_{Z=L-\Delta L} \qquad (3.3.3.52)$$

The development of dynamic models for airlift contactors (ALCs) employed in this work is based mostly on the assumption described above. The mass transfer performance of the ALC depends on several design and operating factors including the gas through-put, liquid phase oxygen concentration (in riser), and contactor geometry particularly the ratio between the downcomer and riser cross sectional areas. We shall be investigating the effects of these factors in the next chapter.

สถาบันวิทยบริการ
จุฬาลงกรณ์มหาวิทยาลัย

Table 3.1 Experimental conditions and the dimensions of the experimental apparatus.

Gas and liquid phases	Air and tap water
Contactor height	1.20 m
Unaerated liquid height	1.08 m
Inner diameter of column	0.1375 m
A_d/A_r [-]	1
Top clearance over split plate	0.03 m
Inlet superficial gas velocity	0.00367-0.0381 $m \cdot s^{-1}$
Liquid feed flow rate	$(6.853\text{-}10.769)x10^{-6}$ $m \cdot s^{-3}$

สถาบันวิทยบริการ
จุฬาลงกรณ์มหาวิทยาลัย

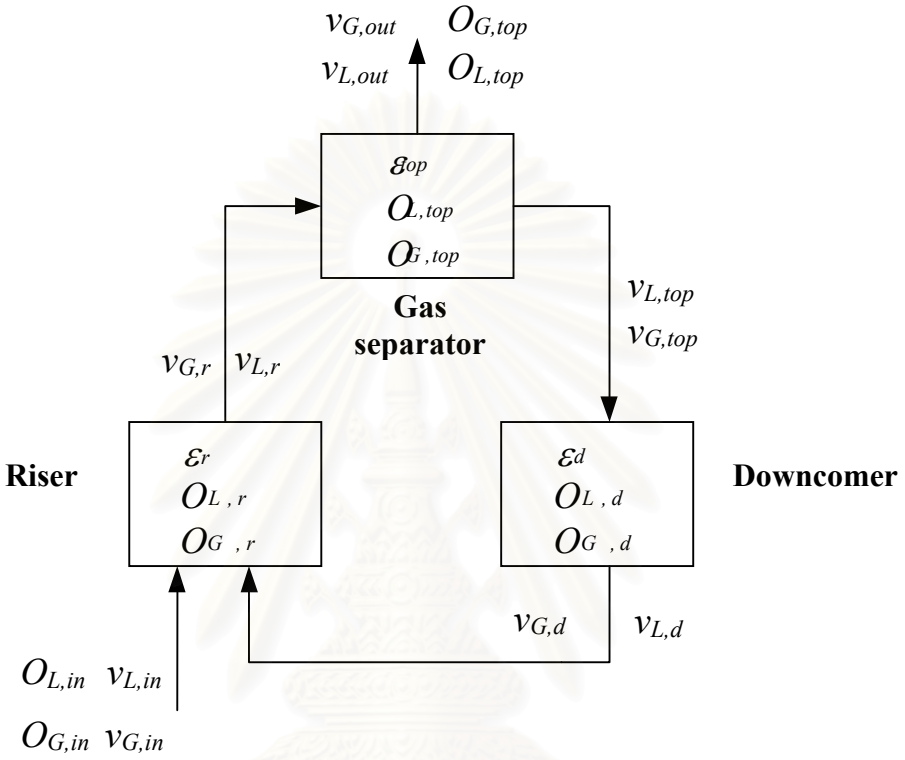

Figure 3.1. Block diagram of CSTR model

สถาบันวิทยบริการ
จุฬาลงกรณ์มหาวิทยาลัย

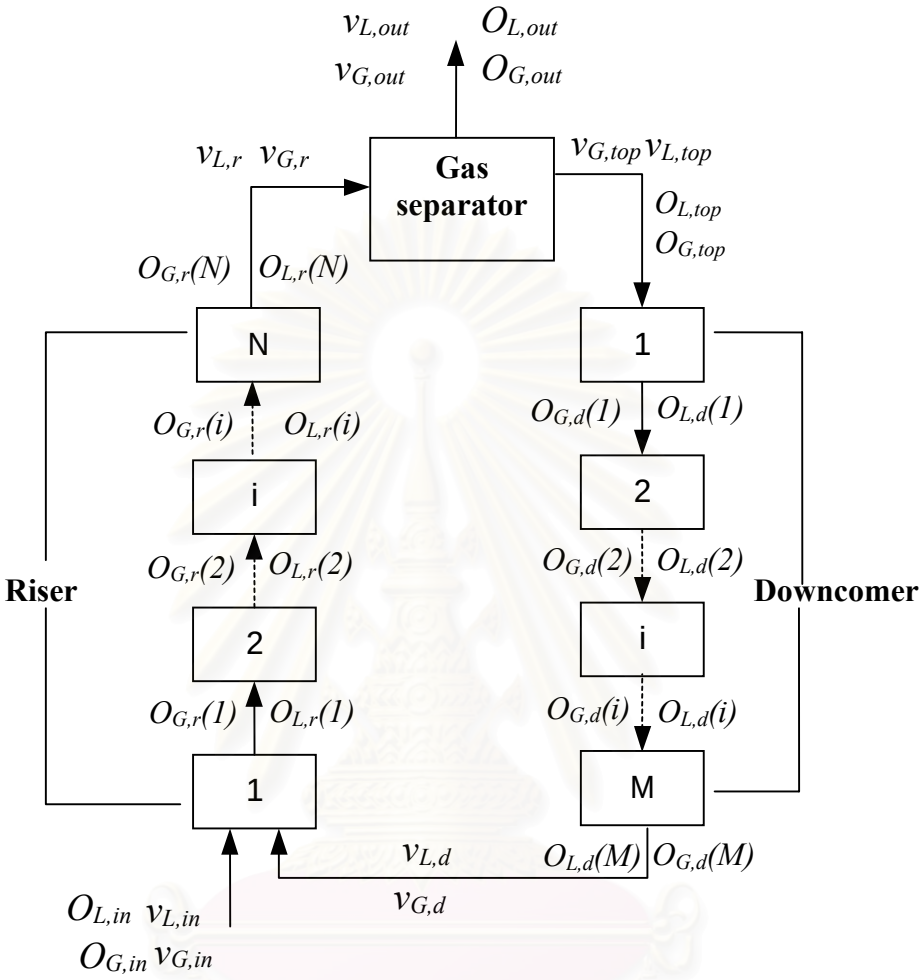

Figure 3.2. Block diagram of CSTRs-in-Series model

สถาบันวิทยบริการ
จุฬาลงกรณ์มหาวิทยาลัย

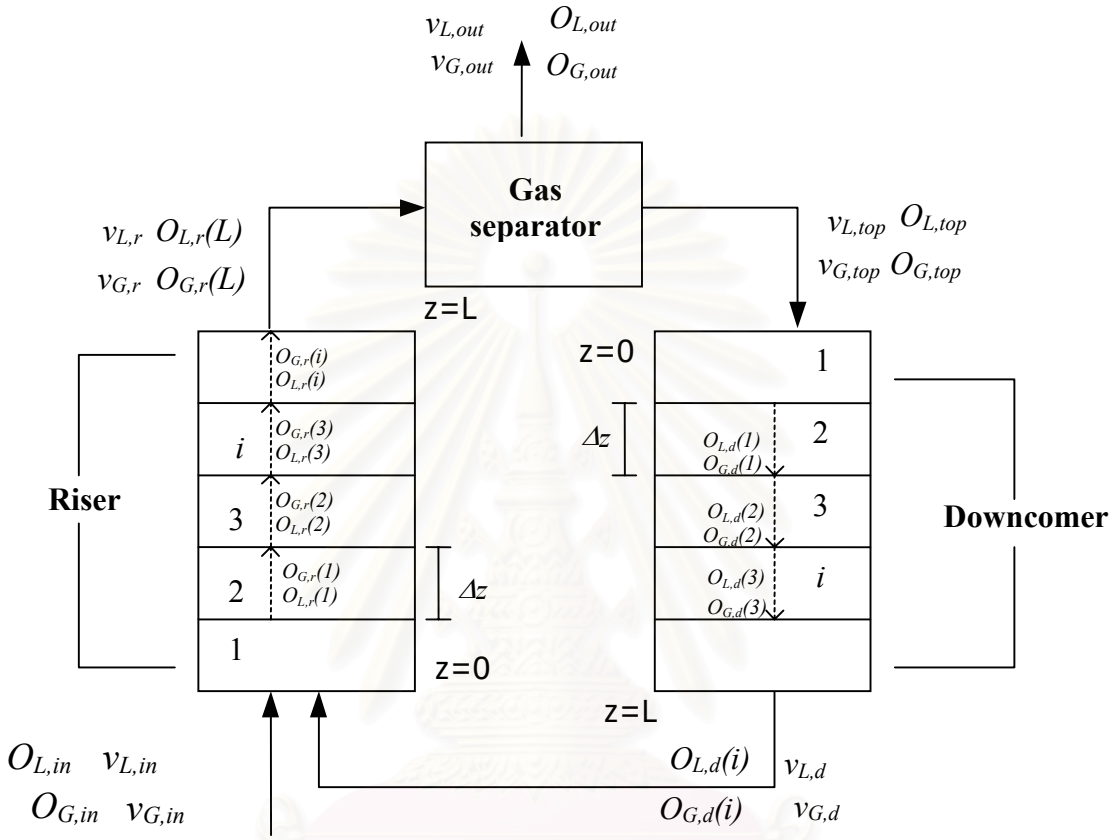

Figure 3.3. Block diagram of Dispersion model

สถาบันวิทยบริการ
จุฬาลงกรณ์มหาวิทยาลัย

CHAPTER 4

Results and discussion

4.1 Normalization of Model Equations

In actual programming stage, it is usually convenient to normalize the continuity equations (Equations 3.3.1.29 to 3.3.3.38). This normally facilitates the solution procedure, particularly in a "stiff" system when a large difference between variables or parameters exists. To normalize the set of equations derived in Chapter 3, the following dimensionless quantities are introduced:

$$\overline{O}_{L,r}(z) = \frac{O_{L,r}(z)}{O_{g,in}} \qquad (4.1.1)$$

$$\overline{O}_{G,r}(z) = \frac{O_{G,r}(z)}{HO_{g,in}} \quad ; \quad O_G^* = \frac{O_G}{H} \qquad (4.1.2)$$

$$\tau = \frac{A_d v_{l,d} t}{V_r} \qquad (4.1.3)$$

$$Z = \frac{z}{L} \qquad (4.1.4)$$

where $O_{g,in}$ = the concentration of oxygen in inlet air [g ▪ l^{-1}]

H = Henry's law constant [l ▪ atm/mg O_2]

L = liquid height in riser and downcomer [m]

For the sake of brevity, the derivation of all dimensionless equations will not be illustrated here, but only equations describing oxygen concentrations in riser (both in gas and liquid phases in the Dispersion model) are detailed as follows.

Substituting the dimensionless quantities in Equations 4.1.1 - 4.1.4 into Equation 3.3.3.26 gives:

$$\frac{\partial}{\partial \tau}\overline{O}_{G,r}(Z) = -v_{G,r}\left[\frac{V_r}{A_d v_{L,d} L}\right]\frac{\partial}{\partial Z}\overline{O}_{G,r}(Z) + D_{G,r}\left[\frac{V_r}{A_d v_{L,d} L^2}\right]\frac{\partial^2}{\partial Z^2}\overline{O}_{G,r}(Z)$$
$$-\frac{(1-\varepsilon_r)}{\varepsilon_r}\left[\frac{V_r}{A_d v_{L,d}}\right]K_L a(\overline{O}_{G,r}(Z) - \overline{O}_{L,r}(Z)) \qquad (4.1.5)$$

Similarly Equation 3.3.3.30 can be converted to:

$$\frac{\partial}{\partial \tau}\overline{O}_{L,r}(Z) = -v_{L,r}\left[\frac{V_r}{A_d v_{L,d} L}\right]\frac{\partial}{\partial Z}\overline{O}_{L,r}(Z) + D_{L,r}\left[\frac{V_r}{A_d v_{L,d} L^2}\right]\frac{\partial^2}{\partial Z^2}\overline{O}_{L,r}(Z)$$
$$+\left[\frac{V_r}{A_d v_{L,d}}\right]K_L a(\overline{O}_{G,r}(Z) - \overline{O}_{L,r}(Z)) \qquad (4.1.6)$$

4.2 Numerical Testing for Appropriateness of the Mathematical Models for Oxygen Mass Transfer in the ALC

4.2.1 Testing by various numerical techniques

The resulting dimensionless equations are linear and solvable by finite difference techniques using the Crank-Nicholson or Forward finite difference criteria, and also the 4th order Runge-Kutta integration method. In the partial differential equation such as PFR model, the space dimension is discretised following the Crank-Nicholson criteria (Kreyszig, 1999). The discretisation both in time and space dimensions ends up with a set of linear algebraic equations which can be solved directly using built-in functions in MATLAB (version 5.3.1).

For the integration method, only the space dimension is discretised by the central finite difference which results in a set of ordinary differential equations that is readily solved using the 4th order Runge-Kutta integrating technique (Kreyszig, 1999).

Intuitively, the testing of numerical solutions of any set of differential equations can be achieved by comparing simulation solutions from various numerical techniques. In this work, this step is accomplished by comparing the simulation results from the Crank Nicholson criteria with those from the 4^{th}-order Runge-Kutta method; results shown in Figure 4.2.1 (simulated from the CSTR model). This comparison indicates good agreement between the prediction of an oxygen concentration profile of liquid phase in the riser of the ALC from the two methods. Note that the predictions of other variables such as gas phase oxygen concentrations in all other sections of the ALC are found to be the same for both numerical methods but the results are not shown for a brevity purpose. It appears that the choice of discretisation does not significantly affect the numerical solutions, and it may be reasonable to conclude that the simulation results from these models are correct.

It is worthwhile to note that varying step size for the time dimension is critical for the accuracy of numerical solutions. In the CSTR model, the optimal step size for all numerical techniques is found to be 0.01 (dimensionless), whilst 0.1 is found to be suitable for the Dispersion model ($\Delta z = 0.07$).

4.2.2 Testing with various modeling techniques

To also prove that the simulation results are correct, it is recommended that simulation results from various modeling techniques are compared. In this case, the solutions from the CSTRs-in-Series model are compared with those from the PFR model. It is known that the solution from the CSTRs-in-Series model will approach that of the PFR when there is an adequate number of tanks in the series. Hence, a simple calculation is carried out such that the number of tanks in the CSTRs-in-Series model can be altered. The simulation results on liquid phase oxygen concentration in the riser from the CSTRs-in-Series model with 5 and 15 tanks in series are plotted together with the results from the PFR model in Figure 4.2.2. The results clearly emphasis the fidelity of the developed models as all of the solutions from the CSTRs-in-Series model lie between those from the CSTR and PFR models. It is interesting, though, to note that the results from the CSTRs-in-Series model become very close to the PFR model even though the number of tanks is as small as five (see Figure 4.2.2).

And when the number of tank reaches fifteen, the solutions from the CSTRs-in-Series model are extremely close to those from the PFR. Hence, it is concluded here that the simulation results are justifiable.

Figure 4.2.2 also displays simulation results from other modeling techniques such as the CSTR and Dispersion models. It is found that the CSTR model predicts the slowest response of the oxygen concentration in the ALC system, whilst the fastest response being that from the Dispersion model. All modeling techniques provide similar response for the liquid phase oxygen concentration, and this response can be divided into two regimes. The first regime is when the oxygen concentration increases rapidly with time indicating a high mass transfer rate between gas and liquid. The second regime following the first regime illustrates a much slower mass transfer rate, and as time approaches infinity, the oxygen concentration reaches the maximum value which is equal to the equilibrium concentration between oxygen in water and in the air. It might be worthwhile to emphasis here that all of the experiment and the simulation starts with the initial condition that there is no dissolved oxygen concentration in the liquid phase, i.e. initial oxygen concentration in water equals zero. When air is sparged into the ALC, oxygen in the air begins to transfer into the liquid phase (water) at the rate equal to the product between the mass transfer coefficient and the driving force of concentration difference between that in water and in the air. The high rate of mass transfer is obtained in the first regime because there is a maximum level of driving force which facilitates in the movement of oxygen from the gas to liquid phases. As time passes, the oxygen concentration in the liquid becomes higher which reduces the driving force for the gas-liquid mass transfer. Hence a slower mass transfer rate is resulted as that observed in the second regime. The dissolved oxygen concentration in the liquid phase finally reaches its equilibrium value when the driving force becomes zero: at this point the net rate of gas-liquid oxygen mass transfer is equal to zero.

4.3 Experimental Confirmation of the Appropriateness of the Mathematical Models for Oxygen Mass Transfer in the ALC

The experimental confirmation of the appropriateness of the mathematical models involves the following tasks:

- The determination of dispersion coefficient of oxygen in the liquid phase using the information on the residence time distribution
- The comparison between simulation results and reported experimental data.

However, there is still an unknown parameter that needs to be estimated in order to solve the mathematical model for the prediction of oxygen concentrations in the ALC, and this is the dispersion coefficient of oxygen in the gas phase. In addition, there is a large deviation in the experimental reported K_La (overall volumetric mass transfer coefficient), and therefore this work treats this parameter as an uncertainty that needs to be re-evaluated by compromising between the simulation and experimental results. In the following discussion, the gas phase dispersion coefficient will be obtained by fitting simulation results to experimental data whereby the K_La will be adjusted within $\pm$50% of the reported value. Note that the experimental data including K_La employed in this investigation are obtained from the work in the same laboratory but still are unpublished elsewhere. (Wongsuchoto and Pavasant, 2000, and Krichnavaruk and Pavasant, 2000) The conditions used in the simulation are exactly identical to those in actual experiments (except the K_La and the gas phase dispersion that remain to be investigated), and these are summarized in Table 4.1. The references in the first column of this table (Cases I to VI) will be used throughout the following discussions.

4.3.1 Estimation of dispersion coefficient of oxygen in the liquid phase in the riser and downcomer of the ALC

The residence time distribution of oxygen in the liquid phase (RTD) can be used to estimate the value of dispersion coefficient in the liquid phase. Results from the RTD experiment (Figure 4.3.1A and 4.3.1B) in the continuous flow ALC reveal that the dispersion coefficient in the riser is higher than that in the downcomer. Figure 4.3.1A is the impulse response curve for the acid tracer which shows that the

residence time in the riser is 83.62 s with the variance of 8421.13 s^2. And according to Equation (3.2.4):

$$\frac{\sigma^2}{t_s^2} = 2\frac{D}{uL} + 8\left[\frac{D}{uL}\right]^2$$

The dispersion coefficient of oxygen in the liquid phase in the riser ($D_{L,r}$) of the ALC is therefore estimated to be 0.05 m^2 s^{-1}. The same experiment was performed to determine the oxygen dispersion coefficient in the downcomer and the results in Figure 4.3.1B show that this coefficient is approximately 0.03 m^2 s^{-1}. This means that the dispersion in the riser of the ALC is almost twice as much as that in the downcomer.

Since the dispersion coefficient in the non-continuous flow (batchwise operation) cannot be easily estimated, this work employs the dispersion coefficients obtained from this experiment in the discussion hereafter.

4.3.2. Effects of operating parameters on the modeling results

In Section 4.3.1, it was indicated that there still existed uncertainties in the values of parameters employed in the model. These parameters are the overall volumetric mass transfer coefficient (K_La) and the gas phase dispersion coefficient (for both riser and downcomer sections). Note that the latter parameter is only used in the Dispersion model. In this section, the influence of these two parameters will be investigated and the oxygen concentration in these section are liquid phase oxygen concentration in the riser.

Effect of the uncertainty in the value of overall volumetric mass transfer coefficient (K_La)

In order to study the effect of overall volumetric mass transfer coefficient, the simulation is performed with the values of K_La ranging from 50% to 150% of the experimental reported value. The results from the CSTR, PFR, and Dispersion models

are shown in Figures 4.3.2A, 4.3.2B, and 4.3.2C, respectively. (All simulations employed the Case III conditions as stated in Table 4.1.)

Theoretically, increasing K_La should result in a more rapid rate of mass transfer from gas bubble to liquid because the overall rate of gas-liquid mass transfer is simply the product between the K_La and the oxygen concentration difference driving force between the two phases (O_G-O_L). Nevertheless, it would be useful to know how the ALC responds to the changes in K_La. The simulation results clearly indicated that the actual calculated rate of mass transfer depends significantly on K_La as increasing K_La results in a reasonably faster responding time for dissolved oxygen concentration to reach its equilibrium level (at about 7 ppm). For instance, increasing K_La from 0.00847 to 0.0185 s^{-1} causes the responding time to reduce from 220 to 110 seconds (at 80% saturation of equilibrium oxygen concentration). In other words, a small increase in K_La causes a notable increase in the rate of gas-liquid mass transfer.

Effect of gas phase dispersion coefficient of oxygen on simulation results from the Dispersion model.

The value of the gas phase dispersion coefficient is estimated from the reported experimental data which were found to be in the range of 1-5 $m^2.s^{-1}$ depending on scales and conditions in the ALC (Rüffer et al., 1994). Unfortunately, the availability of these data is insufficient and these reported values were for the systems with dimensions markedly different from the conditions employed in this work. However, as there were no other alternatives for the estimation of this gas phase dispersion coefficient, the reported value of K_La was used as an initial guess in the estimation procedure. The simulation is then run repeatedly with various K_La around this initial guess to investigate how much this value affects the performance of the system.

Figure 4.3.2D shows that a higher gas phase dispersion coefficient in the riser leads to a faster rate of gas-liquid mass transfer (faster time for liquid phase oxygen concentration to reach its equilibrium level). However, the influence of the gas phase dispersion coefficient in the riser does not seem to be as significant as that of K_La.

Figure 4.3.2D illustrates that increasing the dispersion coefficient from 0.1 to 3.0 $m^2.s^{-1}$ (30 times higher), the responding time for the system to reach 80% saturation concentration only decreases from 260 to 170 seconds. Moreover, the dispersion coefficient of 1 or 3 $m^2.s^{-1}$ does not seem to give meaningful difference in the responding time to reach equilibrium concentration.

The same simulating experiment was performed with varying the gas phase dispersion of oxygen in the downcomer section. Results indicated that there was almost no influence of this dispersion coefficient on the mass transfer rate in the ALC (with conditions of Case III). These results are considered not significant and therefore not shown here.

This section emphasizes one of most significant advantages of the mathematical model which is to investigate the effect of any single parameter in the system. In this case, the most sensitive parameter for the rate of oxygen mass transfer from gas to liquid is found to be the overall volumetric mass transfer coefficient. In the up-coming discussions on the comparative performance between the simulation and the actual experiment, the results from the model will be fitted to the experimental data by adjusting only the K_La and the gas phase dispersion coefficient for oxygen in the riser (and not that in the downcomer).

4.3.3 Predictions of gas phase oxygen concentration in the ALC

The gas phase oxygen concentration is one of the parameters difficult to measure in the actual experiment. This is because gas bubbles move at high speed (can be as high as 80 $cm.s^{-1}$ (Merchuk and Stein, 1981; Clark and Flemmer, 1985)) and the collection of gas samples at such speed is rather troublesome, or may require a highly complicated piece of equipment. The developed mathematical model provides a fruitful information on this parameter which facilitates further understanding in the oxygen mass transfer behavior in the ALC.

Figure 4.3.3 demonstrates the concentration profiles of oxygen in the gas phase at various sections in the ALC. These concentration profiles are obtained from

the Dispersion model where the riser and the downcomer are discretised using the Finite difference method according to the procedure described earlier. The number of discretisation points used in this simulation is equal to 15 both in riser and downcomer beyond which increasing the number of points does not have any effect on simulation results. The displayed oxygen concentration profiles in the riser and downcomer in Figures 4.3.3A and 4.3.3C are from three different positions, or in other words, three different discretisation points. The ‘position 1’ means the first discretisation point, and ‘position 15’ represents the last discretisation point, where ‘position 5’ is somewhere in between the two ends.

The simulation results reveal that the gas phase oxygen concentration in the ALC rises continuously after the inlet-air is switched on. It is noted that both gas and liquid in the ALC at the beginning of the simulation are assumed to have 0% saturation of dissolved oxygen. It is reasonable to conclude that the gas phase oxygen concentration rises rapidly as a result of the addition of oxygen in the gas inlet. Although oxygen is continuously transferred from gas to liquid, the rate of interfacial mass transfer is clearly less than the input rate of oxygen (from gas throughput), and therefore a rise in oxygen concentration in the gas phase is apparent. The initial rise in gas phase oxygen concentration (from 0 to around 80%) occurs in a very short period (approximately 2 seconds), afterwhich it slowly rises and level off at the concentration close to that in the air. This indicates that mixing in the gas phase in the ALC occurs extremely rapidly. However, the profile of liquid phase oxygen concentration does not show this initial rapid-rise regime, and the oxygen concentration continues to increase slowly before reaching its steady state value at about 150 seconds after the air is fed to the system (see Figure 4.3.2). It is possible from this finding that the mass transfer rate in the ALC is still quite low compared to the rate of mixing. As the mass transfer process is batchwise with respect to the liquid phase (but continuous-wise for the gas phase), eventually the oxygen concentration in liquid phase reaches their equilibrium values which ceases the mass transfer process.

In the following discussion, we will investigate how the various parameters affect the behavior of the ALC which will indicate that it is possible to control the rate of gas-liquid mass transfer in the system.

4.3.4 Comparison between simulation results and experimental data

The comparisons of the transient liquid phase oxygen concentration in the riser at various operating parameters from the CSTR and Dispersion models in a semi-batch operated ALC (continuous gas supply without liquid feed) are depicted in Figures 4.3.4A to 4.3.4F. It is found that, in all cases, the Dispersion model is able to accurately predict the behavior of transient oxygen concentration in the liquid phase in riser while the CSTR model always underestimates the rate of mass transfer (lower oxygen concentration profile). The results from the CSTRs-in-Series and PFR models are not shown in this series of figures, but it is known from previous sections that these two models always give lower rate of mass transfer than that of the Dispersion model. This implies that the results from the CSTRs-in-Series and PFR models would also be miscalculated. It can then be concluded from this comparison that the Dispersion model is most suitable for describing the mass transfer behavior of the ALC.

The model seems to be able to predict the performance of the ALC as the simulation results agree well with experimental data in a wide range of operating parameters. It is reminded here that K_La and the gas phase dispersion coefficient of oxygen in the riser, $D_{G,r}$, are adjusted to give the most accurate prediction. Table 4.2 summarizes the results from this sensitivity test for these two parameters. The row with bold characters is the combination employed in the simulation. Note that the value of each parameter, particular K_La, is kept as close as possible to the experimental reported value (Wongsuchoto and Pavasant, 2000). Hence, there might exist conditions (in Table 4.2) that provide better agreement between simulation and experiment, but they are not selected simply because the estimates of parameters are too far from actual values.

Table 4.3 lists all parameters used in the simulation. The liquid phase dispersion coefficients both in riser and downcomer were obtained from the RTD experiment whereas K_La and the gas phase dispersion coefficients in the riser and downcomer were from the data fitting. The resulting estimates of K_La show an interesting capability of the model because all the estimates of K_La in the ALC at low gas flowrate (0.000111 $m^3.s^{-1}$) coincide at approximately 0.013 s^{-1}, and at high gas

flowrate (0.000272 $m^3.s^{-1}$) at about 0.036 s^{-1}. This finding is logical in terms of actual experimental evidence, as high gas flowrates lead to a high level of gas holdup in the ALC which results in a high rate of gas-liquid mass transfer.

The estimates of the gas phase dispersion coefficients also provide a reasonable insight to the actual practice where the coefficient decreases with increasing the ratio between the riser and downcomer cross sectional areas. This is because when this area ratio increases which corresponds to a smaller cross sectional area in the riser, the absolute gas bubble velocity in this section increases. This leads to a smaller portion of gas being recirculated in the system, and therefore a lower level of dispersion.

It is useful to verify these models over a range of operating parameters to avoid a sole agreement between model predictions and experimental results at a single set of parameters. In this work, the operating parameters of interest include the ratio between downcomer and riser cross sectional area (A_d/A_r), the rate of inlet gas flowrate ($Q_{G,in}$), liquid feed flow rate ($Q_{L,F}$), and the height of draft tube (H_{DT}). However, there was no experimental evidence on the ALC with liquid feed flow, this testing is therefore not possible and we will treat this parameter as a special case in the further investigation. In addition, the model is found to be inaccurate for the case of a high draft tube ALC. This limitation of model will also be treated as a special case in the last section of this chapter. In this section, we will investigate the accuracy of the model by verifying the simulation results with experimental data where $Q_{G,in}$, and A_d/A_r were variable.

Increasing inlet gas flowrate ($Q_{G,in}$)

Experiment found that increasing inlet gas flowrate ($Q_{G,in}$) results in a higher rate of oxygen mass transfer from gas to liquid which leads to a faster responding time for the liquid phase oxygen concentration to approach the equilibrium level. Simulation agrees well with experiment as shown in Figures 4.3.4A and 4.3.4B. In these two cases, the A_d/A_r is fixed at 0.067 (Cases I and II) but the inlet gas flowrate in Case I is 0.0001111 and in Case II is 0.000272 $m^2 \cdot s^{-1}$. The responding time for the system to reach 80% saturation concentration, t_{80}, is arbitrarily chosen as an indicator

for comparing the response between the two cases (any other % saturation can also be taken which will give the same result). Increasing the inlet gas flowrate from Case I to Case II causes the reduction in the responding time, i.e. t_{80} decreases from 136 to 50 seconds. The same result is obtained at other values of A_d/A_r (0.43 in Cases III and IV (Figures 4.3.4C and 4.3.4D), and 1.0 in Cases V and VI (Figures 4.3.4E and 4.3.4F)). The reason for this is that increasing $Q_{G,in}$ directly results in an increase in gas holdup, leading to a higher population of gas bubbles in the system. Hence, riser gas holdup increases and so does the K_La which is derived from the higher level of interfacial mass transfer area (a). That is why the result from the curve fitting shows that K_La in the ALC with higher gas flowrate is higher than that in the system with low gas flowrate.

Increasing the ratio between downcomer and riser cross sectional areas (A_d/A_r)

Increasing the ratio between downcomer and riser cross sectional areas (A_d/A_r) effectively leads to an enhancement of gas and liquid velocities in the riser(Garvrilescu and Tudose, 1996). The faster gas velocity in the riser section, in turn, results in a condition even closer to the plug flow. This means a lower dispersion coefficient in the gas phase. In the liquid phase however, the situation is somewhat different as liquid always circulates within the system but gas bubbles do not. Hence, increasing the liquid velocity can well mean a faster self-replacement due to a faster liquid circulation. Garvrilescu and Tudose, 1996 indicated that the faster liquid circulation could result in a faster liquid phase dispersion coefficient. In the present RTD experiment, the liquid phase dispersion coefficient does not seem to vary significantly with varying A_d/A_r (although increasing A_d/A_r from 0.431 to 1.0 decreases the liquid phase dispersion coefficient slightly).

The curve fitting experiment in the simulation shows an impressive prediction of the gas phase dispersion coefficient as increasing this area ratio results in a decrease in the dispersion coefficient. However, both simulation and experiment agree that the effect of A_d/A_r on the rate of gas-liquid mass transfer is marginal, i.e. increasing A_d/A_r from 0.067 to 1, t_{80} only increases from approximately 136 to 158 seconds (Figures 4.3.4A and 4.3.4E).

4.4 Prediction of the Performance of the ALC with Continuous Liquid Feed ($Q_{L,in}$) from the Dispersion Model

The effect of liquid feed flowrate, $Q_{L,in}$, on oxygen concentration profiles in liquid and gas phases in the riser is shown in Figures 4.4A and 4.4B, respectively. Note that the liquid that is fed into the ALC is assumed to contain no dissolved oxygen. The liquid flow into the ALC prevents the system to reach equilibrium oxygen concentration as liquid is continuously removed from the system before a complete mass transfer takes place. In other words, the liquid flow simply reduces the contact time between gas and liquid phases, and if the liquid flow is high enough, there will not be enough time for the gas and liquid to reach their equilibrium concentrations. Figure 4.4A reveals that at a rather low liquid flowrate ($Q_{L,in}$ = 0.00001 $m^3 \cdot s^{-1}$), the steady state dissolved oxygen concentration almost reaches the equilibrium value (93% saturation). Increasing the liquid flowrate results in a decrease in this steady state dissolved oxygen concentration, and when the liquid flowrate reaches 0.001 $m^3 \cdot s^{-1}$, the final oxygen concentration becomes only some 20% of the saturation value.

It is also interesting to look at the gas phase oxygen concentration in the ALC with liquid feed. Figure 4.4B illustrates that the final oxygen concentration in the gas phase depends largely on the liquid flowrate. At relatively low liquid flowrate (e.g. 0.00001 $m^3 \cdot s^{-1}$), the final gas phase oxygen concentration reaches almost 100% saturation. However, when the liquid flow is high (e.g. 0.001 $m^3 \cdot s^{-1}$), the final steady state oxygen concentration is only 88% of the saturation. The reason for this was already given in the above paragraph.

In terms of the rate of mass transfer between gas and liquid, since we know that

$$\text{Oxygen mass flux} = N_{O2} = K_L a \, \Delta O = K_L a \, \Delta (O_G - O_L)$$

and if it is assumed that $K_L a$ does not depend significantly on the liquid feed, oxygen mass flux from the gas to liquid phases varies according to the concentration difference driving force, ΔO. This ΔO can be obtained by subtracting the oxygen concentration in Figure 4.4B (gas phase) with that in Figure 4.4A (liquid phase at the

same operating conditions). Therefore if we have a low level of oxygen concentration in the liquid phase and a high level of oxygen concentration in the gas phase, a high mass transfer rate can be achieved. The simulation illustrates that, at steady state, the concentration difference, ΔO, for the ALC with low liquid flow is smaller than that with high liquid flow. For instance, at $Q_{L,in} = 0.00001\ m^3 \cdot s^{-1}$, $\Delta O \approx 0.065$, and at $Q_{L,in} = 0.001\ m^3 \cdot s^{-1}$, $\Delta O \approx 0.682$. This means that a higher gas-liquid mass transfer can be obtained by increasing the liquid flowrate into the ALC. This knowledge can be applied to real applications where a high mass transfer is necessary.

4.5 The Prediction of Oxygen Mass Transfer Behavior in a High Draft Tube ALC by the Dispersion Model

The model is further tested for its generality by rendering the height of the ALC one of the variables. The liquid phase oxygen concentration in the riser with predicted by Dispersion model are compared with experimental reported data from a 2 m draft tube concentric ALC as shown in Figure 4.5 (experimental data from Krichnavaruk and Pavasant, 2000). However, the comparison clearly shows that there is a large discrepancy between the predicted and the real concentration profiles, although the trends from the two are similar. This, in effect, means that the Dispersion model lacks some crucial information about the mass transport in the high ALC.

It might be possible that the following phenomena take place in the system but not considered in the model:

- The overall mass transfer in the high ALC is not homogeneous in various sections of the ALC, e.g. K_La in the riser might be higher than that in the downcomer.
- There exists a deviation of the gas holdup along the height of the contactor.
- The column height might affect the oxygen solubility, i.e. static pressure causes a decrease in oxygen solubility by a factor of 1.6. Hence, there will be a large difference between the equilibrium oxygen concentration at the bottom and the top of the column (Dhaouadi et al.,1997).

In addition, there might also be some other nonidealities that exist in the high column which have not been included in the developed mathematical model. Further investigations on these points are urgently needed to complete the knowledge of mass transport in the ALC.

สถาบันวิทยบริการ
จุฬาลงกรณ์มหาวิทยาลัย

Table 4.1 Operating parameters used in the simulations

Case	A_d/A_r	H_0 [m]	$Q_{g,in}$[$m^3 . s^{-1}$]	$v_{L,d}$ [$m . s^{-1}$]	$K_L a_S$ [s^{-1}]	$\varepsilon_r = \varepsilon_{top}$	ε_d
I	0.067	1.018	0.000111	0.50	0.0132	0.050	0.020
II	0.067	1.018	0.000272	0.50	0.0360	0.080	0.045
III	0.431	1.018	0.000111	0.50	0.0133	0.030	0.018
IV	0.431	1.018	0.000272	0.50	0.0336	0.075	0.061
V	1.000	1.018	0.000111	0.25	0.0130	0.035	0.020
VI	1.000	1.018	0.000272	0.30	0.0360	0.075	0.050

Note : subscript *s* = the simulation result

สถาบันวิทยบริการ
จุฬาลงกรณ์มหาวิทยาลัย

Table 4.2 Sensitivity analysis in various cases of the simulation results by the Dispersion model

Case I	K_La [s^{-1}]	$D_{G,r}$ [$m^2.s^{-1}$]	t_{80} [s]
Experimental data	0.012	-	140
Simulation results	0.012	0.3	205.12
	0.012	0.5	186.88
	0.012	0.7	177.77
	0.012	1	171.08
	0.012	3	159.08
	0.012	5	156.59
	0.006	3	293.76
	0.0084	3	216.66
	0.0132	***3***	***146.47***
	0.0144	3	136.75
	0.0156	3	127.63

Case II	K_La [s^{-1}]	$D_{G,r}$ [$m^2.s^{-1}$]	t_{80} [s]
Experimental data	0.03	-	50
Simulation results	0.03	0.3	81.44
	0.03	0.5	74.15
	0.03	0.7	70.50
	0.03	1	67.76
	0.03	3	62.90
	0.03	5	61.69
	0.015	3	117.60
	0.021	3	86.30
	0.033	3	57.74
	0.036	***3***	***53.48***
	0.039	3	50.14

Case III	K_La [s^{-1}]	$D_{G,r}$ [$m^2.s^{-1}$]	t_{80} [s]
Experimental data	0.0121	-	140
Simulation results	0.0121	0.3	223.01
	0.0121	0.5	205.25
	0.0121	1	187.54
	0.0121	3	173.37
	0.0121	5	170.39
	0.0121	7	168.88
	0.0121	9	168.26
	0.00605	3	311.16
	0.00847	3	232.89
	0.01331	***3***	***160.61***
	0.01573	3	140.54
	0.01815	3	125.51

Case IV	K_La [s^{-1}]	$D_{G,r}$ [$m^2.s^{-1}$]	t_{80} [s]
Experimental data	0.021	-	60
Simulation results	0.021	0.5	104.63
	0.021	0.3	111.25
	0.021	1	97.78
	0.021	3	90.93
	0.021	5	90.70
	0.021	7	90.60
	0.0105	3	170.06
	0.0147	3	125.51
	0.0231	3	85.03
	0.0273	3	73.93
	0.0315	3	65.71
	0.0336	***3***	***62.35***

สถาบันวิทยบริการ
จุฬาลงกรณ์มหาวิทยาลัย

Case V	K_La [s^{-1}]	$D_{G,r}$ [$m^2.s^{-1}$]	t_{80} [s]
Experimental data	0.011	-	160
Simulation results	0.011	0.5	172.24
	0.011	1.5	158.89
	0.011	2	156.97
	0.011	3	154.74
	0.011	4	153.60
	0.0077	1	246.35
	0.0099	1	199.53
	0.011	1	183.24
	0.0121	1	169.80
	0.0132	***1***	***158.69***
	0.0143	1	149.24

Case VI	K_La [s^{-1}]	$D_{G,r}$ [$m^2.s^{-1}$]	t_{80} [s]
Experimental data	0.036	-	70
Simulation results	0.036	0.3	80.07
	0.036	0.5	73.69
	0.036	***0.7***	***70.23***
	0.036	1	66.84
	0.036	2	63.58
	0.036	3	62.12
	0.0168	0.7	125.54
	0.021	0.7	106.20
	0.0252	0.7	94.32
	0.0338	0.7	76.68
	0.0359	0.7	73.93
	0.038	0.7	71.32
	0.0401	0.7	68.88

Note: t_{80} is the responding time for the system to reach 80% saturation concentration

Table 4.3: Simulation Parameters

Case	K_La_{exp} [s^{-1}]	K_La_S [s^{-1}]	$D_{G,r}$ [$m^2 . s^{-1}$]	$D_{L,r}$ [$m^2 . s^{-1}$]	$D_{G,d}$ [$m^2 . s^{-1}$]	$D_{L,d}$ [$m^2 . s^{-1}$]
I	0.0121	0.0132	3	0.05	0.3	0.03
II	0.0300	0.0360	3	0.05	0.3	0.03
III	0.0120	0.0133	3	0.05	0.3	0.03
IV	0.0210	0.0336	3	0.05	0.3	0.03
V	0.0110	0.0132	1	0.03	0.8	0.01
VI	0.0250	0.0360	0.7	0.05	0.3	0.02

Note : subscript

exp = the experimental data

s = the simulation result

สถาบันวิทยบริการ
จุฬาลงกรณ์มหาวิทยาลัย

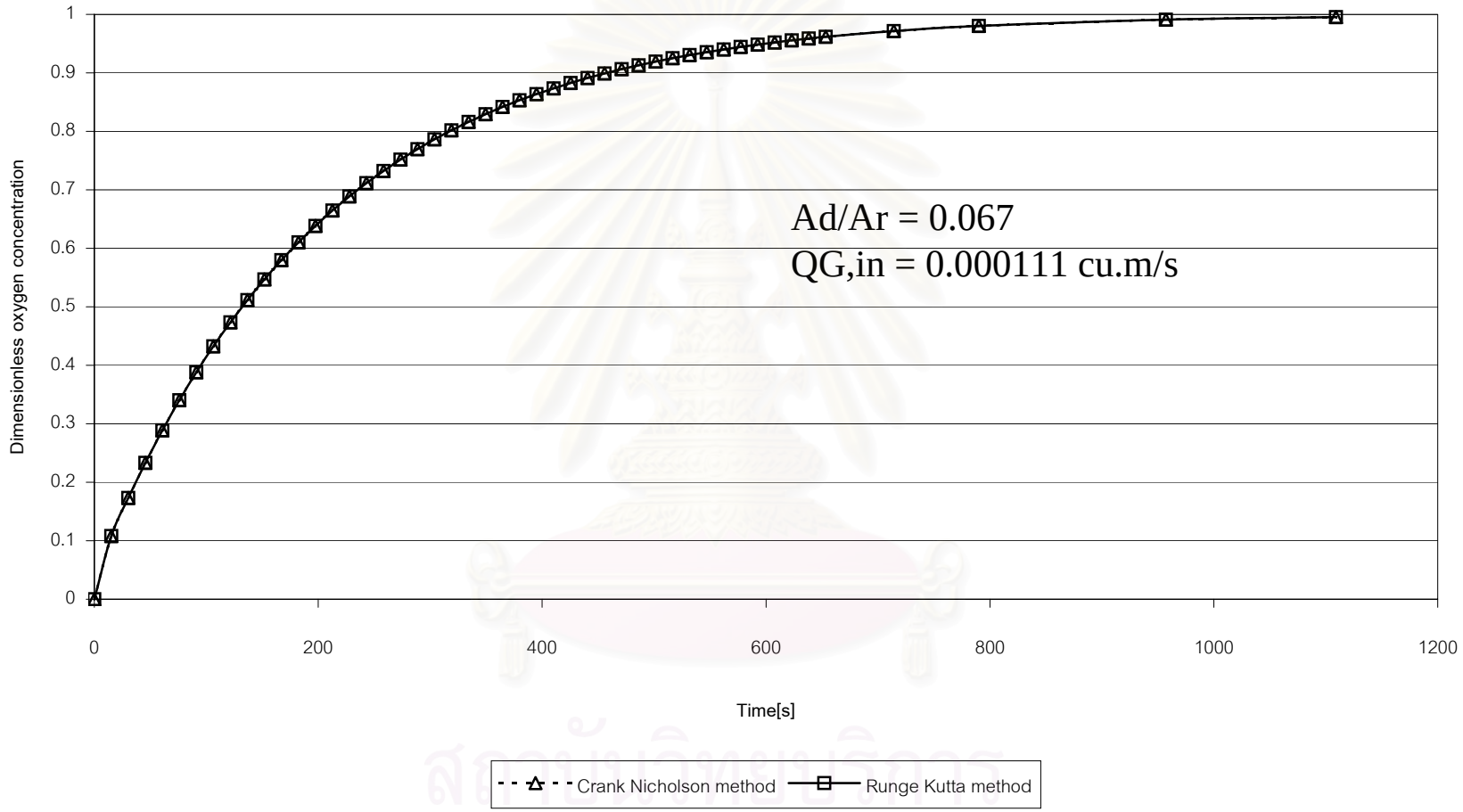

Figure 4.2.1. Comparison between the predicted riser oxygen concentration from CSTR (Crank Nicholson) and Runge-Kutta methods (case I)

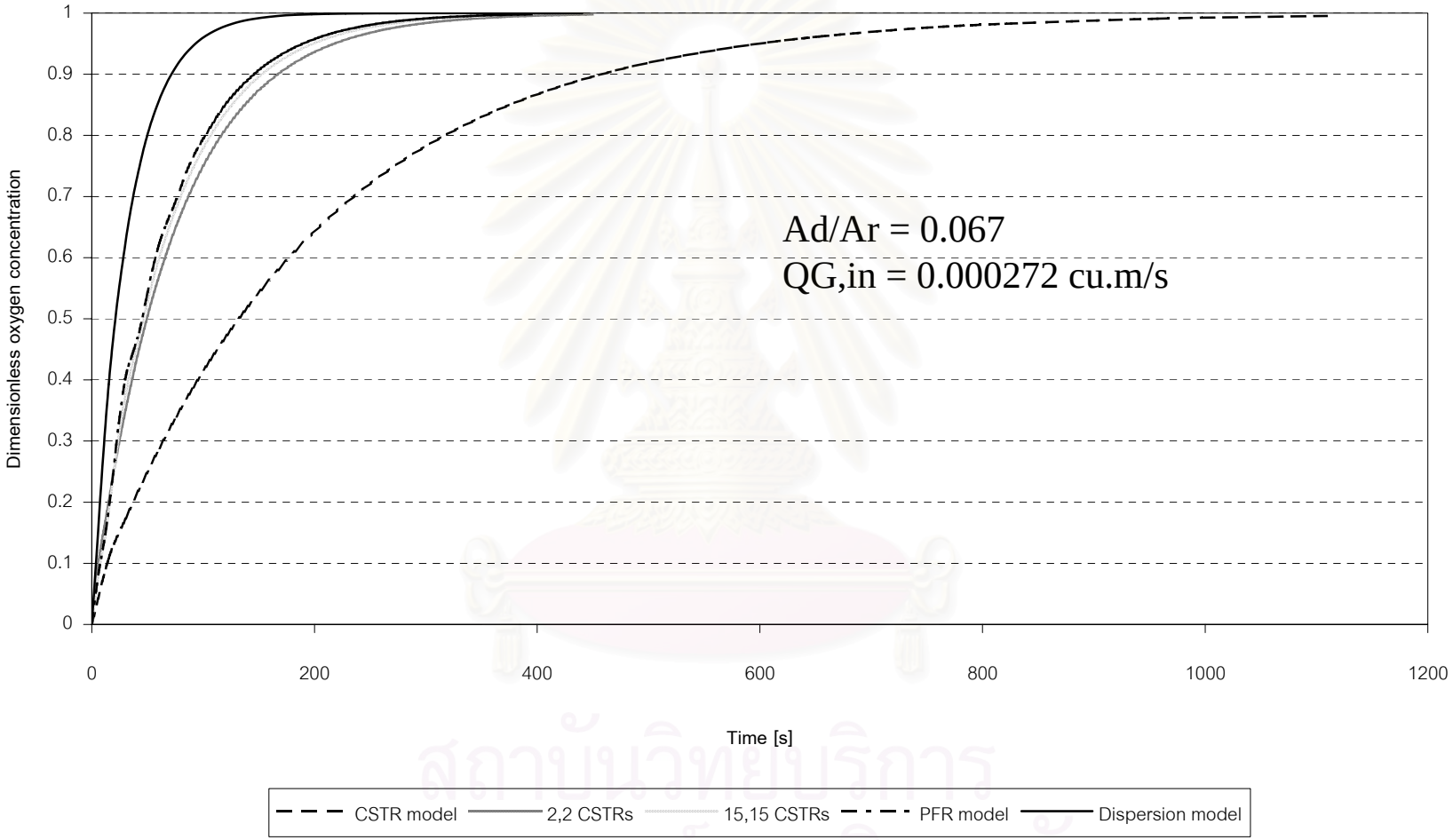

Figure 4.2.2 Comparison between the predicted riser oxygen concentration from CSTR, CSTRs-in-series, PFR, and Dispersion models (Case II)

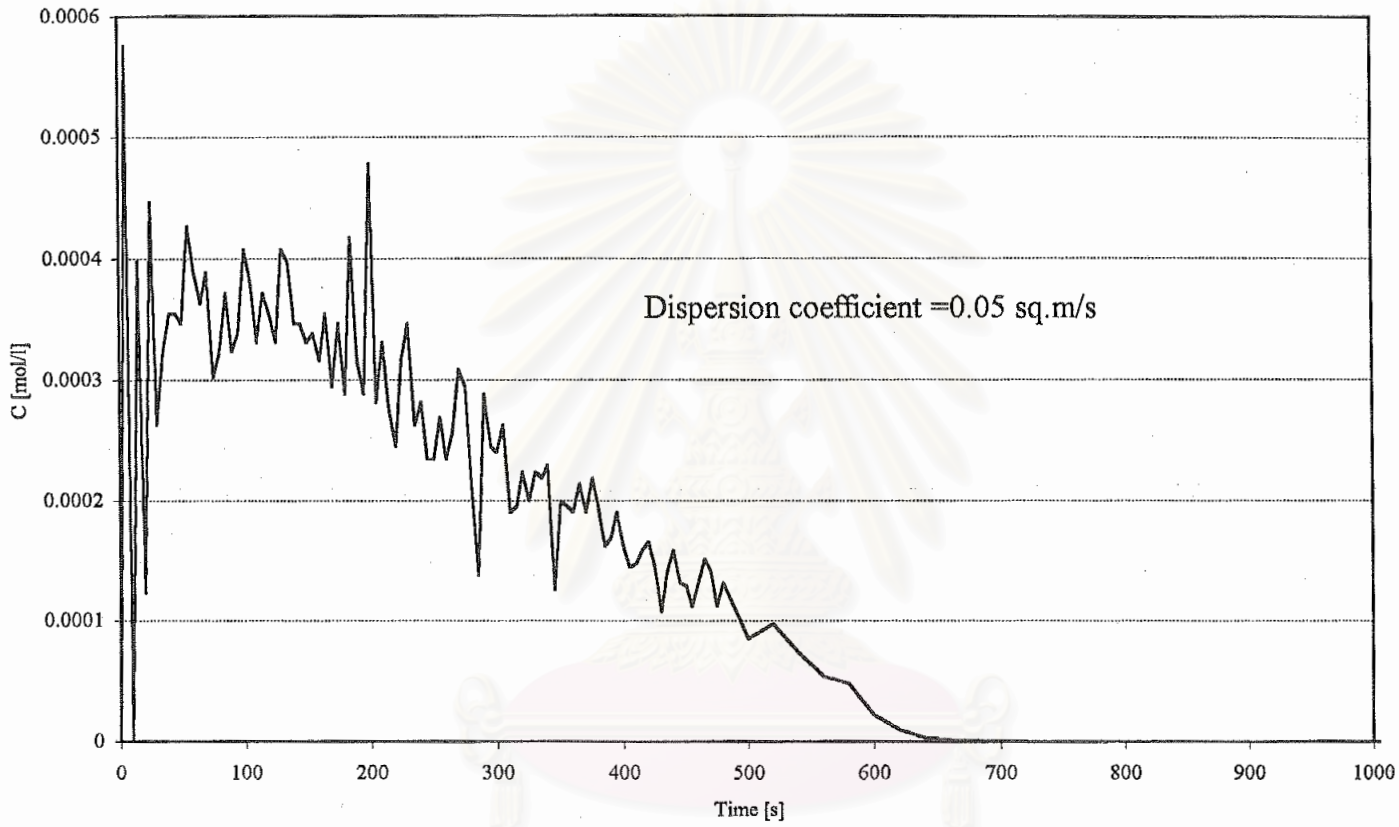

Figure 4.3.1A The responding C curve from the impulse tracer experiment in the riser section of the Split type ALC.
($Q_{g,in}$=0.0000557 $m^3.s^{-1}$ A_d/A_r=1 H_{DT}=1.08 m)

สถาบันวิทยบริการ
จุฬาลงกรณ์มหาวิทยาลัย

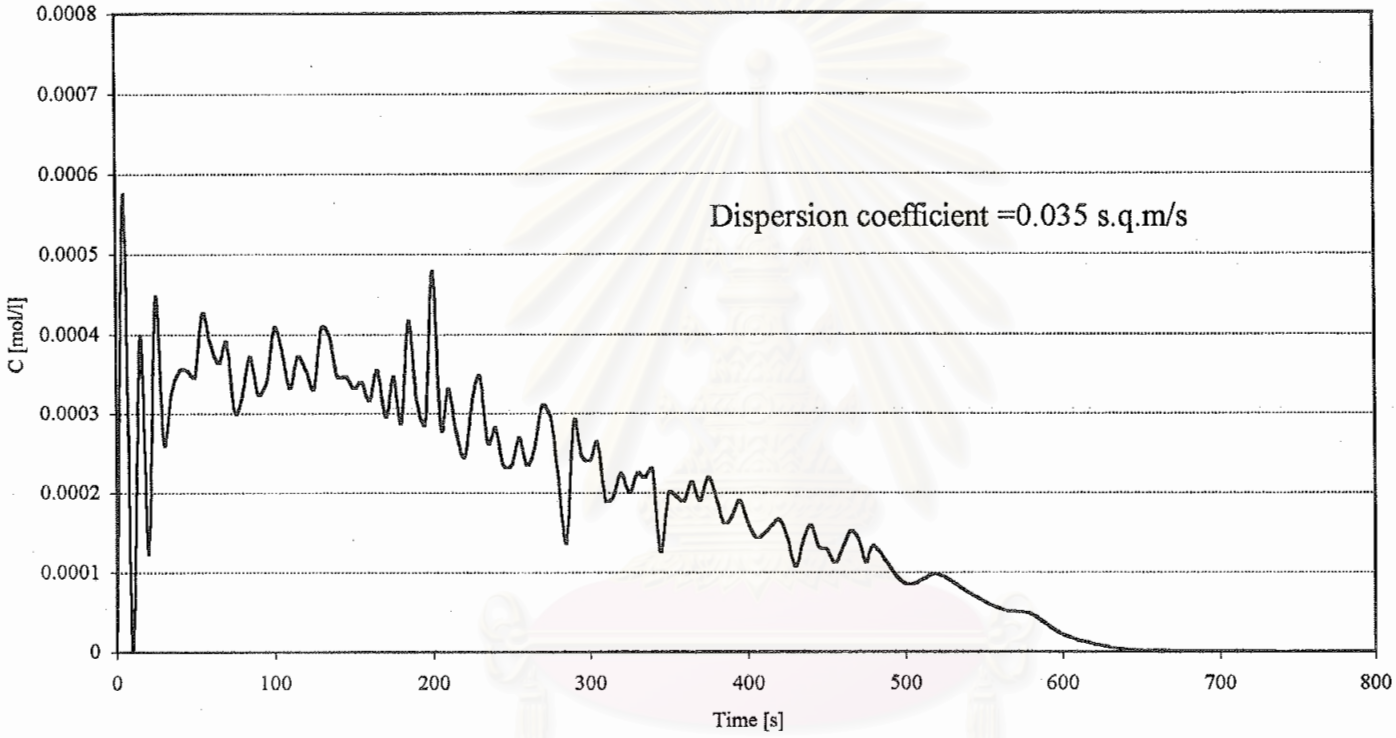

Figure 4.3.1B The responding C curve from the impulse tracer experiment in the downcomer section of the Split type ALC.
(Qg,in=0.0000557 $m^3.s^{-1}$ Ad/Ar=1 HDT=1.08 m)

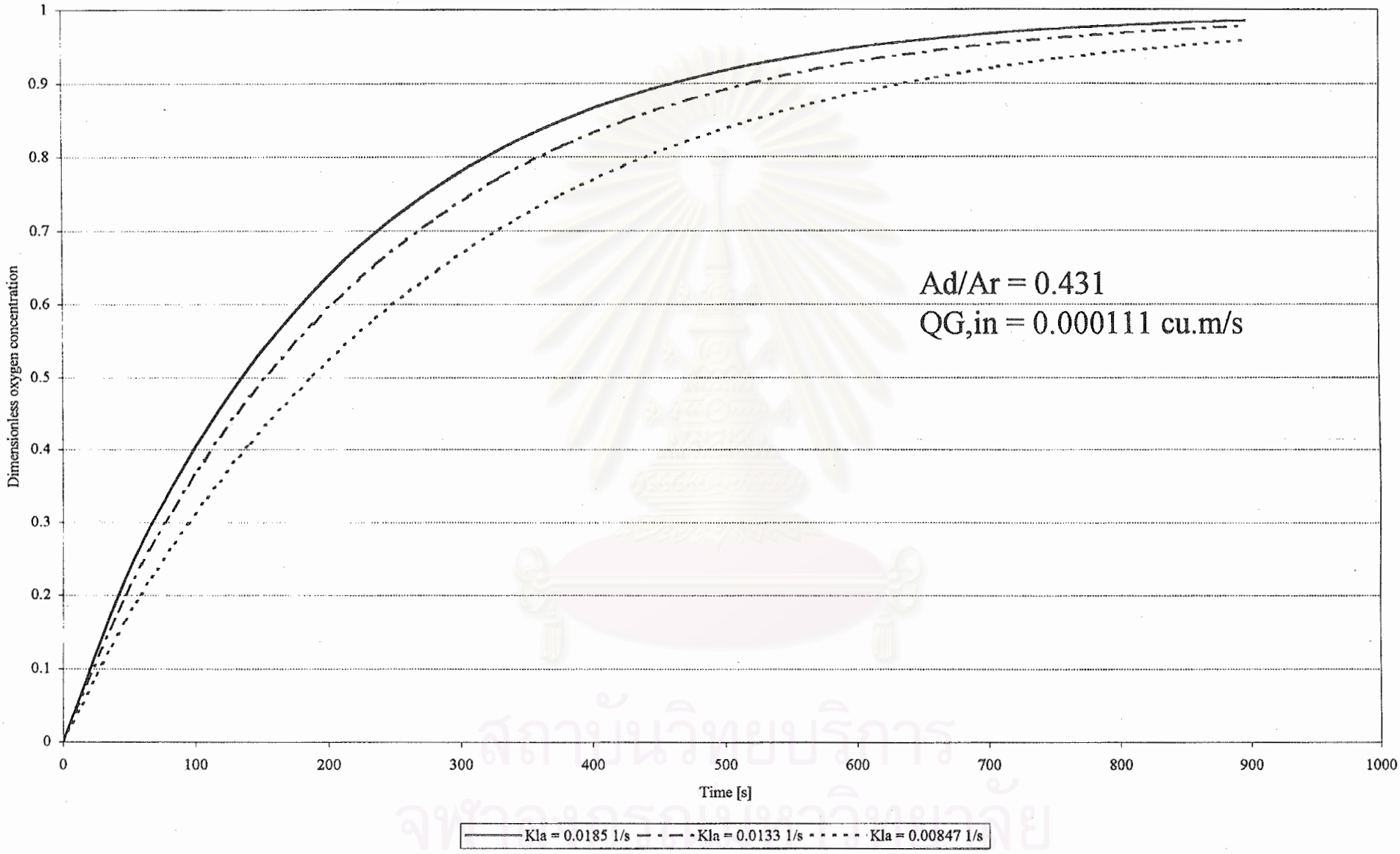

Figure 4.3.2A. Effect of the overall volumetric mass transfer coefficient (K_La) on the prediction from the CSTR model (case III)

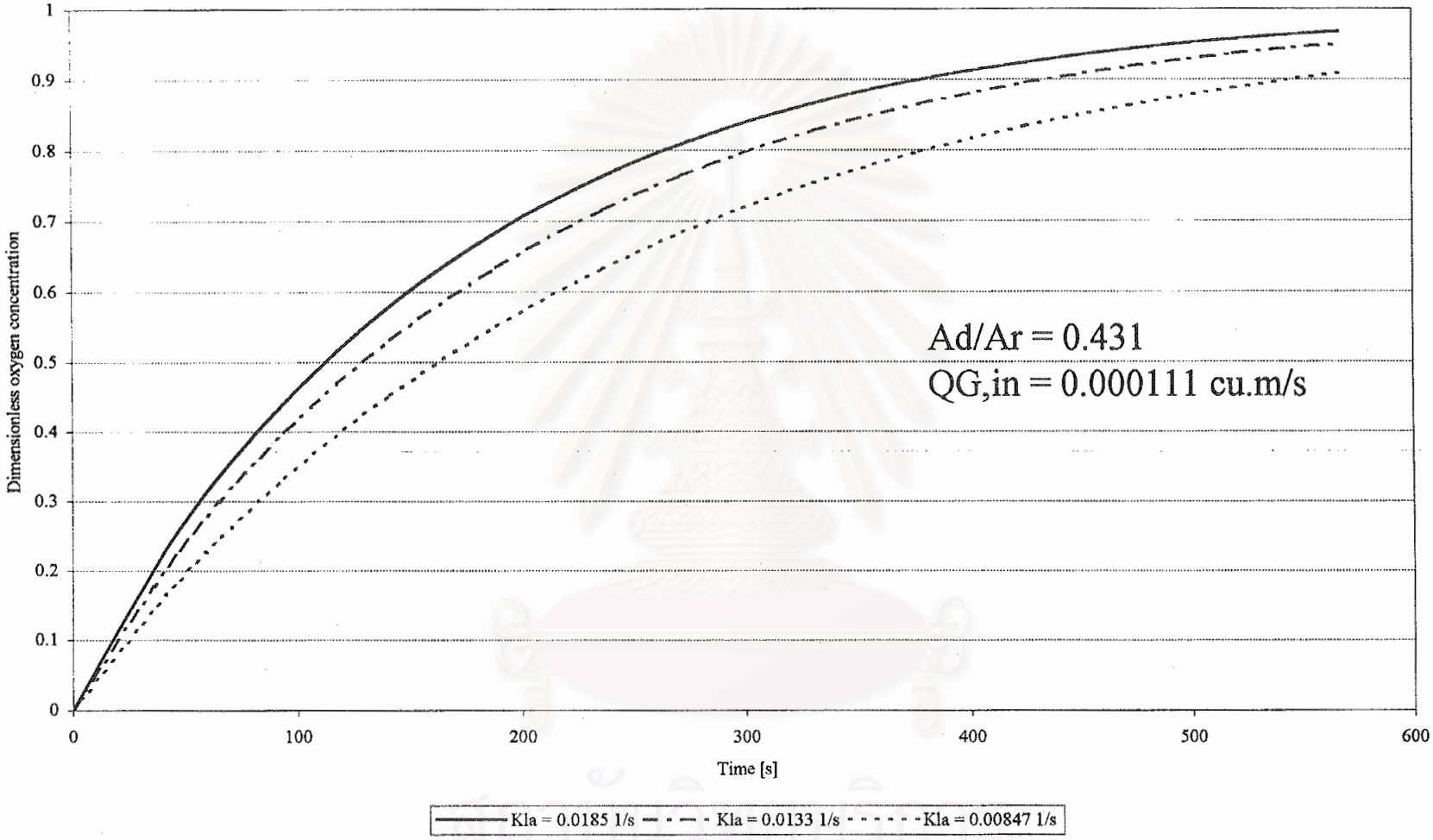

Figure 4.3.2B. Effect of the overall volumetric mass transfer coefficient (K_La) on the prediction from the PFR model (case III)

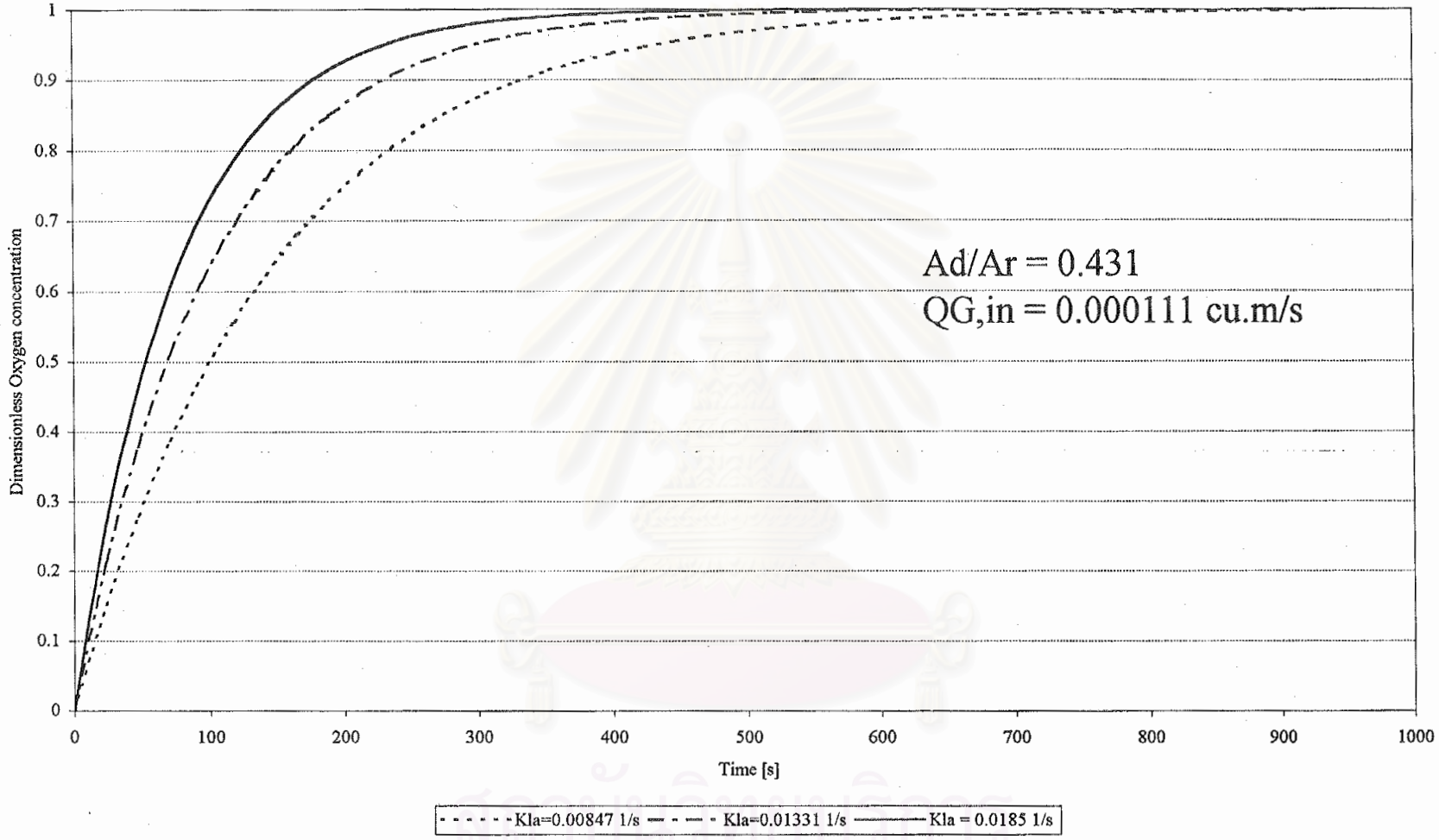

Figure 4.3.2C. Effect of the overall volumetric mass transfer coefficient (K_La) on the prediction from the Dispersion model (case III)

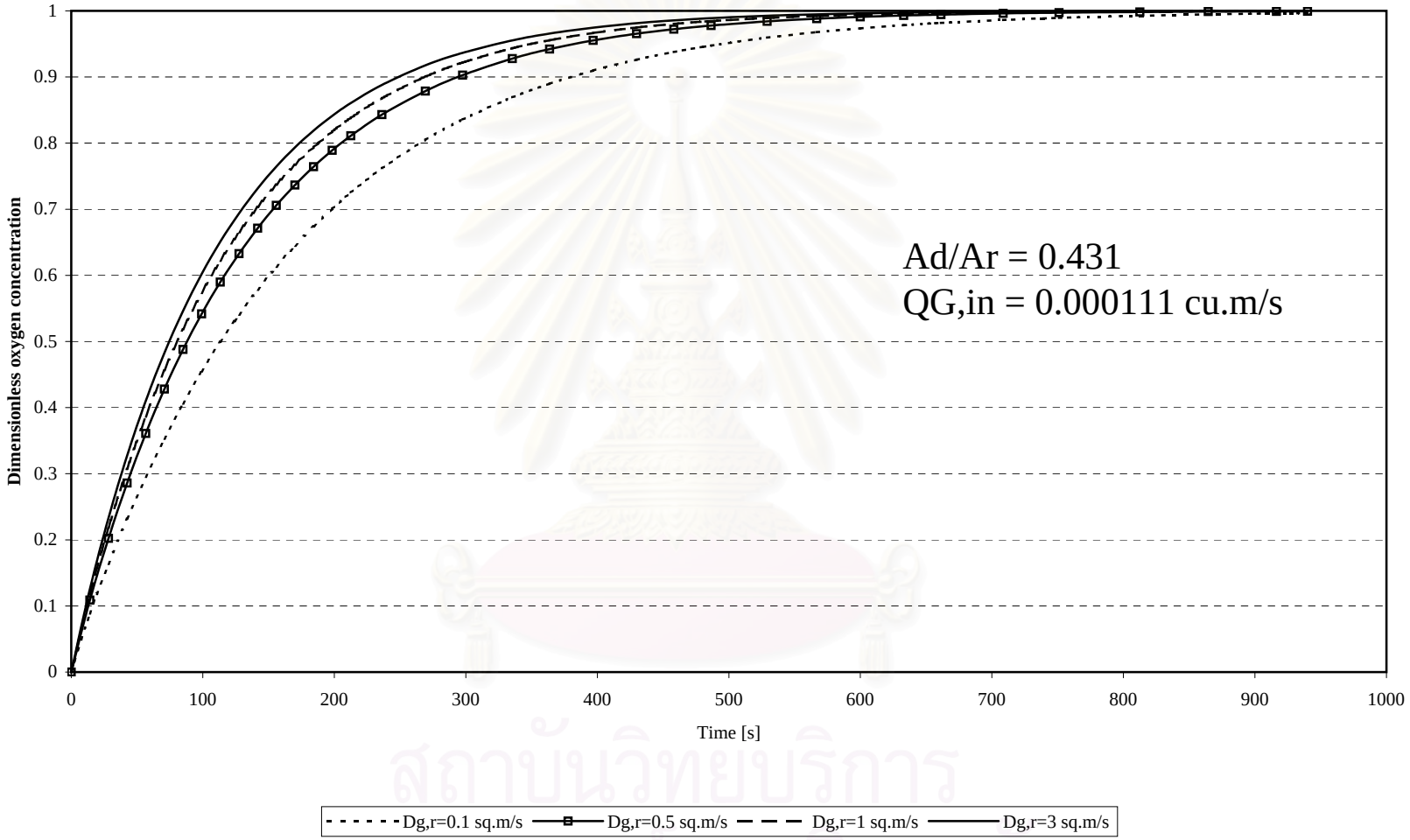

Figure 4.3.2D. Comparison of experimental data and simulation results (Dispersion model) obtained at various values of gas dispersion coefficients in riser (Case III)

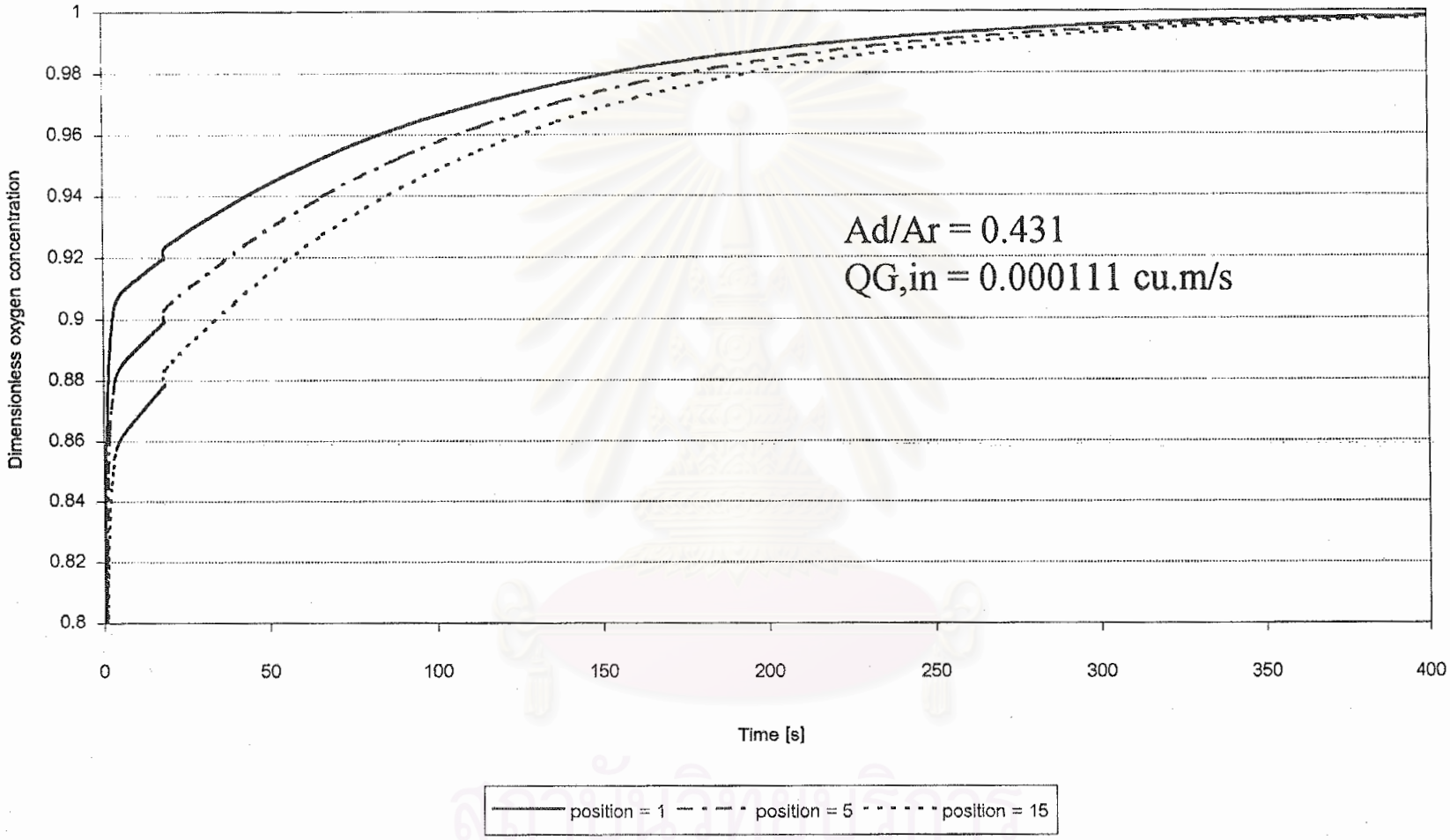

Figure 4.3.3A. Predicted riser oxygen concentration profile in gas phase by Dispersion model (Case III)

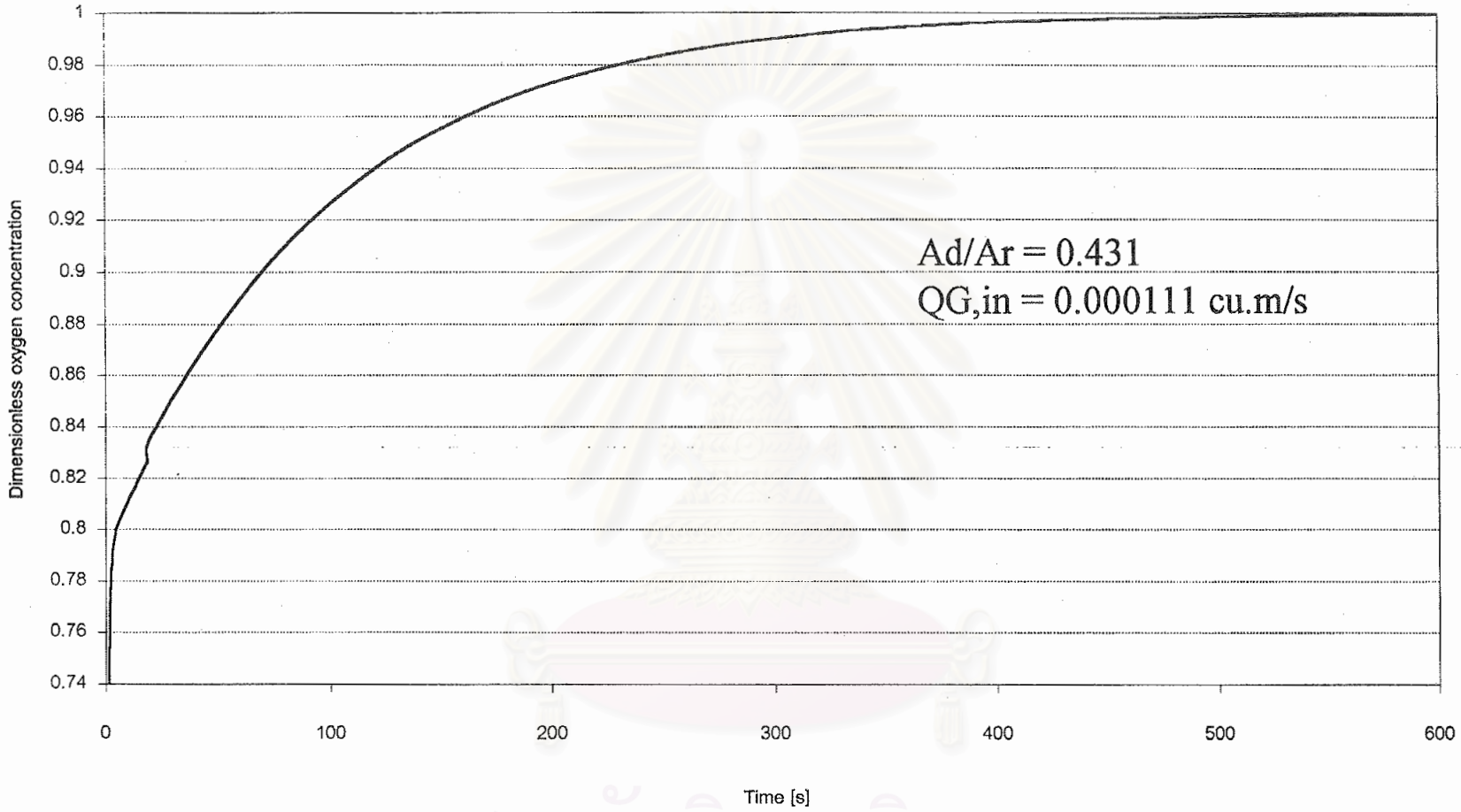

Figure 4.3.3B. Predicted gas separator oxygen concentration profile in gas phase by Dispersion model (Case III)

สถาบันวิทยบริการ
จุฬาลงกรณ์มหาวิทยาลัย

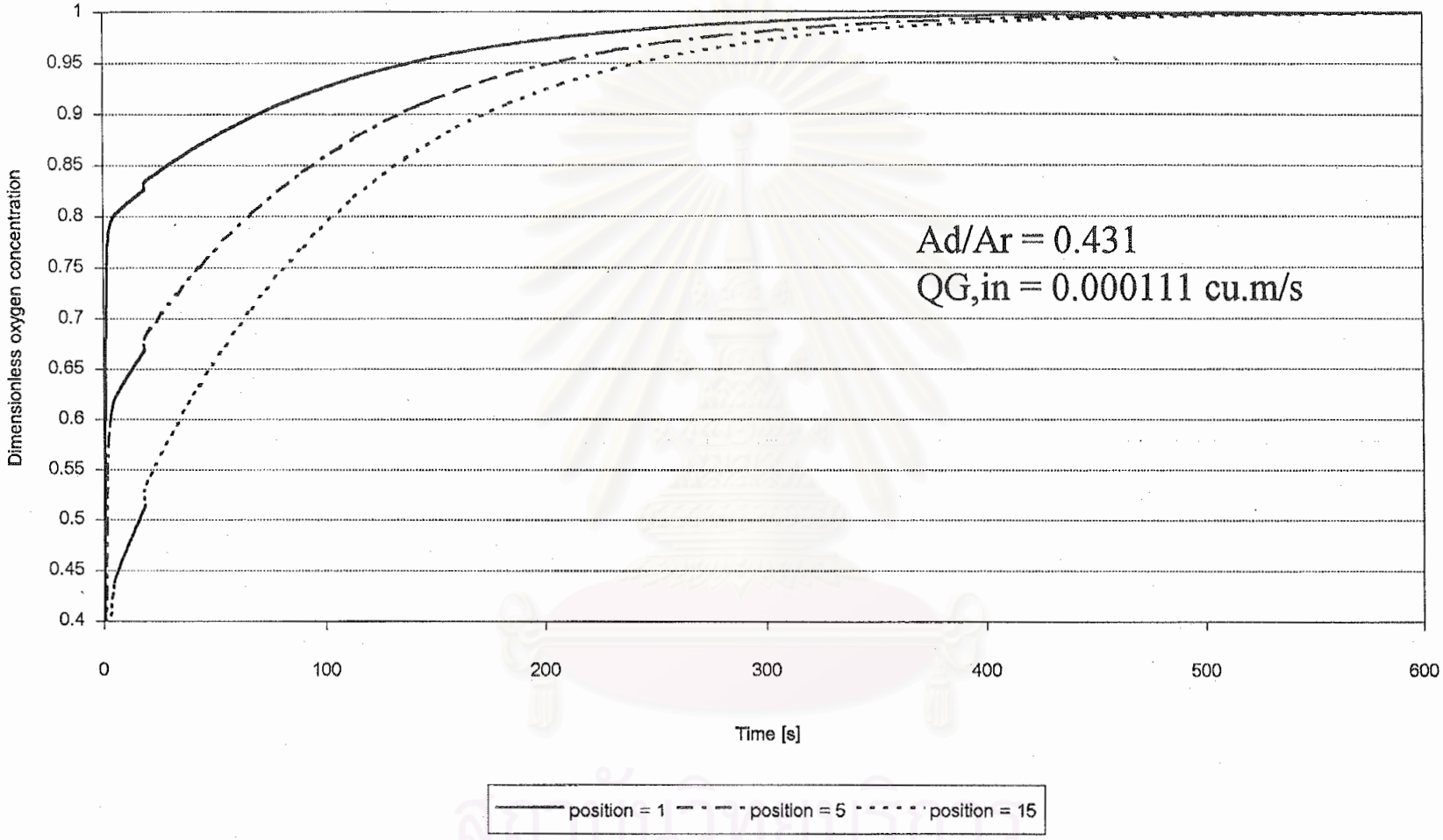

Figure 4.3.3C. Predicted downcomer oxygen concentration profile in gas phase by Dispersion model (Case III)

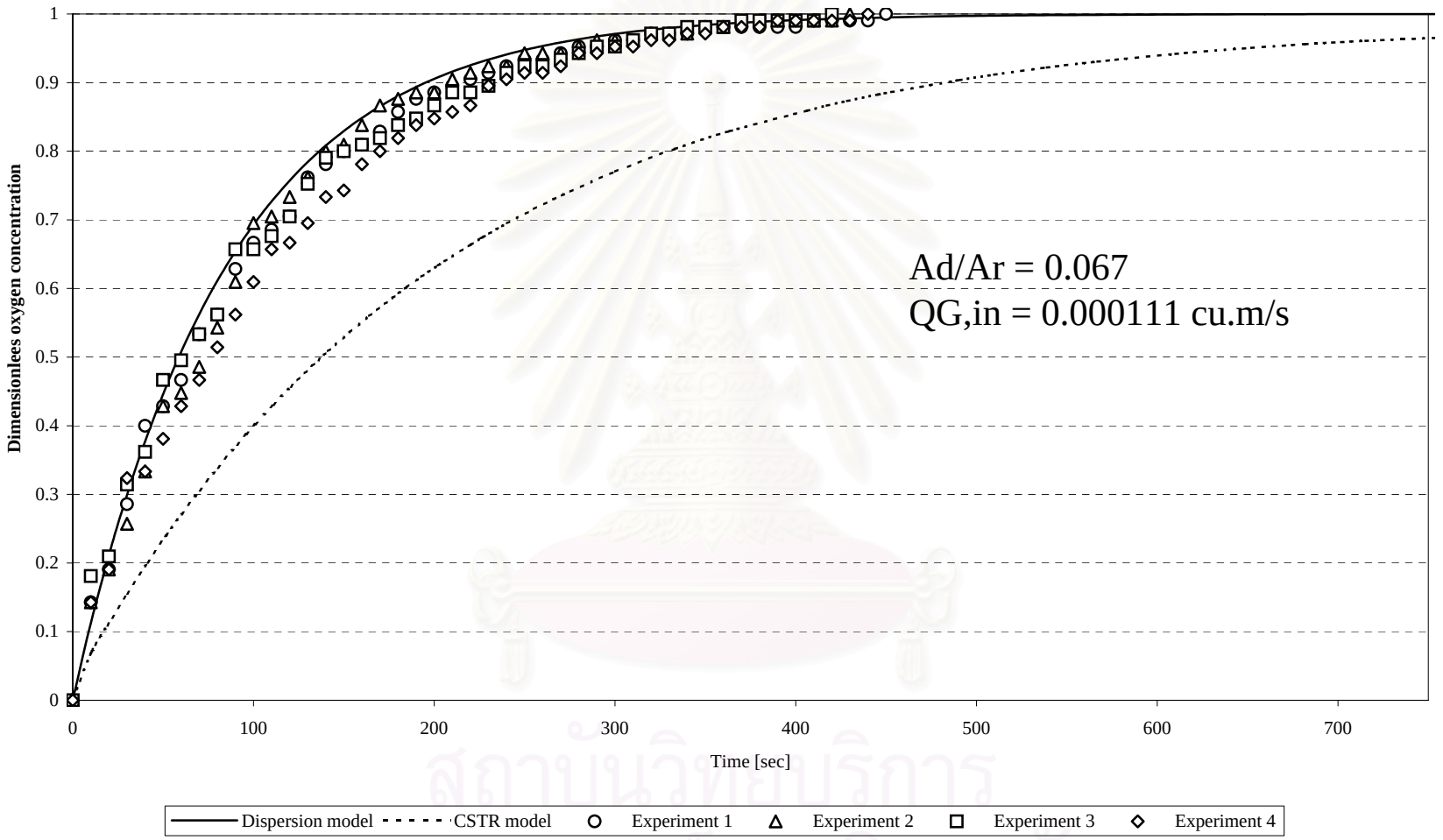

Figure 4.3.4A. Comparison between simulation results (Dispersion and CSTR models) and reported experimental data (Case I)

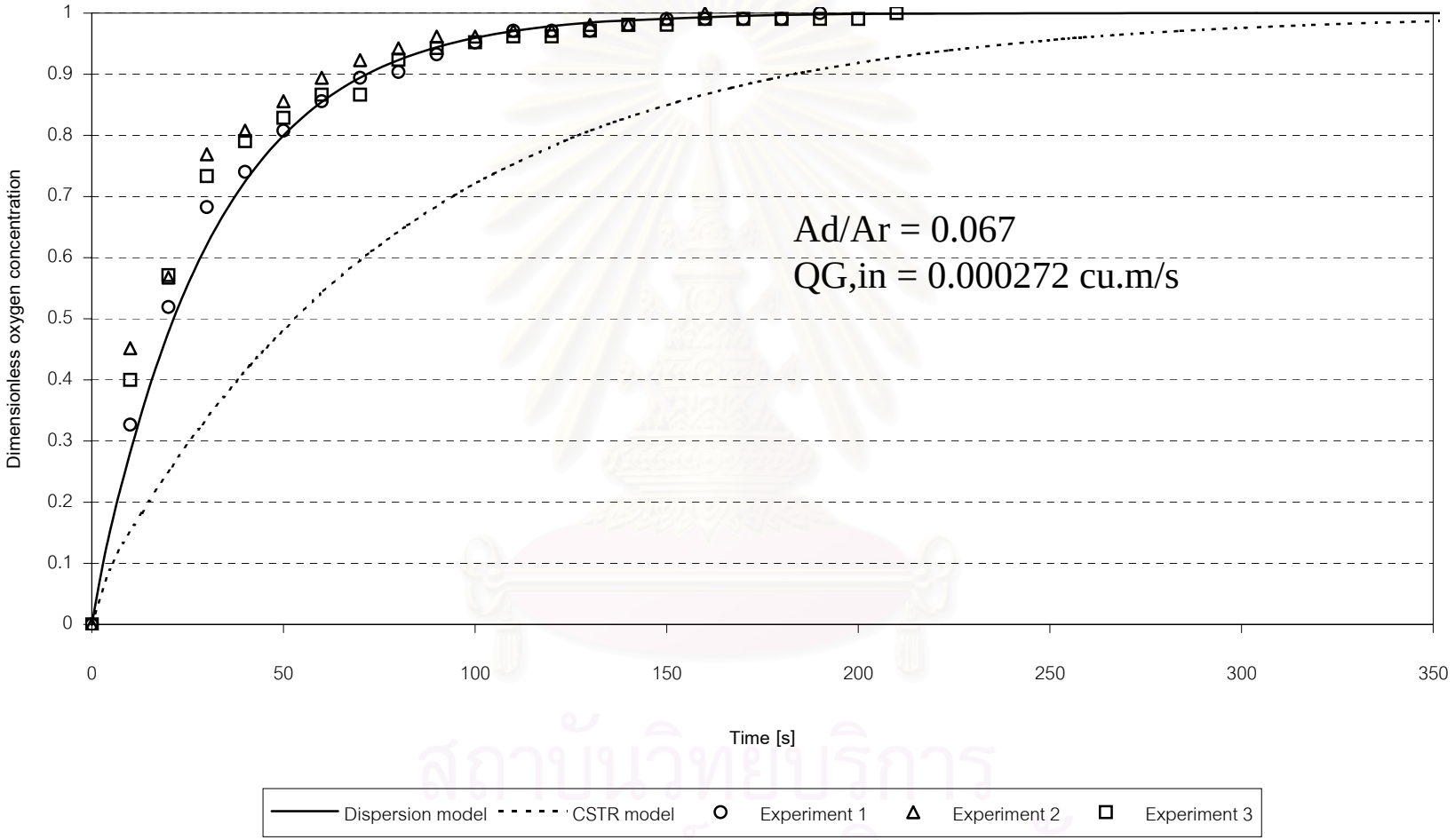

Figure 4.3.4B. Comparison between simulation results (Dispersion and CSTR models) and reported experimental data (Case II)

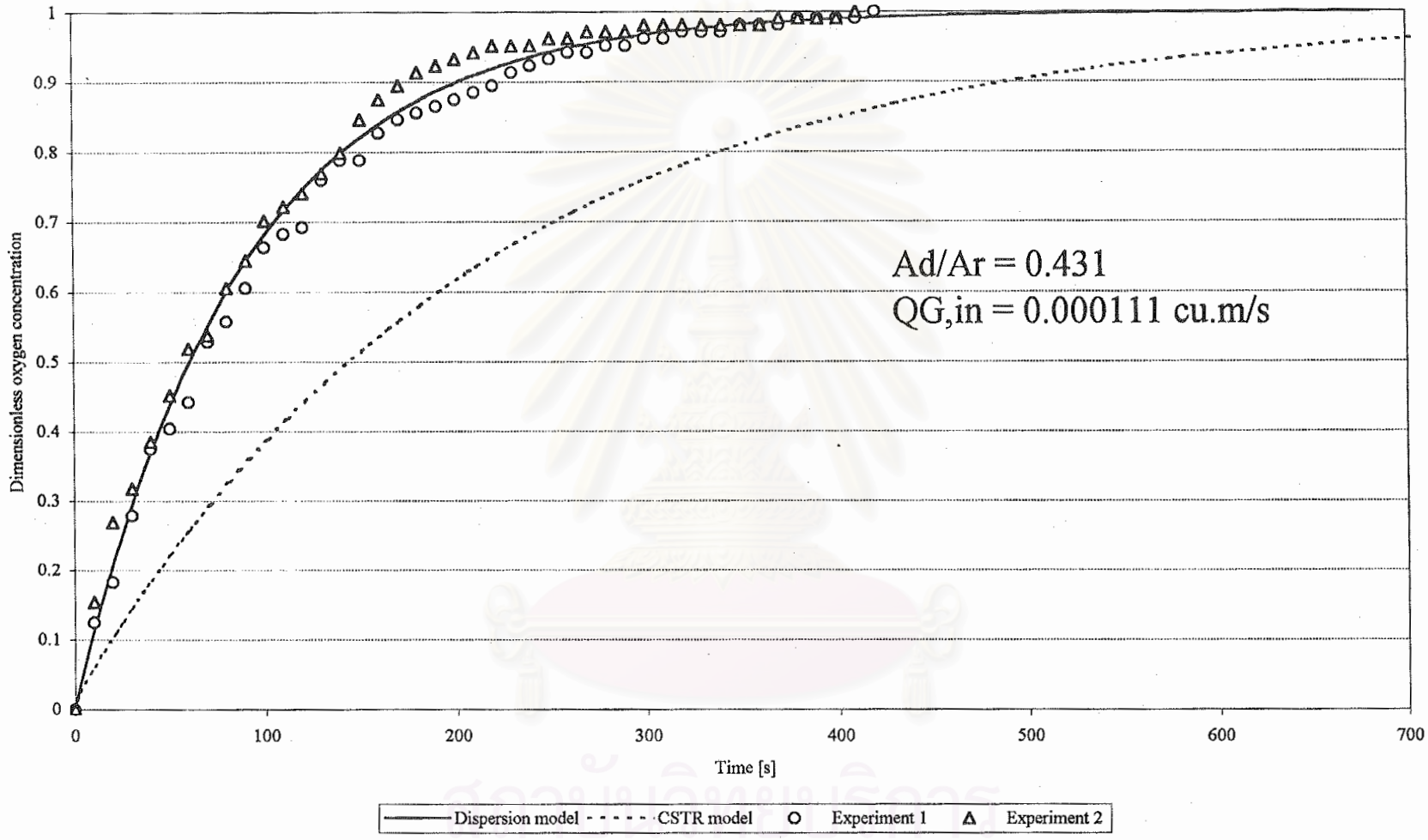

Figure 4.3.4C. Comparison between simulation results (Dispersion and CSTR models) and reported experimental data (Case III)

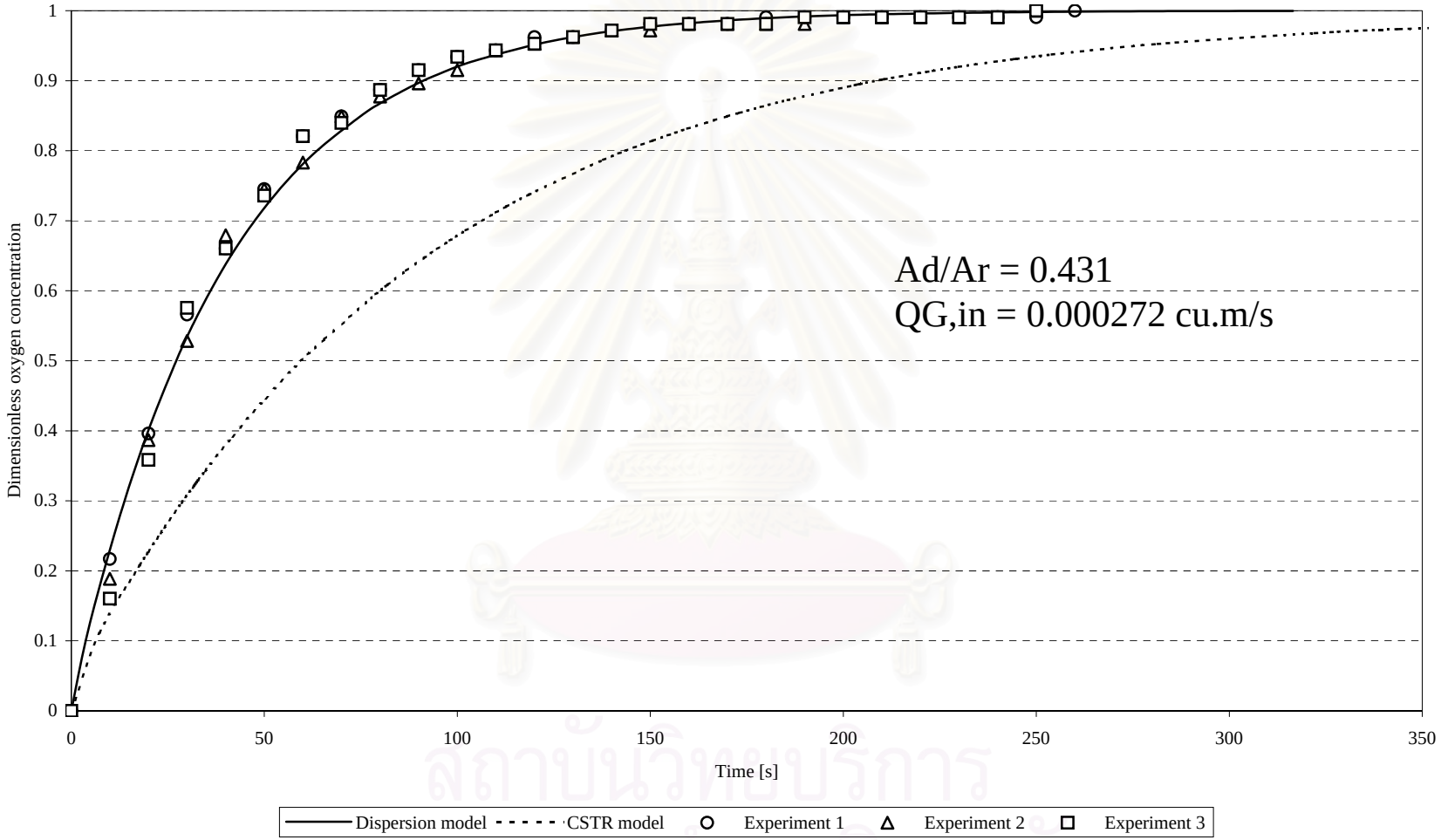

Figure 4.3.4D. Comparison between simulation results (Dispersion and CSTR models) and reported experimental data (Case IV)

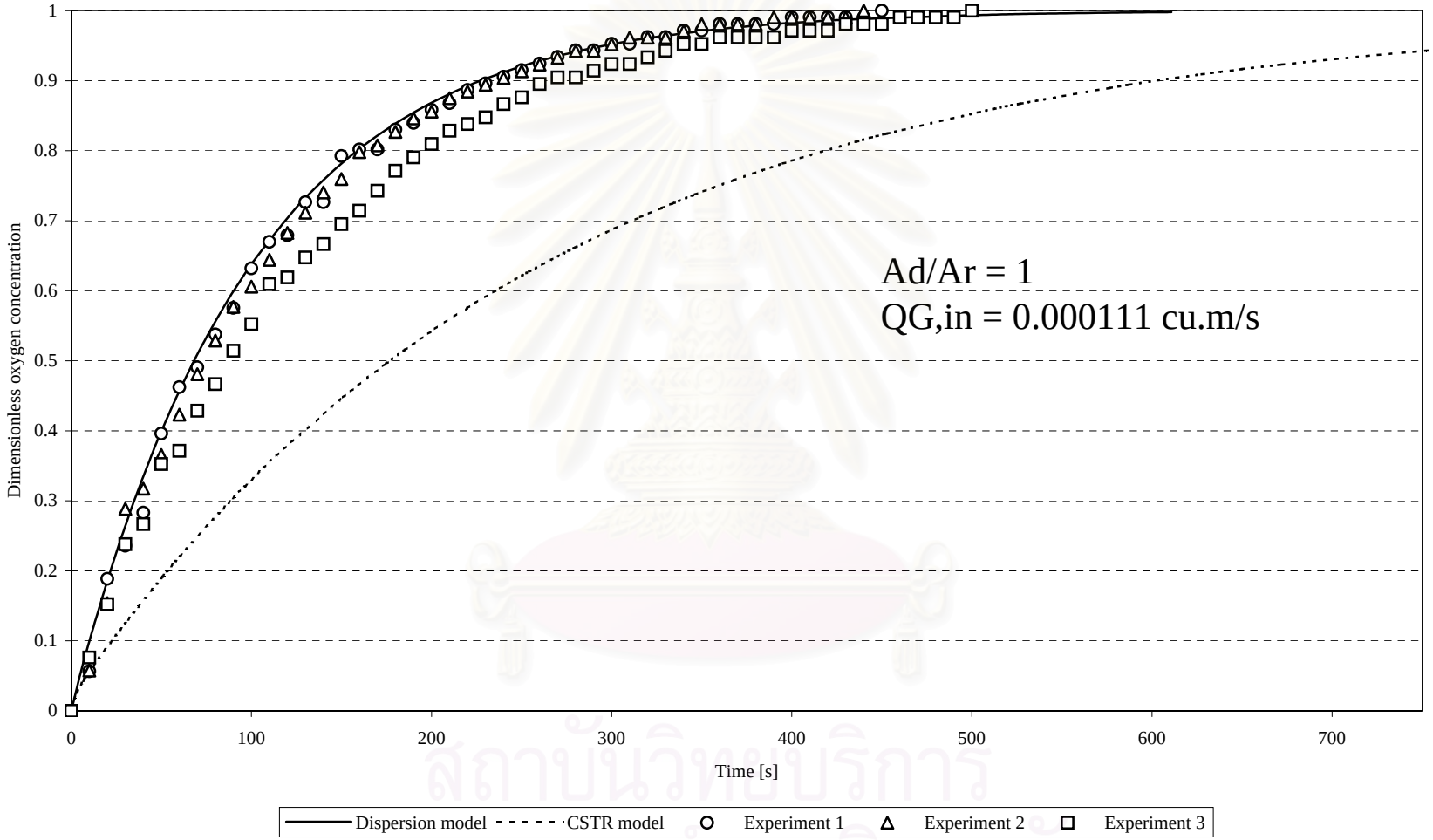

Figure 4.3.4E. Comparison between simulation results (Dispersion and CSTR models) and reported experimental data (Case V)

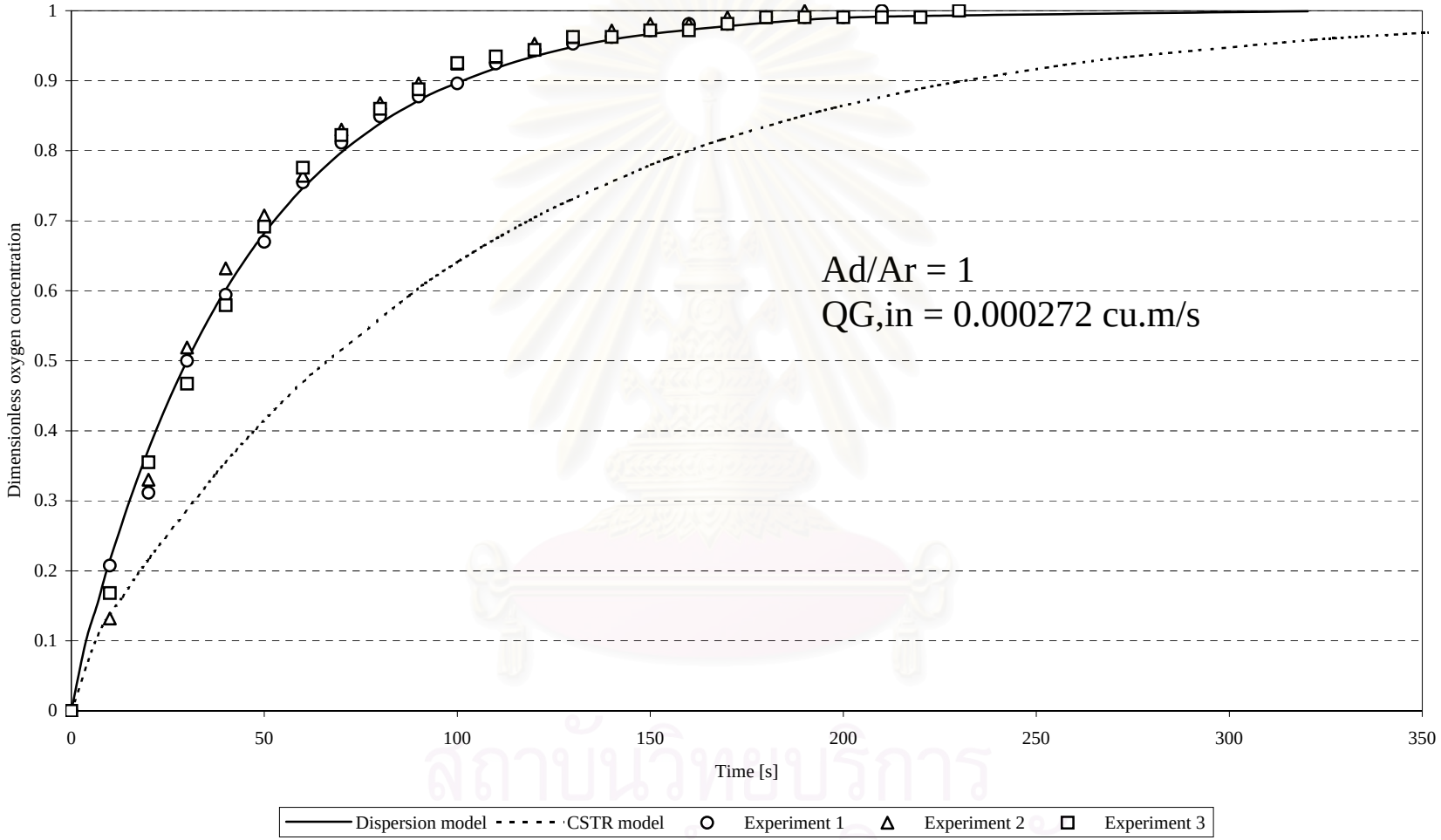

Figure 4.3.4F. Comparison between simulation results (Dispersion and CSTR models) and reported experimental data (Case VI)

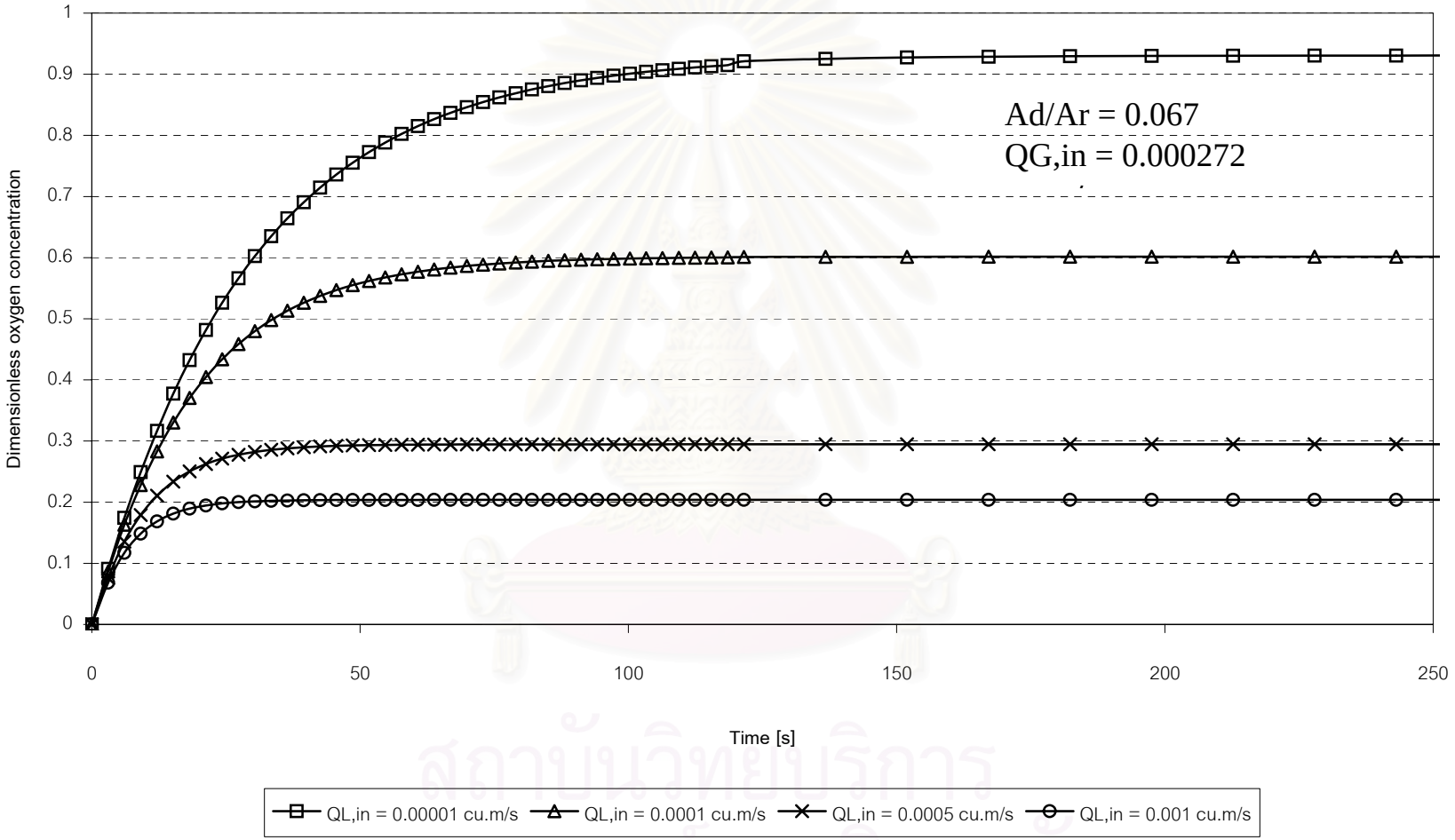

Figure 4.4A. Effect of liquid feed flow rate ($Q_{L,in}$) on liquid phase oxygen concentration in the riser section (Case II)

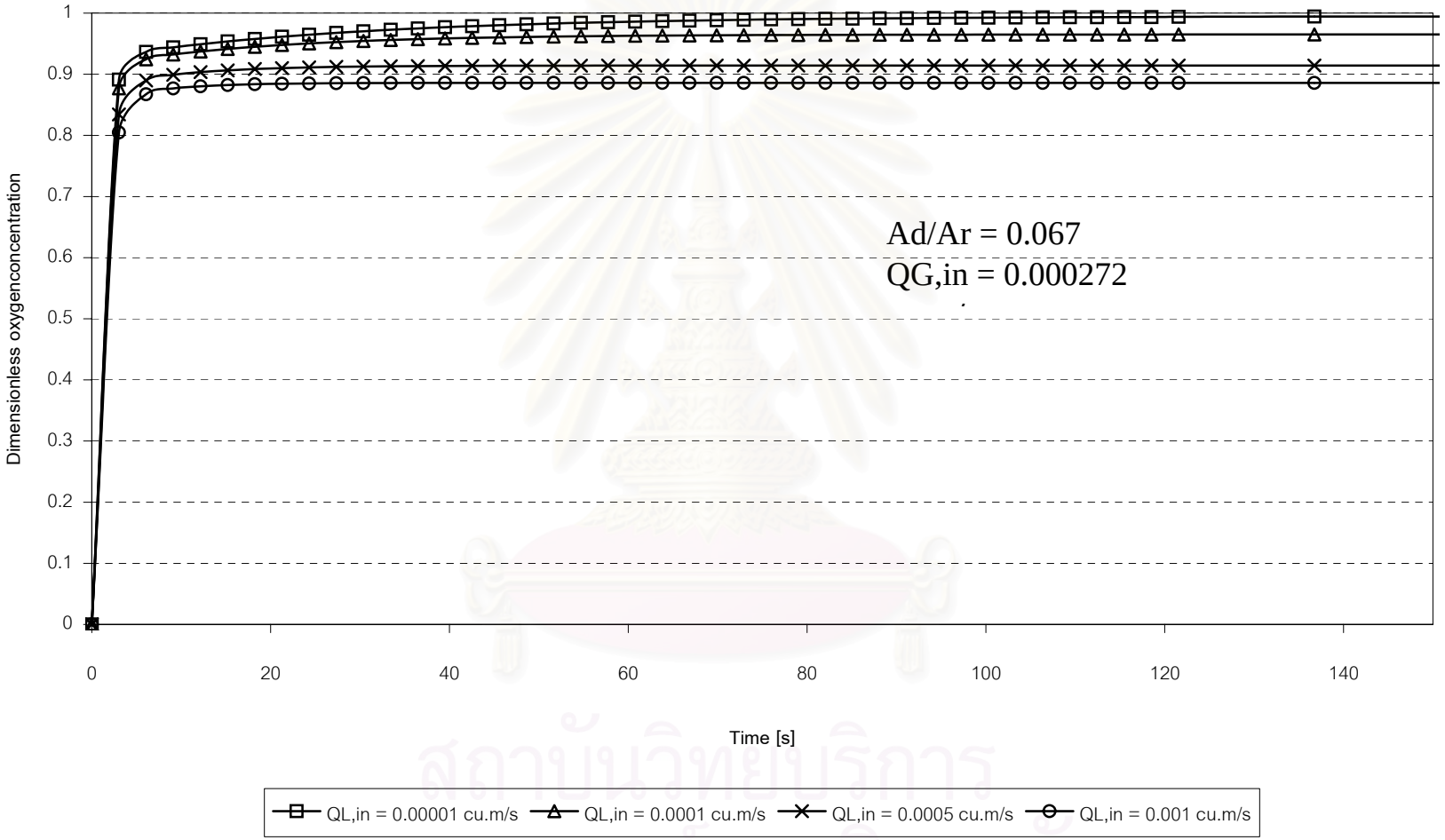

Figure 4.4B. Effect of liquid feed flow rate ($Q_{L,in}$) on gas phase oxygen concentration in the riser section (Case II)

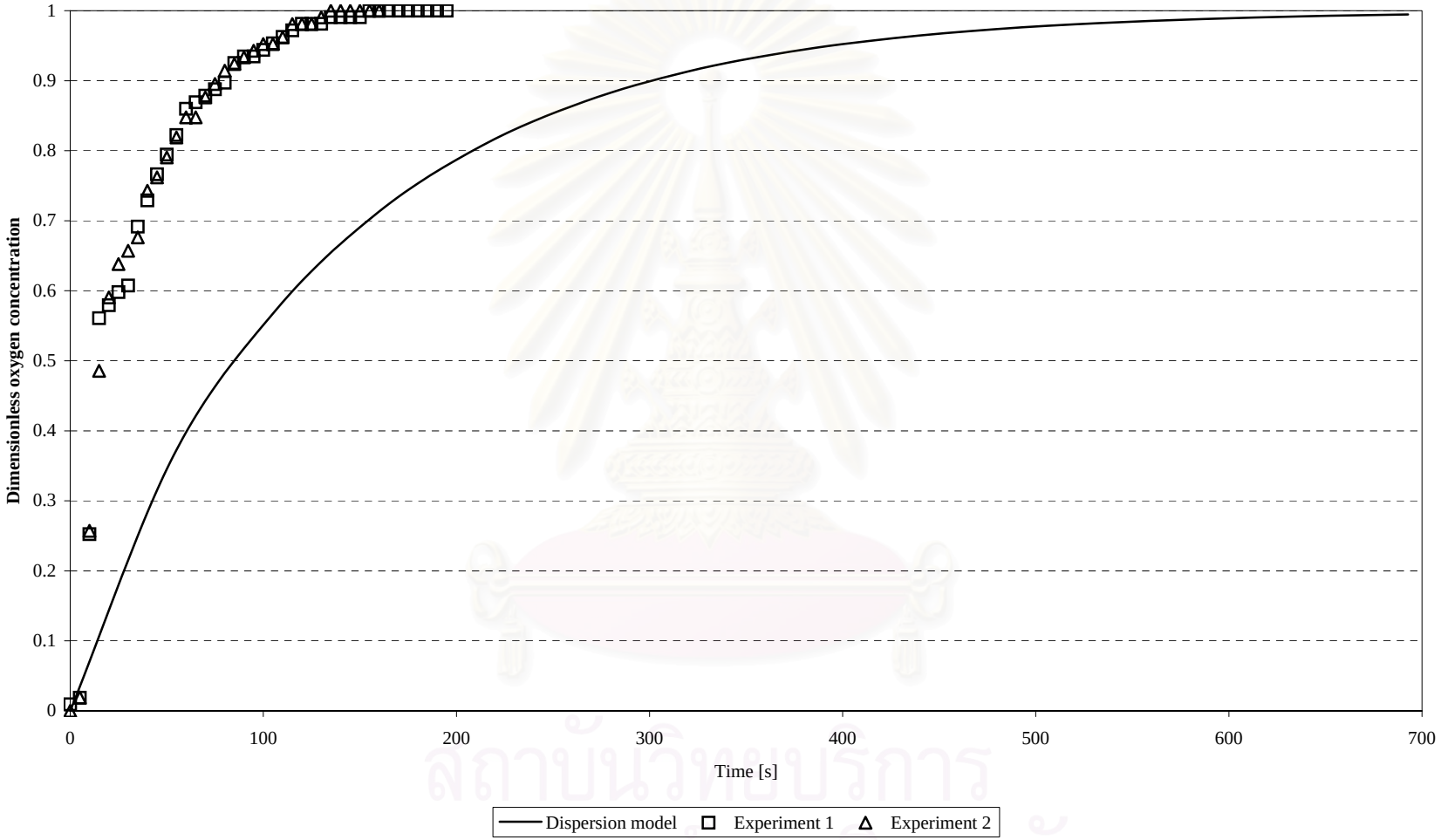

Figure 4.5. Comparison between simulation results (Dispersion model) and reported experimental data (for the large scale ALC)

CHAPTER 5

Conclusions and Recommendations

5.1 Validity of the Developed Mathematical Models

The transient gas-liquid oxygen mass transfer in the ALC was successfully described by mathematical models based on continuity equations both in gas and liquid phases. The model was able to predict not only oxygen concentration in liquid phase, but also the oxygen concentration in gas phase. The major achievements include:

(*i*) ***Numerical testing for appropriateness of mathematical models for oxygen mass transfer in the ALC***

The mathematical models were tested by both numerical and various modeling techniques. The testung of numerical solutions from the Crank Nicholson criteria and the 4^{th}-order Runge-Kutta method indicated a good agreement between the prediction of oxygen concentration profile in the ALC and the experimental reported data. The CSTR model was found to predict the slowest oxygen mass transfer rate, whilst the Dispersion model was the most rapid. Solutions from the PFR and CSTRs-in-Series models lied between the CSTR and Dispersion models.

(*ii*) ***Experimental confirmation of the appropriateness of the mathematical models for oxygen mass transfer in the ALC***

- The simulation results clearly indicated that increasing the overall volumetric mass transfer coefficient (K_La) and the gas phase dispersion coefficient ($D_{G,r}$) resulted in a higher rate of mass transfer. However, the influence of the gas phase dispersion coefficient in the riser was not as significant as that of K_La.

- The simulated gas phase oxygen concentration by the Dispersion model revealed that the mixing in the gas phase is extremely rapid when compared to the rate of gas-liquid mass transfer.
- The Dispersion model was found to be most accurate in describing the transient gas-liquid mass transfer behavior in the ALC. The best simulation results were obtained from the sensitivity analysis of the two uncertain parameters, i.e. K_La and $D_{G,r}$. The model was proven to be able to describe the mass transfer performance in the ALC with variable design and operating parameters.

(*iii*) *Prediction of the performance of the ALC with continuous liquid feed ($Q_{L,in}$) from the Dispersion model*

The effect of liquid feed flowrate ($Q_{L,in}$) on oxygen concentration profiles in gas and liquid phases in the riser was predicted. It was found that increasing $Q_{L,in}$ resulted in decreases in the steady state dissolved oxygen concentrations both in gas and liquid phases. However, at this condition, an increase in the mass transfer rate was obtained from a large concentration difference driving force between the two phases.

(*iv*) *The prediction of oxygen mass transfer behavior in a high draft tube ALC by the Dispersion model.*

The simulation results showed that there was a large discrepancy between the prediction and the real concentration profiles for a high draft tube ALC. This might have taken place due to the lack of some crucial knowledge on mass transport in the system. Several possibilities that caused this inaccuracy were proposed at the end of the previous chapter which included an uncertainty in the estimations of bubble velocity, overall mass transfer coefficient in each section of the ALC, variations in the gas holdups along the height of the contactor, etc. Further attention in this area is therefore needed.

5.2 Concluding Remarks

Although the model still shows some weaknesses in describing the performance of the ALC, this work contributes significantly to the existing knowledge on the actual transport phenomena that take place in the system. It has been shown that the ALC could well be described by a set of simple continuity equations where each part of the ALC could be represented by a fundamental reactor type such as a CSTR, PFR with or without the dispersion term. The derivation of the model has been made rather clear and simple, which helps in a further modification to include other incidents that might occur in the ALC. For instance, a reaction term might easily be inserted into the right hand side of the continuity equation in a similar fashion with the mass transfer term. The outcome from this work is therefore considered beneficial for the design of a small scale ALC.

สถาบันวิทยบริการ
จุฬาลงกรณ์มหาวิทยาลัย

REFERENCE

Andre, G., Robinson, C.W., Moo-Young, M., 1983. New Criteria for Application of the Well-Mixed Model to Gas-Liquid Mass Transfer Studies. *Chem.Engng.Sci.* **38**(11): 1845-1854.

Bello, R. A., Robinson, C. W. and Moo-Young, M., 1984. Liquid circulation and mixing characteristics of airlift contactors. *Can. J. chem. Engng.* **62**: 573-577.

Bello, R. A., Robinson, C. W. and Moo-Young, M., 1985. Gas hold-up and overall volumetric oxygen transfer coefficient in airlift contactors. *Biotechnol. Bioeng.* **27**: 369-381.

Calvo E.G., 1989. A fluid dynamic model for airlift loop reactors. *Chem.Eng.Sci.* **44** (2):321-323.

Calvo E.G., and Leton, P., 1991. A fluid dynamic model for bubble columns and airlift reactors. *Chem. Eng.Sci.* **46**:2947-2951.

Clark, N.N. and Flemmer, R.L. 1985. Prediction in the holdup in two-phase bubble upflow and downflow using the Zuber and Findlay drift-flux model. *AIChE. J*. **31**:500-503.

Chisti, M. Y. and Moo-Young, M.,1988. Hydrodynamics and oxygen transfer in pneumatic devices. *Biotechnol. Bioeng.* **31**:487-494.

Chisti, M.Y., Halard, M. and Moo-Young, M., 1988. Liquid circulation in airlift reactors. *Chem. Eng. Sci.* **43**:451-457.

Choi, K.H., 1999. A Mathematical Model for Unsteady-State Oxygen Transfer in an External-Loop Airlift Reactor. *Korean, Chem. Eng*. **16**(4):441-448.

Dhaouadi, H., Poncin, S., Hornut, J.M., and Wild, G., 1996. Hydrodynamics of Airlift reactor: Experimental and Modeling. *Chem. Eng.Sci*. **51**(11):2625-2630.

Dhaouadi H., Poncin, S., Hornut, J.M., Wild, G., Oinas, P., and Korpijarvi, J., 1997. Mass transfer in an external-loop airlift reactor: experiments and modeling. *Chem. Eng.Sci.* **52**(21/22): 3909-3917.

Gavrilescu, M., and Tudose, R.Z., 1998. Modelling of liquid velocity in concentric-tube airlift reactors. *Chem. Eng.J.* **69**: 85-91.

Kemblowski, Z., Przywarski, J. and Diab, A., 1993, An average gas hold-up and liquid circulation velocity in airlift reactors with external loop. *Chem. Eng. Sci.* **48**: 4023-4035.

Kreyszig, E., '*Advanced Engineering Mathematics*, 8th Edn. Wiley, New York 1999.

Krichnavaruk, S. and Pavasant, P., 2000. unpublished report.

Levenspiel O., '*Chemical Reaction Engineering*, 2nd Edn. Wiley, New York 1972.

Merchuk, J. C. and Stein, Y., 1981, Local hold-up and liquid velocity in air-lift reactors. *AIChE.J.* **27:** 377-388.

Merchuk, J. C. and Siegel, M.H., 1988, Airlift reactors in chemical and biological technology. *J. Chem. Technol. Biotechnol.* **41**: 105-120.

Rüffer, H. M., Liwei Wan, Lübbert, A. and Schügerl, K., 1994, Interpretation of gas residence time distributions in large airlift tower loop reactors. *Bioproc. Eng.* **11**: 153-159.

Sáez, A.E., Marquez., M.A., Roberts, G.W., and Carbonell, R.G., 1998, Hydrodynamic Model for Gas-Lift Reactors. *AIChE.J.* **44**(6): 1413-1422.

Shamlou, P. A., Pollard, D.J. and Iaon, A.P., 1995, Volumetric mass transfer coefficient in concentric tube airlift bioreactors. *Chem. Eng. Sci.* **50**: 1579 – 1590.

Verlaan, P., Tramper, J. and Riet, V., 1986, A Hydrodynamic Model for an airlift-Loop Bioreactor with External Loop. *Chem. Eng. J.* **33**: B43-B53.

Verlaan, P., Van Eijs, A. M. M., Tramper, J., Van't Riet, K. and Luyben, K. Ch. A. M., 1989, Estimation of an airlift-loop reactor. *Chem. Eng. Sci.* **44**, 1139-1146.

Wongsuchoto, P. and Pavasant, P., 2000. unpublished report.

Zhao, M., Niranjan, D., Davidson, J. F., 1994, Mass transfer to viscous liquids in bubble columns and airlift reactors: Influence of baffles. *Chem. Eng. Sci.* **49**: 2359-2369.

Zuber N. and Findlay J.A., 1965, Average volumetric concentration in two-phase flow system. *J. Heat Transfer-Transactions of the ASME* ,**Serie C**(6): 453-457.

APPENDICES

สถาบันวิทยบริการ
จุฬาลงกรณ์มหาวิทยาลัย

Appendix A

Program source codes

This appendix presents all of the main programs used in this work. The following table gives information about what category of each program was used in this work. All programs were written in MATLAB(VERSION 5.3.1)

Program Name	Usage
CSTR Model	All regions(riser, gas separator and downcomer) were considered as completely mixed zone.
CSTRs-in-Series Model	The riser and downcomer were modeled by CSTRs-in series, whilst the CSTR were used to represent in gas separator.
Dispersion Model 1	The riser and downcomer were considered as a plug flow region with dispersion, where as the gas separator were modeled as a region of completely mixed. The model is discretised following the Crank-Nicholson criteria.
Dispersion Model 2	The riser and downcomer were considered as a plug flow region with dispersion, where as the gas separator were modeled as a region of completely mixed. The model is discretised following the Forward finite difference criteria.

สถาบันวิทยบริการ
จุฬาลงกรณ์มหาวิทยาลัย

```
#-----------------------------------------------

%File Name:CSTR MODEL
%Programe Cstr behavior in all section of retactor

#-----------------------------------------------

clear

H1=input('Unaereated Height in reactor (Riser and
Downcomer) = ');
Hd=input('Dispersion Height in reactor = ');
A1=input('Cross sectional Area in section of Riser = ');
A2=input('Cross sectional Area in section of gas
seperator = ');
ratio=input('Ad/Ar ratio = ');
A3=A1*ratio;

vl_downcomer=input('liquid velocity in downcomer =  ');
e1=input('gas hold up in riser = ');
e3=input('gas hold up in gas separator = ');
kla=input('kla of reactor = ');
e2=e1;
%density of liquid phase (1000 kg/m^3))
denst=1000;
%('diameter of bubble (0.005 m))
d_bubble=0.005;
%('surface tension of liquid phase (0.07275 kg/sec^2))
s_tension=0.07275;
Qg_in=input('inlet gas flowrate = ');
Ql_in=input('liquid feed flow rate = ');

tfinal=input('input final time =') ;
del_t=input('input step size of time = ');
tin=0;
t=tin:del_t:tfinal;
h=del_t;

H2=Hd-H1;
V1=A1*H1;
V2=A2*H2;
V3=A3*H1;

vl_riser=((1-e3)*A3*vl_downcomer+Ql_in)/((1-e1)*A1);
vl_top=((1-e1)*vl_riser*A1-Ql_in)/((1-e2)*A3);
x=2.14*s_tension/(denst*d_bubble)+(0.505*10*d_bubble);
ub_terminal=sqrt(x);
v_slip=ub_terminal*(1-e1)^0.702;
vg_riser=vl_riser+v_slip;
vg_downcomer=(vg_riser*A1*e1-Qg_in)/(A3*e3);
vg_top=vg_downcomer*e3/e2;

t_factor=V1/(A3*vl_downcomer);


%COEFICIENT OF RISER(CSTR)
alpha1=e3*A3*vg_downcomer*t_factor/(e1*V1);
beta1=A1*vg_riser*t_factor/V1;
gamma1=((1-e1)/e1)*kla*V1*t_factor/V1;
ceta1=Qg_in*t_factor/(e1*V1);

coef1=(1-e3)*A3*vl_downcomer*t_factor/((1-e1)*V1);
coef2=A1*vl_riser*t_factor/(V1);
coef3=kla*t_factor;

%COEFICIENT OF GAS SEPARATOR(CSTR)
alpha2=e1*A1*vg_riser*t_factor/(e2*V2);
beta2=vg_top*A3*t_factor/V2;
gamma2=((1-e2)/e2)*kla*t_factor;
ceta2=Qg_in*t_factor/(e2*V2);

coef4=(1-e1)*vl_riser*A1*t_factor/((1-e2)*V2);
coef5=A3*vl_top*t_factor/V2;
coef6=kla*t_factor;
coef_6=Ql_in*t_factor/((1-e2)*V2);
```

```
%COEFICIENT OF DOWNCOMER(CSTR)
alpha3=e2*A3*vg_top*t_factor/(e3*V3);
beta3=vg_downcomer*t_factor;
gamma3=((1-e3)/e3)*kla*t_factor;

coef7=(1-e2)*A3*vl_top*t_factor/((1-e3)*V3);
coef8=A3*vl_downcomer*t_factor/V3;
coef9=kla*t_factor;

%SET UP INITIAL AND BOUNDARY CONDITIONS
Og_riser(1)=1;
Og_top(1)=1;
Og_downcomer(1)=1;
Ol_riser(1)=0;
Ol_top(1)=0;
Ol_downcomer(1)=0;
Olr(1,1)=0;
%SOLVE FOR OXYGEN RESPONSE
%Programe Beginning

% FIND OXYGEN CONCENTRATION WITH TIME

for i=1:length(t)-1;
%Rungr Kutta
%SET UP k l m n
k1=h*(alpha1*Og_downcomer(i)-gamma1*(Og_riser(i)-
Ol_riser(i))-beta1*Og_riser(i)+ceta1);
l1=h*(coef1*Ol_downcomer(i)-coef2*Ol_riser(i)+coef3*
(Og_riser(i)-Ol_riser(i)));
m1=h*(alpha2*Og_riser(i)-beta2*Og_top(i)-gamma2*(Og_top
(i)-Ol_top(i))-ceta2*Og_top(i));
n1=h*(coef4*Ol_riser(i)-coef5*Ol_top(i)+coef6*(Og_top
(i)-Ol_top(i))-coef_6*Ol_top(i));
o1=h*(alpha3*Og_top(i)-beta3*Og_downcomer(i)-gamma3*
(Og_downcomer(i)-Ol_downcomer(i)));
p1=h*(coef7*Ol_top(i)-coef8*Ol_downcomer(i)+coef9*
(Og_downcomer(i)-Ol_downcomer(i)));

k2=h*(alpha1*(Og_downcomer(i)+o1/2)-gamma1*((Og_riser
(i)+k1/2)-(Ol_riser(i)+l1/2))-beta1*(Og_riser
(i)+k1/2)+ceta1);
l2=h*(coef1*(Ol_downcomer(i)+p1/2)-coef2*(Ol_riser
(i)+l1/2)+coef3*((Og_riser(i)+k1/2)-(Ol_riser
(i)+l1/2)));
m2=h*(alpha2*(Og_riser(i)+k1/2)-beta2*(Og_top(i)+m1/2)-
gamma2*((Og_top(i)+m1/2)-(Ol_top(i)+n1/2))-ceta2*(Og_top
(i)+m1/2));
n2=h*(coef4*(Ol_riser(i)+l1/2)-coef5*(Ol_top
(i)+n1/2)+coef6*((Og_top(i)+m1/2)-(Ol_top(i)+n1/2))-
coef_6*Ol_top(i));
o2=h*(alpha3*(Og_top(i)+m1/2)-beta3*(Og_downcomer
(i)+o1/2)-gamma3*((Og_downcomer(i)+o1/2)-(Ol_downcomer
(i)+p1/2)));
p2=h*(coef7*(Ol_top(i)+n1/2)-coef8*(Ol_downcomer
(i)+p1/2)+coef9*((Og_downcomer(i)+o1/2)-(Ol_downcomer
(i)+p1/2)));

k3=h*(alpha1*(Og_downcomer(i)+o2/2)-gamma1*((Og_riser
(i)+k2/2)-(Ol_riser(i)+l2/2))-beta1*(Og_riser
(i)+k2/2)+ceta1);
l3=h*(coef1*(Ol_downcomer(i)+p2/2)-coef2*(Ol_riser
(i)+l2/2)+coef3*((Og_riser(i)+k2/2)-(Ol_riser
(i)+l2/2)));
m3=h*(alpha2*(Og_riser(i)+k2/2)-beta2*(Og_top(i)+m2/2)-
gamma2*((Og_top(i)+m2/2)-(Ol_top(i)+n2/2))-ceta2*(Og_top
(i)+m2/2));
n3=h*(coef4*(Ol_riser(i)+l2/2)-coef5*(Ol_top
(i)+n2/2)+coef6*((Og_top(i)+m2/2)-(Ol_top(i)+n2/2))-
coef_6*Ol_top(i));
o3=h*(alpha3*(Og_top(i)+m2/2)-beta3*(Og_downcomer
(i)+o2/2)-gamma3*((Og_downcomer(i)+o2/2)-(Ol_downcomer
(i)+p2/2)));
p3=h*(coef7*(Ol_top(i)+n2/2)-coef8*(Ol_downcomer
(i)+p2/2)+coef9*((Og_downcomer(i)+o2/2)-(Ol_downcomer
(i)+p2/2)));
```

```
k4=h*(alpha1*(Og_downcomer(i)+o3)-gamma1*((Og_riser
(i)+k3)-(Ol_riser(i)+l3))-beta1*(Og_riser(i)+k3)+ceta1);
l4=h*(coef1*(Ol_downcomer(i)+p3)-coef2*(Ol_riser
(i)+l3)+coef3*((Og_riser(i)+k3)-(Ol_riser(i)+l3)));
m4=h*(alpha2*(Og_riser(i)+k3)-beta2*(Og_top(i)+m3)-
gamma2*((Og_top(i)+m3)-(Ol_top(i)+n3))-ceta2*(Og_top
(i)+m3));
n4=h*(coef4*(Ol_riser(i)+l3)-coef5*(Ol_top(i)+n3)+coef6*
((Og_top(i)+m3)-(Ol_top(i)+n3))-coef_6*Ol_top(i));
o4=h*(alpha3*(Og_top(i)+m3)-beta3*(Og_downcomer(i)+o3)-
gamma3*((Og_downcomer(i)+o3)-(Ol_downcomer(i)+p3)));
p4=h*(coef7*(Ol_top(i)+n3)-coef8*(Ol_downcomer
(i)+p3)+coef9*((Og_downcomer(i)+o3)-(Ol_downcomer
(i)+p3)));

Og_riser(i+1)=Og_riser(i)+1/6*(k1+2*k2+2*k3+k4);
Ol_riser(i+1)=Ol_riser(i)+1/6*(l1+2*l2+2*l3+l4);
Og_top(i+1)=Og_top(i)+1/6*(m1+2*m2+2*m3+m4);
Ol_top(i+1)=Ol_top(i)+1/6*(n1+2*n2+2*n3+n4);
Og_downcomer(i+1)=Og_downcomer(i)+1/6*(o1+2*o2+2*o3+o4);
Ol_downcomer(i+1)=Ol_downcomer(i)+1/6*(p1+2*p2+2*p3+p4);

if floor((i-1)/500)==ceil((i-1)/500)
   fprintf('i=%f \n',i);
end

end

   k=1;
   for i=1:length(t)-1
      if floor((i-1)/1000)==ceil((i-1)/1000)
         Olrn(k,1) = Ol_riser(i) ;
         k = k+1;
      end
   end

save effectkla Olrn -ascii;
```

```
figure(1)
plot(t,Ol_riser,'r');
title('CSTR Ol riser  ');
xlabel('time(-) ');
ylabel('concentration of Ol_r(-) ');
grid on

figure(2)
plot(t,Og_riser,'r');
title('Og riser ');
xlabel('time(-) ');
ylabel('concentration of Og_r(-) ');
grid on

figure(4)
subplot(211);plot(t,Ol_top,'r');
ylabel('concentration of Ol_t ');
grid on
subplot(212);plot(t,Og_top,'b');
xlabel('time ');
ylabel('concentration of Og_t ');
grid on

figure(5)
plot(t,Ol_downcomer,'r');
title('Ol downcomer');
xlabel('time ');
ylabel('concentration of Ol_d ');
grid on

figure(6)
plot(t,Og_downcomer,'r');
title('Og downcomer');
xlabel('time ');
ylabel('concentration of Og_d ');
grid on

#------------------END-----------------------
```

```
#-----------------------------------------------

%File Name:CSTRs-in-Series MODEL
%Programe CSTRs-in-Series in RISER and DOWNCOMER

#-----------------------------------------------

clear

H1=input('Unaereated Height in reactor (Riser and
Downcomer) = ');
Hd=input('Dispersion Height in reactor = ');
A1=input('Cross sectional Area in section of Riser = ');
A2=input('Cross sectional Area in section of gas
seperator = ');
ratio=input('Ad/Ar ratio = ');
A3=A1*ratio;

vl_downcomer=input('liquid velocity in downcomer =  ');
e1=input('gas hold up in riser = ');
e3=input('gas hold up in gas separator = ');
kla=input('kla of reactor = ');
e2=e1;
%density of liquid phase (1000 kg/m^3))
denst=1000;
%('diameter of bubble (0.005 m))
d_bubble=0.005;
%('surface tension of liquid phase (0.07275 kg/sec^2))
s_tension=0.07275;
Qg_in=input('inlet gas flowrate = ');
Ql_in=input('liquid feed flow rate = ');

tfinal=input('input final time (500)=') ;
del_t=input('input delta_t(0-0.9) = ');
tin=0;
t=tin:del_t:tfinal;
h=del_t;

H2=Hd-H1;

m=input('enter number of interval(CSTRs-in-Series) in
riser = ');
n=input('enter number of interval(CSTRs-in-Series) in
downcomer = ');

H2=Hd-H1;
Vr=A1*H1;
Vtop=A2*H2;
Vd=A3*H1;

V1=Vr/m;
V2=Vtop;
V3=Vd/n;

vl_riser=((1-e3)*A3*vl_downcomer+Ql_in)/((1-e1)*A1);
vl_top=((1-e1)*vl_riser*A1-Ql_in)/((1-e2)*A3);
x=2.14*s_tension/(denst*d_bubble)+(0.505*10*d_bubble);
ub_terminal=sqrt(x);
v_slip=ub_terminal*(1-e1)^0.702;
vg_riser=vl_riser+v_slip;
vg_downcomer=(vg_riser*A1*e1-Qg_in)/(A3*e3);
vg_top=vg_downcomer*e3/e2;

%COEFICIENT OF RISER(CSTR in series)
%At first point of CSTR in series
alpha1=e3*vg_downcomer*Vr*del_t/(2*e1*vl_downcomer*V1);
beta1=A1*vg_riser*Vr*del_t/(2*A3*vl_downcomer*V1);
gamma1=(1-e1)*kla*Vr*del_t/(2*e1*A3*vl_downcomer);
ceta1=Qg_in*Vr*del_t/(e1*A3*vl_downcomer*V1);

coef1=(1-e3)*Vr*del_t/(2*(1-e1)*V1);
coef2=A1*vl_riser*Vr*del_t/(2*A3*vl_downcomer*V1);
coef3=kla*Vr*del_t/(2*A3*vl_downcomer);

%At i=2 to i=m of CSTR in series
alpha1_1=A1*vg_riser*Vr*del_t/(2*A3*vl_downcomer*V1);
```

```
beta1_1=alpha1_1;
gamma1_1=(1-e1)*kla*Vr*del_t/(2*e1*A3*vl_downcomer);

coef1_1=A1*vl_riser*Vr*del_t/(2*A3*vl_downcomer*V1);
coef2_1=coef1_1;
coef3_1=kla*Vr*del_t/(2*A3*vl_downcomer);

%COEFICIENT OF GAS SEPARATOR(CSTR)
alpha2=e1*A1*vg_riser*Vr*del_t/(2*e2*A3*vl_downcomer*V2)
;
beta2=vg_top*Vr*del_t/(2*vl_downcomer*V2);
gamma2=(1-e2)*kla*Vr*del_t/(2*e2*A3*vl_downcomer);
ceta2=Vr*Qg_in*del_t/(2*e2*A3*vl_downcomer*V2);

coef4=(1-e1)*vl_riser*A1*Vr*del_t/(2*A3*(1-
e2)*vl_downcomer*V2);
coef5=vl_top*Vr*del_t/(2*vl_downcomer*V2);
coef6=kla*Vr*del_t/(2*A3*vl_downcomer);
coef_6=Ql_in*Vr*del_t/(2*(1-e2)*A3*vl_downcomer*V2);

%COEFICIENT OF DOWNCOMER(Cstr in series)
%GAS PHASE COEFICIENT
% i=1 first point
alpha3=e2*vg_top*Vr*del_t/(2*e3*vl_downcomer*V3);
beta3=(vg_downcomer*Vr*del_t)/(2*vl_downcomer*V3);
gamma3=(1-e3)*kla*Vr*del_t/(2*e3*A3*vl_downcomer);

% i=2,.....,m
alpha3_1=vg_downcomer*Vr*del_t/(2*vl_downcomer*V3);
beta3_1=alpha3_1;
gamma3_1=gamma3;

%LIQUID PHASE COEFICIENT
% i=1 first point
coef7=(1-e2)*vl_top*Vr*del_t/(2*(1-e3)*vl_downcomer*V3);
coef8=(Vr*del_t)/(2*V3);
coef9=kla*Vr*del_t/(2*A3*vl_downcomer);

%i=2,.....,m
coef7_1=Vr*del_t/(2*V3);
coef8_1=coef7_1;
coef9_1=coef9;

%SET UP INITIAL AND BOUNDARY CONDITIONS
for j=1:1:m
   Og_riser(1,j)=1;
end
   Og_top(1,1)=1;
for j=1:1:n
   Og_downcomer(1,j)=1;
end

for j=1:1:m
   Ol_riser(1,j)=0;
end
Ol_top(1,1)=0;
for j=1:1:n
   Ol_downcomer(1,j)=0;
end

%SOLVE FOR OXYGEN RESPONSE
%Programe Beginning

%SET UP INITIAL VALUE IN METRIX A

for i=1:1:2*n+2*m+2
   for j=1:1:2*n+2*m+2
      A(i,j)=0;
   end
end

%SET UP METRIX A IS (2n+4)*(2n+4)
%Metrix A Of CSTR in series in Riser
%First point in gas phase
A(1,1)=1+beta1+gamma1;
A(1,m+1)=-gamma1;
```

```
A(1,2*m+n+2)=-alpha1;

j=2;
k=2;
while j<=m
   if k>=2&k<=m
      A(j,k-1)=-alpha1_1;
      A(j,k)=(1+beta1_1+gamma1_1);
      A(j,k+m)=-gamma1_1;
   end
   j=j+1;
   k=k+1;
end

%First point in liquid phase
A(m+1,1)=-coef3;
A(m+1,m+1)=1+coef2+coef3;
A(m+1,2*m+2*n+2)=-coef1;

j=m+2;
k=m+2;
while j<=2*m
   if k>=m+2&k<=2*m
      A(j,k-1)=-coef1_1;
      A(j,k)=(1+coef2_1+coef3_1);
      A(j,k-m)=-coef3_1;
   end
   j=j+1;
   k=k+1;
end

%Metrix A Of CSTR in Gas seperator
A(2*m+1,m)=-alpha2;
A(2*m+1,2*m+1)=1+beta2+gamma2+ceta2;
A(2*m+1,2*m+2)=-gamma2;
A(2*m+2,2*m)=-coef4;
A(2*m+2,2*m+1)=-coef6;
A(2*m+2,2*m+2)=1+coef5+coef6+coef_6;

%Metrix A Of cstr in series in Downcomer
%First point of tank in series in gas phase
A(2*m+3,2*m+1)=-alpha3;
A(2*m+3,2*m+3)=1+beta3+gamma3;
A(2*m+3,2*m+n+3)=-gamma3;

j=2*m+4;
k=2*m+4;
while j<=2*m+n+2
   if k>=2*m+4&k<=2*m+n+2
      A(j,k-1)=-alpha3_1;
      A(j,k)=1+beta3_1+gamma3_1;
      A(j,k+n)=-gamma3_1;
   end
   j=j+1;
   k=k+1;
end

%First point of tank in series in liquid phase
A(2*m+n+3,2*m+2)=-coef7;
A(2*m+n+3,2*m+n+3)=1+coef8+coef9;
A(2*m+n+3,2*m+3)=-coef9;

j=2*m+n+4;
k=2*m+n+4;
while j<=2*m+2*n+2
   if k>=2*m+n+4&k<=2*m+2*n+2
      A(j,k-1)=-coef7_1;
      A(j,k)=1+coef8_1+coef9_1;
      A(j,k-n)=-coef9_1;
   end
   j=j+1;
   k=k+1;
end

metrixA=[A(1:2*m+2*n+2,1:2*m+2*n+2)];
```

สถาบันวิทยบริการ
จุฬาลงกรณ์มหาวิทยาลัย

```
% FIND OXYGEN CONCENTRATION WITH TIME

for i=1:length(t)-1;

%SET UP METRIX B

%SET UP METRIX B IN THE PART OF GAS AND LIQUID PHASE IN
RISER

% Gas phase i=1
b(1,1)=(1-beta1-
gamma1)*Og_riser(i,1)+alpha1*Og_downcomer
(i,n)+gamma1*Ol_riser(i,1)+ceta1;

% Gas phase i=2,.....,m
for j=2:1:m
   b(j,1)=alpha1_1*Og_riser(i,j-1)+(1-beta1_1-
gamma1_1)*Og_riser(i,j)+gamma1_1*Ol_riser(i,j);
end

% Liquid phase i=1
b(m+1,1)=(1-coef2-
coef3)*Ol_riser(i,1)+coef1*Ol_downcomer(i,n)+coef3*Og_ri
ser(i,1);

% Liquid phase i=2,.....,m
for j=m+2:1:2*m
   b(j,1)=coef1_1*Ol_riser(i,j-1-m)+(1-coef2_1-
coef3_1)*Ol_riser(i,j-m)+coef3_1*Og_riser(i,j-m);
end

%Gas phase in GAS SEPERATOR

b(2*m+1,1)=(1-beta2-gamma2-
ceta2)*Og_top(i,1)+alpha2*Og_riser(i,m)+gamma2*Ol_top
(i,1);

%LIQUID phase in GAS SEPERATOR

b(2*m+2,1)=(1-coef5-coef6-
coef_6)*Ol_top(i,1)+coef4*Ol_riser(i,m)+coef6*Og_top
(i,1);

%SET UP METRIX B IN THE PART OF GAS PHASE AND LIQUID
PHASE IN DOWNCOMER

% Gas phase i=1
b(2*m+3,1)=(1-beta3-
gamma3)*Og_downcomer(i,1)+alpha3*Og_top(i,1)+gamma3*Ol_d
owncomer(i,1);

% Gas phase i=2,.....,n
for j=2*m+4:1:2*m+n+2
   b(j,1)=alpha3_1*Og_downcomer(i,j-1-(2*m+2))+(1-
beta3_1-gamma3_1)*Og_downcomer(i,j-
(2*m+2))+gamma3_1*Ol_downcomer(i,j-(2*m+2));
end

% Liquid phase i=1
b(2*m+n+3,1)=(1-coef8-coef9)*Ol_downcomer
(i,1)+coef7*Ol_top(i,1)+coef9*Og_downcomer(i,1);

% Liquid phase i=2,.....,n
for j=2*m+n+4:1:2*m+2*n+2
   b(j,1)=coef7_1*Ol_downcomer(i,j-1-(2*m+n+2))+(1-
coef8_1-coef9_1)*Ol_downcomer(i,j-
(2*m+n+2))+coef9_1*Og_downcomer(i,j-(2*m+n+2));
end

B=[b(1:2*m+2*n+2,1)];

O(1:2*m+2*n+2,1)=inv(metrixA)*B;

for j=1:1:m
   Og_riser(i+1,j)=O(j,1);
end
```

```
for j=m+1:1:2*m
   Ol_riser(i+1,j-m)=O(j,1);
end

Og_top(i+1,1)=O(2*m+1,1);
Ol_top(i+1,1)=O(2*m+2,1);

for j=2*m+3:1:2*m+n+2
   Og_downcomer(i+1,j-(2*m+2))=O(j,1);
end

for j=2*m+n+3:1:2*m+2*n+2
   Ol_downcomer(i+1,j-(2*m+n+2))=O(j,1);
end

if floor((i-1)/500)==ceil((i-1)/500)
   fprintf('i=%f \n',i);
end

end

   k=1;
   for i=1:length(t)-1
      if floor((i-1)/20)==ceil((i-1)/20)
         Olrn(k,1) = Ol_riser(i,m) ;
         k = k+1;
      end %if
   end %for i
save tankinseries Olrn -ascii;


if m==1&n==1
   figure(1)
   plot(t,Ol_riser,'r');
   xlabel('time ');
   ylabel('concentration of Ol_r ');
   grid on
   figure(2)
   plot(t,Og_riser,'b');
   xlabel('time ');
   ylabel('concentration of Og_r ');
   grid on

   figure(3)
   plot(t,Ol_top,'r');
   xlabel('time ');
   ylabel('concentration of Ol_t ');
   grid on

   figure(4)
   plot(t,Og_top,'b');
   xlabel('time ');
   ylabel('concentration of Og_t ');
   grid on

   figure(5)
   plot(t,Ol_downcomer,'r');
   xlabel('time ');
   ylabel('concentration of Ol_d ');
   grid on

   figure(6)
   plot(t,Og_downcomer,'b');
   xlabel('time ');
   ylabel('concentration of Og_d ');
   grid on
else
   figure(1)
   plot(t,Ol_riser,'r');
   title('Ol riser');
   xlabel('time ');
   ylabel('concentration of Ol_r ');
   grid on
```

สถาบันวิทยบริการ
จุฬาลงกรณ์มหาวิทยาลัย

```
figure(2)
if m==1
   plot(t,Og_riser,'r');
   title('Og riser');
   xlabel('time ');
   ylabel('concentration of Og_r ');
   grid on
else
   figure(2)
   plot(t,Og_riser,'r');
   title('Og riser');
   xlabel('time ');
   ylabel('concentration of Og_r ');
   grid on
   figure(3)
   mesh(Og_riser);
   title('Og riser');
   grid on
end

figure(4)
subplot(211);plot(t,Ol_top,'r');
ylabel('concentration of Ol_t ');
grid on
subplot(212);plot(t,Og_top,'b');
xlabel('time ');
ylabel('concentration of Og_t ');
grid on

figure(5)
plot(t,Ol_downcomer,'r');
title('Ol downcomer');
xlabel('time ');
ylabel('concentration of Ol_d ');
grid on

figure(6)
   if n==1
      plot(t,Og_downcomer,'r');
      title('Og downcomer');
      xlabel('time ');
      ylabel('concentration of Og_d ');
      grid on
   else
      figure(6)
      plot(t,Og_downcomer,'r');
      title('Og downcomer');
      xlabel('time ');
      ylabel('concentration of Og_d ');
      grid on
      figure(7)
      mesh(Og_downcomer);
      title('Og downcomer');
      grid on
   end
end


#----------------END-------------------------
```

สถาบันวิทยบริการ
จุฬาลงกรณ์มหาวิทยาลัย

```
#-----------------------------------------------------

%File Name:DISPERSION MODEL 1
%Programe PFR with or without Dispersion term in RISER
and DOWNCOMER
%Discretisation by Crank-Nicholson method

#-----------------------------------------------------

clear

H1=input('Unaereated Height in reactor (Riser and
Downcomer) = ');
Hd=input('Dispersion Height in reactor = ');
A1=input('Cross sectional Area in section of Riser = ');
A2=input('Cross sectional Area in section of gas
seperator = ');
ratio=input('Ad/Ar ratio = ');
A3=A1*ratio;

vl_downcomer=input('liquid velocity in downcomer =  ');
e1=input('gas hold up in riser = ');
e3=input('gas hold up in gas separator = ');
kla=input('kla of reactor = ');
e2=e1;
%density of liquid phase (1000 kg/m^3))
denst=1000;
%('diameter of bubble (0.005 m))
d_bubble=0.005;
%('surface tension of liquid phase (0.07275 kg/sec^2))
s_tension=0.07275;
Qg_in=input('inlet gas flowrate = ');
Ql_in=input('liquid feed flow rate = ');
m=input('enter number of interval(PFR) in riser m= ');
n=input('enter number of interval(PFR) in downcomer n=
');
disp1=input('gas phase dispersion coefficient in riser
of the contactor = ');
disp2=input('liquid phase dispersion coefficient in
riser of the contactor = ');
del_z1=1/m;
disp3=input('gas phase dispersion coefficient in
downcomer of the contactor = ');
disp4=input('liquid phase dispersion coefficient in
downcomer of the contactor = ');
del_z2=1/n;

tfinal=input('input final time =') ;
del_t=input('input step size of time = ');
tin=0;
t=tin:del_t:tfinal;

H=H1;
H2=Hd-H1;
V1=A1*H1;
V2=A2*H2;
V3=A3*H1;

vl_riser=((1-e3)*A3*vl_downcomer+Ql_in)/((1-e1)*A1);
vl_top=((1-e1)*vl_riser*A1-Ql_in)/((1-e2)*A3);
x=2.14*s_tension/(denst*d_bubble)+(0.505*10*d_bubble);
ub_terminal=sqrt(x);
v_slip=ub_terminal*(1-e1)^0.702;
vg_riser=vl_riser+v_slip;
vg_downcomer=(vg_riser*A1*e1-Qg_in)/(A3*e3);
vg_top=vg_downcomer*e3/e2;

Q=Qg_in/(A3*e3);
vg_r=(vg_riser*A1*e1)/(A3*e3);
V=V1+V2+V3;
time=V1/(A3*vl_downcomer);

t_factor=V1/(A3*vl_downcomer);
z_factor=1/H;

%COEFICIENT OF RISER(PFR)
```

```
%GAS PHASE COEFICIENT
alpha1=(disp1*(z_factor^2)*t_factor*del_t)/
(del_z1*del_z1);
beta1=-(vg_riser*z_factor*t_factor*del_t)/del_z1;
gamma1=((1-e1)/e1)*kla*t_factor*del_t;
if alpha1~=0
   COEFA1=alpha1;
   COEFB1=2+(2*alpha1)+beta1+gamma1;
   COEFC1=alpha1+beta1;
   COEFD1=2-beta1-(2*alpha1)-gamma1;
   COEFE1=gamma1;
else
   COEFB1=2-beta1+gamma1;
   COEFC1=beta1;
   COEFD1=2+beta1-gamma1;
   COEFE1=gamma1;
end

%LIQUID PHASE COEFICIENT
coef1=-(vl_riser*z_factor*t_factor*del_t)/(del_z1);
coef2=(disp2*(z_factor^2)*t_factor*del_t)/
(del_z1*del_z1);
coef3=kla*t_factor*del_t;
if coef2~=0
   COEFA2=coef2;
   COEFB2=2+(2*coef2)+coef1+coef3;
   COEFC2=coef1+coef2;
   COEFD2=2-(2*coef2)-coef1-coef3;
   COEFE2=coef3;
else
   COEFB2=2-coef1+coef3;
   COEFC2=coef1;
   COEFD2=2+coef1-coef3;
   COEFE2=coef3;
end

%COEFICIENT OF GAS SEPARATOR(CSTR)
alpha2=e1*A1*vg_riser*t_factor*del_t/(2*e2*V2);
beta2=vg_top*A3*t_factor*del_t/(2*V2);
gamma2=(1-e2)*kla*t_factor*del_t/(2*e2);
ceta2=Qg_in*t_factor*del_t/(2*e2*V2);

coef4=(1-e1)*vl_riser*A1*t_factor*del_t/(2*(1-e2)*V2);
coef5=A3*vl_top*t_factor*del_t/(2*V2);
coef6=kla*t_factor*del_t/2;
coef_6=Ql_in*t_factor*del_t/(2*(1-e2)*V2);

%COEFICIENT OF DOWNCOMER(PFR)
%GAS PHASE COEFICIENT
alpha3=(disp3*(z_factor^2)*t_factor*del_t)/
(del_z2*del_z2);
beta3=-(vg_downcomer*z_factor*t_factor*del_t)/(del_z2);
gamma3=((1-e3)/e3)*kla*t_factor*del_t;
if alpha3~=0
   COEFA3=alpha3;
   COEFB3=2+(2*alpha3)+beta3+gamma3;
   COEFC3=alpha3+beta3;
   COEFD3=2-beta3-(2*alpha3)-gamma3;
   COEFE3=gamma3;
else
   COEFB3=2-beta3+gamma3;
   COEFC3=beta3;
   COEFD3=2+beta3-gamma3;
   COEFE3=gamma3;
end

%LIQUID PHASE COEFICIENT
coef7=-(vl_downcomer*z_factor*t_factor*del_t)/(del_z2);
coef8=(disp4*(z_factor^2)*t_factor*del_t)/
(del_z2*del_z2);
coef9=kla*t_factor*del_t;
if coef8~=0
   COEFA4=coef8;
   COEFB4=2+(2*coef8)+coef7+coef9;
   COEFC4=coef7+coef8;
   COEFD4=2-(2*coef8)-coef7-coef9;
```

```
   COEFE4=coef9;
else
   COEFB4=2-coef7+coef9;
   COEFC4=coef7;
   COEFD4=2+coef7-coef9;
   COEFE4=coef9;
end

%SET UP INITIAL AND BOUNDARY CONDITIONS
for j=1:1:m
   Og_riser(1,j)=1;
end

Og_top(1,1)=1;

for j=1:1:n
   Og_downcomer(1,j)=1;
end

for j=1:1:m
   Ol_riser(1,j)=0;
end

Ol_top(1,1)=0;

for j=1:1:n
   Ol_downcomer(1,j)=0;
end

%SOLVE FOR OXYGEN RESPONSE
%Programe Beginning
%SET UP INITIAL VALUE IN METRIX A
for i=1:1:2*n+2*m+2
   for j=1:1:2*n+2*m+2
      A(i,j)=0;
   end
end

%SET UP METRIX A IS (2m+2n+2)*(2m+2n+2)
%Metrix A OF PFR in Riser
% PFR in gas phase
%First point of PFR in gas phase
A(1,1)=e1*A1*vg_riser;
A(1,2*m+n+2)=-e3*A3*vg_downcomer;

j=2;
k=1;
while j<=m-1
   if k>=1&k<=m-2
      if alpha1~=0
         A(j,k)=-COEFA1;
         A(j,k+1)=COEFB1;
         A(j,k+2)=-COEFC1;
         A(j,k+1+m)=-COEFE1;
      else
         A(j,k)=COEFC1;
         A(j,k+1)=COEFB1;
         A(j,k+1+m)=-COEFE1;
      end
   end
   j=j+1;
   k=k+1;
end

%End point of PFR in gas phase
A(m,m-1)=-1;
A(m,m)=1;

%First point of PFR in liquid phase
A(m+1,m+1)=-(1-e1)*A1*vl_riser;
A(m+1,2*m+2*n+2)=(1-e3)*A3*vl_downcomer;

j=m+2;
k=m+1;
while j<=2*m-1
   if k>=m+1&k<=2*m-2
```

```
      if coef2~=0
         A(j,k)=-COEFA2;
         A(j,k+1)=COEFB2;
         A(j,k+2)=-COEFC2;
         A(j,k+1-m)=-COEFE2;
      else
         A(j,k)=COEFC2;
         A(j,k+1)=COEFB2;
         A(j,k+1-m)=-COEFE2;
      end
   end
   j=j+1;
   k=k+1;
end

%End point of PFR in liquid phase
A(2*m,2*m-1)=-1;
A(2*m,2*m)=1;

%Metrix A Of CSTR in Gas seperator
A(2*m+1,m)=-alpha2;
A(2*m+1,2*m+1)=1+beta2+gamma2+ceta2;
A(2*m+1,2*m+2)=-gamma2;
A(2*m+2,2*m)=-coef4;
A(2*m+2,2*m+1)=-coef6;
A(2*m+2,2*m+2)=1+coef5+coef6+coef_6;

%Metrix A Of PFR in Downcomer
%First point of PFR in gas phase
A(2*m+3,2*m+1)=-1;
A(2*m+3,2*m+3)=1;

j=2*m+4;
k=2*m+3;
while j<=2*m+n+1
   if k>=2*m+3&k<=2*m+n
      if alpha3~=0
         A(j,k)=-COEFA3;
         A(j,k+1)=COEFB3;
         A(j,k+2)=-COEFC3;
         A(j,k+1+n)=-COEFE3;
      else
         A(j,k)=COEFC3;
         A(j,k+1)=COEFB3;
         A(j,k+1+n)=-COEFE3;
      end
   end
   j=j+1;
   k=k+1;
end
%End point of PFR in gas phase
A(2*m+n+2,2*m+n+1)=-1;
A(2*m+n+2,2*m+n+2)=1;

%First point of PFR in liquid phase
A(2*m+n+3,2*m+2)=-1;
A(2*m+n+3,2*m+n+3)=1;

j=2*m+n+4;
k=2*m+n+3;
while j<=2*m+2*n+1
   if k>=2*m+n+3&k<=2*m+2*n
      if coef8~=0
         A(j,k)=-COEFA4;
         A(j,k+1)=COEFB4;
         A(j,k+2)=-COEFC4;
         A(j,k+1-n)=-COEFE4;
      else
         A(j,k)=COEFC4;
         A(j,k+1)=COEFB4;
         A(j,k+1-n)=-COEFE4;
      end
   end
   j=j+1;
   k=k+1;
end
```

สถาบันวิทยบริการ
จุฬาลงกรณ์มหาวิทยาลัย

```
%End point of PFR in liquid phase
A(2*m+2*n+2,2*m+2*n+1)=-1;
A(2*m+2*n+2,2*m+2*n+2)=1;

metrixA=[A(1:2*m+2*n+2,1:2*m+2*n+2)];

%SET UP METRIX B
%SET UP METRIX B IN THE PART OF GAS PHASE IN RISER

for i=1:length(t)-1;

   b(1,1)=(2*Qg_in)+(e3*A3*vg_downcomer*Og_downcomer
(i,n))-(e1*A1*vg_riser*Og_riser(i,1));

for j=2:1:m-1
   if alpha1~=0
      b(j,1)=(COEFC1*Og_riser(i,j+1))+(COEFD1*Og_riser
(i,j))+COEFA1*Og_riser(i,j-1)+(COEFE1*Ol_riser(i,j));
   else
      b(j,1)=(-COEFC1*Og_riser(i,j-1))+(COEFD1*Og_riser
(i,j))+(COEFE1*Ol_riser(i,j));
   end
end

b(m,1)=Og_riser(i,m-1)-Og_riser(i,m);

%SET UP METRIX B IN THE PART OF LIQUID PHASE IN RISER
b(m+1,1)=((1-e1)*A1*vl_riser*Ol_riser(i,1))-((1-
e3)*A3*vl_downcomer*Ol_downcomer(i,n));

for j=m+2:1:2*m-1
   if coef2~=0
      b(j,1)=(COEFC2*Ol_riser(i,j+1-m))+(COEFD2*Ol_riser
(i,j-m))+(COEFA2*Ol_riser(i,j-1-m))+(COEFE2*Og_riser
(i,j-m));
   else
      b(j,1)=(-COEFC2*Ol_riser(i,j-1-m))+
(COEFD2*Ol_riser(i,j-m))+(COEFE2*Og_riser(i,j-m));
   end
end

b(2*m,1)=Ol_riser(i,m-1)-Ol_riser(i,m);

%Gas phase in GAS SEPERATOR
b(2*m+1,1)=(1-beta2-gamma2-
ceta2)*Og_top(i,1)+alpha2*Og_riser(i,m)+gamma2*Ol_top
(i,1);
%LIQUID phase in GAS SEPERATOR
b(2*m+2,1)=(1-coef5-coef6-
coef_6)*Ol_top(i,1)+coef4*Ol_riser(i,m)+coef6*Og_top
(i,1);

%SET UP METRIX B IN THE PART OF GAS PHASE IN DOWNCOMER
b(2*m+3,1)=Og_top(i,1)-Og_downcomer(i,1);

for j=2*m+4:1:2*m+n+1
   if alpha3~=0
      b(j,1)=(COEFC3*Og_downcomer(i,j+1-(2*m+2)))+
(COEFD3*Og_downcomer(i,j-(2*m+2)))+(COEFA3*Og_downcomer
(i,j-1-(2*m+2)))+(COEFE3*Ol_downcomer(i,j-(2*m+2)));
   else
      b(j,1)=(-COEFC3*Og_downcomer(i,j-1-(2*m+2)))+
(COEFD3*Og_downcomer(i,j-(2*m+2)))+(COEFE3*Ol_downcomer
(i,j-(2*m+2)));
   end
end

b(2*m+n+2,1)=Og_downcomer(i,n-1)-Og_downcomer(i,n);

%SET UP METRIX B IN THE PART OF LIQUID PHASE IN
DOWNCOMER
b(2*m+n+3,1)=Ol_top(i,1)-Ol_downcomer(i,1);

for j=2*m+n+4:1:2*m+2*n+1
```

```
   if coef8~=0
      b(j,1)=(COEFC4*Ol_downcomer(i,j+1-(2*m+n+2)))+
(COEFD4*Ol_downcomer(i,j-
(2*m+n+2)))+(COEFA4*Ol_downcomer(i,j-1-(2*m+n+2)))+
(COEFE4*Og_downcomer(i,j-(2*m+n+2)));
   else
      b(j,1)=(-COEFC4*Ol_downcomer(i,j-1-(2*m+n+2)))+
(COEFD4*Ol_downcomer(i,j-
(2*m+n+2)))+(COEFE4*Og_downcomer(i,j-(2*m+n+2)));
   end
end

b(2*m+2*n+2,1)=Ol_downcomer(i,n-1)-Ol_downcomer(i,n);

B=[b(1:2*m+2*n+2,1)];

O(1:2*m+2*n+2,1)=inv(metrixA)*B;

for j=1:1:m
   Og_riser(i+1,j)=O(j,1);
end

for j=m+1:1:2*m
   Ol_riser(i+1,j-m)=O(j,1);
end

%Olr(i+1,1)=O(2*m,1);
Og_top(i+1,1)=O(2*m+1,1);
Ol_top(i+1,1)=O(2*m+2,1);

for j=2*m+3:1:2*m+n+2
   Og_downcomer(i+1,j-(2*m+2))=O(j,1);
end

for j=2*m+n+3:1:2*m+2*n+2
   Ol_downcomer(i+1,j-(2*m+n+2))=O(j,1);
end
```

```
if floor((i-1)/300)==ceil((i-1)/300)
   fprintf('i=%f \n',i);
end

end

   k=1;
   for i=1:length(t)-1
      if floor((i-1)/50)==ceil((i-1)/50)
         Olrm(k,1) = Ol_riser(i,m) ;
         Olt(k,1) = Ol_top(i,1) ;
         Oldn(k,1) = Ol_downcomer(i,n) ;
         k = k+1;
      end
   end

   k=1;
   for i=1:1:40
      if floor((i-1)/2)==ceil((i-1)/2)
         Ogr_1(k,1) = Og_riser(i,1) ;
         Ogr_5(k,1) = Og_riser(i,5) ;
         Ogr_15(k,1) = Og_riser(i,m) ;
         Ogt1(k,1) = Og_top(i,1) ;
         Ogd_1(k,1) = Og_downcomer(i,1) ;
         Ogd_5(k,1) = Og_downcomer(i,5) ;
         Ogd_15(k,1) = Og_downcomer(i,n);
         k = k+1;
      end
   end

   k=1;
   for i=41:length(t)-1
      if floor((i-1)/50)==ceil((i-1)/50)
         Ogr_11(k,1) = Og_riser(i,1) ;
         Ogr_55(k,1) = Og_riser(i,5) ;
         Ogr_m15(k,1) = Og_riser(i,m) ;
         Ogt2(k,1) = Og_top(i,1) ;
         Ogd_11(k,1) = Og_downcomer(i,1) ;
```

สถาบันวิทยบริการ
จุฬาลงกรณ์มหาวิทยาลัย

```
        Ogd_55(k,1) = Og_downcomer(i,5) ;
        Ogd_m15(k,1) = Og_downcomer(i,n);
        k = k+1;
      end
   end

save Ogr_1 Ogr_1 -ascii;
save Ogr_11 Ogr_11 -ascii;
save Ogr_5 Ogr_5 -ascii;
save Ogr_55 Ogr_55 -ascii;
save Ogr_15 Ogr_15 -ascii;
save Ogr_m15 Ogr_m15 -ascii;
save Ogt1 Ogt1 -ascii;
save Ogt2 Ogt2 -ascii;
save Ogd_1 Ogd_1 -ascii;
save Ogd_11 Ogd_11 -ascii;
save Ogd_5 Ogd_5 -ascii;
save Ogd_55 Ogd_55 -ascii;
save Ogd_15 Ogd_15 -ascii;
save Ogd_m15 Ogd_m15 -ascii;

figure(1)
plot(t,Ol_riser,'r');
title('Ol riser  ');
xlabel('time(-) ');
ylabel('concentration of Ol_r(-) ');
grid on

figure(2)
plot(t,Og_riser,'r');
title('Figure 4.3.3A  ');
xlabel('T [s] ');
ylabel('Dimensionless oxygen concentration ');
grid on

figure(3)
plot(t,Ol_top,'r');
ylabel('concentration of Ol_t ');
grid on

figure(4)
plot(t,Og_top,'b');
title('Figure 4.3.3B ');
xlabel('T [s] ');
ylabel('Dimensionless oxygen concentration ');
grid on

figure(5)
plot(t,Ol_downcomer,'r');
title('Ol downcomer');
xlabel('time ');
ylabel('concentration of Ol_d ');
grid on

figure(6)
plot(t,Og_downcomer,'r');
title('Figure 4.3.3C ');
xlabel('T [s] ');
ylabel('Dimensionless oxygen concentration ');
grid on

#---------------------END-----------------------
```

สถาบันวิทยบริการ
จุฬาลงกรณ์มหาวิทยาลัย

```
#-----------------------------------------------------

%File Name:DISPERSION MODEL 2
%Programe PFR with or without Dispersion term in RISER
and DOWNCOMER
%Discretisation by Implicit method

#-----------------------------------------------------

clear

H1=input('Unaereated Height in reactor (Riser and
Downcomer) = ');
Hd=input('Dispersion Height in reactor = ');
A1=input('Cross sectional Area in section of Riser = ');
A2=input('Cross sectional Area in section of gas
seperator = ');
ratio=input('Ad/Ar ratio = ');
A3=A1*ratio;

vl_downcomer=input('liquid velocity in downcomer =  ');
e1=input('gas hold up in riser = ');
e3=input('gas hold up in gas separator = ');
kla=input('kla of reactor = ');
e2=e1;
denst=input('density of liquid phase (1000 kg/m^3)');
d_bubble=input('diameter of bubble (0.005 m)');
s_tension=input('surface tension of liquid phase
(0.07275 kg/sec^2)');
Qg_in=input('inlet gas flowrate = ');
Ql_in=input('liquid feed flow rate = ');
m=input('enter number of interval(Dispersion model) in
riser m= ');
n=input('enter number of interval(Dispersion model) in
downcomer n= ');
disp1=input('gas phase dispersion coefficient in riser
of the contactor = ');
disp2=input('liquid phase dispersion coefficient in
riser of the contactor = ');
del_z1=1/m;
disp3=input('gas phase dispersion coefficient in
downcomer of the contactor = ');
disp4=input('liquid phase dispersion coefficient in
downcomer of the contactor = ');
del_z2=1/n;

tfinal=input('input final time =') ;
del_t=input('input step size of time = ');
tin=0;
t=tin:del_t:tfinal;

H2=Hd-H1;
V1=A1*H1;
V2=A2*H2;
V3=A3*H1;

vl_riser=((1-e3)*A3*vl_downcomer+Ql_in)/((1-e1)*A1);
vl_top=((1-e1)*vl_riser*A1-Ql_in)/((1-e2)*A3);
x=2.14*s_tension/(denst*d_bubble)+(0.505*10*d_bubble);
ub_terminal=sqrt(x);
v_slip=ub_terminal*(1-e1)^0.702;
vg_riser=vl_riser+v_slip;
vg_downcomer=(vg_riser*A1*e1-Qg_in)/(A3*e3);
vg_top=vg_downcomer*e3/e2;

Q=Qg_in/(A3*e3);
vg_r=(vg_riser*A1*e1)/(A3*e3);
V=V1+V2+V3;
time=V1/(A3*vl_downcomer);

t_factor=V1/(A3*vl_downcomer);
z_factor=1/H1;

%COEFICIENT OF RISER
%GAS PHASE COEFICIENT
```

```
beta1=-(vg_riser*z_factor*t_factor*del_t)/(2*del_z1);
alpha1=(disp1*(z_factor^2)*t_factor*del_t)/(del_z1^2);
gamma1=((1-e1)/e1)*kla*t_factor*del_t;
if alpha1~=0
   COEFA1=beta1-alpha1;
   COEFB1=1+(2*alpha1)+gamma1;
   COEFC1=alpha1+beta1;
   COEFD1=gamma1;
else
   COEFA1=beta1;
   COEFB1=1+gamma1;
   COEFC1=beta1;
   COEFD1=gamma1;
end

%LIQUID PHASE COEFICIENT
coef1=-(vl_riser*z_factor*t_factor*del_t)/(2*del_z1);
coef2=(disp2*(z_factor^2)*t_factor*del_t)/(del_z1^2);
coef3=kla*t_factor*del_t;
if coef2~=0
   COEFA2=coef3;
   COEFB2=coef1-coef2;
   COEFC2=1+(2*coef2)+coef3;
   COEFD2=coef1+coef2;
else
   COEFA2=coef3;
   COEFB2=coef1;
   COEFC2=1+coef3;
   COEFD2=coef1;
end

%COEFICIENT OF GAS SEPARATOR
alpha2=e1*A1*vg_riser*t_factor*del_t/(e2*V2);
beta2=A3*vg_top*t_factor*del_t/V2;
gamma2=(1-e2)*kla*t_factor*del_t/e2;
ceta2=Qg_in*t_factor*del_t/(e2*V2);

coef4=(1-e1)*vl_riser*A1*t_factor*del_t/((1-e2)*V2);
coef5=A3*vl_top*t_factor*del_t/V2;
coef6=kla*t_factor*del_t;
coef_6=Ql_in*t_factor*del_t/((1-e2)*V2);

%COEFICIENT OF DOWNCOMER
%GAS PHASE COEFICIENT
beta3=-(vg_downcomer*z_factor*t_factor*del_t)/
(2*del_z2);
alpha3=(disp3*(z_factor^2)*t_factor*del_t)/(del_z2^2);
gamma3=((1-e3)/e3)*kla*t_factor*del_t;
if alpha3~=0
   COEFA3=beta3-alpha3;
   COEFB3=1+2*alpha3+gamma3;
   COEFC3=alpha3+beta3;
   COEFD3=gamma3;
else
   COEFA3=beta3;
   COEFB3=1+gamma3;
   COEFC3=beta3;
   COEFD3=gamma3;
end

%LIQUID PHASE COEFICIENT
coef7=-(vl_downcomer*z_factor*t_factor*del_t)/
(2*del_z2);
coef8=(disp4*(z_factor^2)*t_factor*del_t)/(del_z2^2);
coef9=kla*t_factor*del_t;
if coef8~=0
   COEFA4=coef9;
   COEFB4=coef7-coef8;
   COEFC4=1+2*coef8+coef9;
   COEFD4=coef7+coef8;
else
   COEFA4=coef9;
   COEFB4=coef7;
   COEFC4=1+coef9;
   COEFD4=coef7;
end
```

```
%SET UP INITIAL AND BOUNDARY CONDITIONS
for j=1:1:m
   Og_riser(1,j)=0;
end

Og_top(1,1)=0;

for j=1:1:n
   Og_downcomer(1,j)=0;
end

for j=1:1:m
   Ol_riser(1,j)=0;
end

Ol_top(1,1)=0;

for j=1:1:n
   Ol_downcomer(1,j)=0;
end

%SOLVE FOR OXYGEN RESPONSE
%Programe Beginning
%SET UP INITIAL VALUE IN METRIX A
for i=1:1:2*n+2*m+2
   for j=1:1:2*n+2*m+2
      A(i,j)=0;
   end
end

%SET UP METRIX A IS (2m+2n+2)*(2m+2n+2)
%Metrix A OF Dispersion model

%Riser
%First point of Dispersion model in gas phase
A(1,1)=e1*A1*vg_riser;
A(1,2*m+n+2)=-e3*A3*vg_downcomer;

j=2;
k=1;
while j<=m-1
   if k>=1&k<=m-2
         A(j,k)=COEFA1;
         A(j,k+1)=COEFB1;
         A(j,k+2)=-COEFC1;
         A(j,k+1+m)=-COEFD1;
   end
   j=j+1;
   k=k+1;
end

%End point of Dispersion model in gas phase
A(m,m-1)=-1;
A(m,m)=1;

%First point of Dispersion model in liquid phase
A(m+1,m+1)=-(1-e1)*A1*vl_riser;
A(m+1,2*m+2*n+2)=(1-e3)*A3*vl_downcomer;

j=m+2;
k=m+1;
while j<=2*m-1
   if k>=m+1&k<=2*m-2
         A(j,k)=COEFB2;
         A(j,k+1)=COEFC2;
         A(j,k+2)=-COEFD2;
         A(j,k+1-m)=-COEFA2;
   end
   j=j+1;
   k=k+1;
end

%End point of Dispersion model in liquid phase
A(2*m,2*m-1)=-1;
A(2*m,2*m)=1;
```

สถาบันวิทยบริการ
จุฬาลงกรณ์มหาวิทยาลัย

```
%Metrix A Of Dispersion model in Gas seperator
A(2*m+1,m)=-alpha2;
A(2*m+1,2*m+1)=1+beta2+gamma2+ceta2;
A(2*m+1,2*m+2)=-gamma2;
A(2*m+2,2*m)=-coef4;
A(2*m+2,2*m+1)=-coef6;
A(2*m+2,2*m+2)=1+coef5+coef6+coef_6;

%Metrix A Of Dispersion model in Downcomer
%First point of Dispersion model in gas phase
A(2*m+3,2*m+1)=-1;
A(2*m+3,2*m+3)=1;

j=2*m+4;
k=2*m+3;
while j<=2*m+n+1
   if k>=2*m+3&k<=2*m+n
         A(j,k)=COEFA3;
         A(j,k+1)=COEFB3;
         A(j,k+2)=-COEFC3;
         A(j,k+1+n)=-COEFD3;
   end
   j=j+1;
   k=k+1;
end
%End point of Dispersion model in gas phase
A(2*m+n+2,2*m+n+1)=-1;
A(2*m+n+2,2*m+n+2)=1;

%First point of Dispersion model in liquid phase
A(2*m+n+3,2*m+2)=-1;
A(2*m+n+3,2*m+n+3)=1;

j=2*m+n+4;
k=2*m+n+3;
while j<=2*m+2*n+1
   if k>=2*m+n+3&k<=2*m+2*n
         A(j,k)=COEFB4;
         A(j,k+1)=COEFC4;
         A(j,k+2)=-COEFD4;
         A(j,k+1-n)=-COEFA4;
   end
   j=j+1;
   k=k+1;
end

%End point of PFR in liquid phase
A(2*m+2*n+2,2*m+2*n+1)=-1;
A(2*m+2*n+2,2*m+2*n+2)=1;

metrixA=[A(1:2*m+2*n+2,1:2*m+2*n+2)];

%SET UP METRIX B
%SET UP METRIX B IN THE PART OF GAS PHASE IN RISER
% i=time, j=position

for i=1:length(t)-1;

   b(1,1)=Qg_in;

for j=2:1:m-1
      b(j,1)=Qg_riser(i,j);
end

b(m,1)=0;

%SET UP METRIX B IN THE PART OF LIQUID PHASE IN RISER
b(m+1,1)=0;

for j=m+2:1:2*m-1
      b(j,1)=Ol_riser(i,j-m);
end

b(2*m,1)=0;
```

```
%Gas phase in GAS SEPERATOR
b(2*m+1,1)=Og_top(i,1);
%LIQUID phase in GAS SEPERATOR
b(2*m+2,1)=Ol_top(i,1);

%SET UP METRIX B IN THE PART OF GAS PHASE IN DOWNCOMER
b(2*m+3,1)=0;

for j=2*m+4:1:2*m+n+1
      b(j,1)=Og_downcomer(i,j-(2*m+2));
end

b(2*m+n+2,1)=0;

%SET UP METRIX B IN THE PART OF LIQUID PHASE IN
DOWNCOMER
b(2*m+n+3,1)=0;

for j=2*m+n+4:1:2*m+2*n+1
      b(j,1)=Ol_downcomer(i,j-(2*m+n+2));
end

b(2*m+2*n+2,1)=0;

B=[b(1:2*m+2*n+2,1)];

O(1:2*m+2*n+2,1)=inv(metrixA)*B;

for j=1:1:m
   Og_riser(i+1,j)=O(j,1);
end

for j=m+1:1:2*m
   Ol_riser(i+1,j-m)=O(j,1);
end

%Olr(i+1,1)=O(2*m,1);
Og_top(i+1,1)=O(2*m+1,1);
Ol_top(i+1,1)=O(2*m+2,1);

for j=2*m+3:1:2*m+n+2
   Og_downcomer(i+1,j-(2*m+2))=O(j,1);
end

for j=2*m+n+3:1:2*m+2*n+2
   Ol_downcomer(i+1,j-(2*m+n+2))=O(j,1);
end

if floor((i)/300)==ceil((i)/300)
   fprintf('i=%f \n',i);
end

end

   k=1;
   for i=1:length(t)-1
      if floor((i)/50)==ceil((i)/50)
         Olrm(k,1) = Ol_riser(i,m) ;
         Olt(k,1) = Ol_top(i,1) ;
         Oldn(k,1) = Ol_downcomer(i,n) ;
         k = k+1;
      end
   end

   k=1;
   for i=1:1:40
      if floor((i))==ceil((i))
         Ogr_1(k,1) = Og_riser(i,1) ;
         Ogr_5(k,1) = Og_riser(i,5) ;
         Ogr_15(k,1) = Og_riser(i,m) ;
         Ogt1(k,1) = Og_top(i,1) ;
         Ogd_1(k,1) = Og_downcomer(i,1) ;
         Ogd_5(k,1) = Og_downcomer(i,5) ;
         Ogd_15(k,1) = Og_downcomer(i,n);
         k = k+1;
      end
```

สถาบันวิทยบริการ
จุฬาลงกรณ์มหาวิทยาลัย

```
   end


   k=1;
   for i=41:length(t)-1
      if floor((i)/50)==ceil((i)/50)
         Ogr_11(k,1) = Og_riser(i,1) ;
         Ogr_55(k,1) = Og_riser(i,5) ;
         Ogr_m15(k,1) = Og_riser(i,m) ;
         Ogt2(k,1) = Og_top(i,1) ;
         Ogd_11(k,1) = Og_downcomer(i,1) ;
         Ogd_55(k,1) = Og_downcomer(i,5) ;
         Ogd_m15(k,1) = Og_downcomer(i,n);
         k = k+1;
      end
   end

save Ogr_1 Ogr_1 -ascii;
save Ogr_11 Ogr_11 -ascii;
save Ogr_5 Ogr_5 -ascii;
save Ogr_55 Ogr_55 -ascii;
save Ogr_15 Ogr_15 -ascii;
save Ogr_m15 Ogr_m15 -ascii;

save Ogt1 Ogt1 -ascii;
save Ogt2 Ogt2 -ascii;


save Ogd_1 Ogd_1 -ascii;
save Ogd_11 Ogd_11 -ascii;
save Ogd_5 Ogd_5 -ascii;
save Ogd_55 Ogd_55 -ascii;
save Ogd_15 Ogd_15 -ascii;
save Ogd_m15 Ogd_m15 -ascii;

ratio=A3/A1;
fprintf('Value of t = %0.4f\n',time);
fprintf('Value of Ad/Ar = %0.3f\n',ratio);
fprintf('Value of Ad = %0.5f\n',A3);
fprintf('Value of Ar = %0.5f\n',A1);
fprintf('Value of V1 = %0.5f\n',V1);
fprintf('Value of V2 = %0.5f\n',V2);
fprintf('Value of V3 = %0.5f\n',V3);
fprintf('Value of V = %0.5f\n',V);
fprintf('Value of vg_r = %0.3f\n',vg_r);
fprintf('Value of Q = %0.4f\n',Q);
fprintf('Value of v_slip = %0.3f\n',v_slip);
fprintf('Value of vg_riser = %0.3f\n',vg_riser);
fprintf('Value of vg_top = %0.3f\n',vg_top);
fprintf('Value of vg_downcomer = %0.3f\n',vg_downcomer);
fprintf('Value of vl_riser = %0.3f\n',vl_riser);
fprintf('Value of vl_top = %0.3f\n',vl_top);
fprintf('Value of vl_downcomer = %0.3f\n',vl_downcomer);

figure(1)
plot(t,Ol_riser,'r');
title('Ol riser  ');
xlabel('T [-] ');
ylabel('Dimensionless oxygen concentration ');
grid on

figure(2)
plot(t,Og_riser,'r');
title('Figure 4.3.3A  ');
xlabel('T [-] ');
ylabel('Dimensionless oxygen concentration ');
grid on

figure(3)
plot(t,Ol_top,'r');
xlabel('T [-] ');
ylabel('Dimensionless oxygen concentration ');
grid on

figure(4)
plot(t,Og_top,'b');
```

```
title('Figure 4.3.3B ');
xlabel('T [-] ');
ylabel('Dimensionless oxygen concentration ');
grid on

figure(5)
plot(t,Ol_downcomer,'r');
title('Ol downcomer');
xlabel('T [-] ');
ylabel('Dimensionless oxygen concentration ');
grid on

figure(6)
plot(t,Og_downcomer,'r');
title('Figure 4.3.3C ');
xlabel('T [-] ');
ylabel('Dimensionless oxygen concentration ');
grid on


#---------------------END------------------------
```

สถาบันวิทยบริการ
จุฬาลงกรณ์มหาวิทยาลัย

Appendix B

Residence time distributions in gas-liquid contactors

Sontaya Krichnavaruk, Sarit Chotchakornpant, Vichian Suksoir, and Prasert Pavasant

Department of Chemical Engineering, Faculty of Engineering, Chulalongkorn University. Thailand

Abstract

Residence time distributions in various types of gas-liquid contactors, i.e. bubble column, airlift contactors were investigated. Results clearly illustrated that, within the chosen operating conditions, the bubble column comprised two regions: the first one could be described as a perfectly mixed compartment and the other as a dead zone. By injecting tracer at different column heights, the locations of dead zone were estimated to be at the bottom part of the bubble column. In other cases, the RTD explicitly demonstrated that, with the two types of ALCs used in this work, all sections of the ALCs including riser, downcomer, and gas separator behaved closer to a completely mixed zone than plug flow. Dead zones were also found to exist in the column. However, unlike the case of bubble columns, this zone was not only at the bottom part, but was expected to be at various points in the column.

Key words: residence time distribution, airlift contactor, split airlift contactor, gas-liquid contactor

สถาบันวิทยบริการ
จุฬาลงกรณ์มหาวิทยาลัย

Introduction

One of the parameters commonly used to evaluate the flow behavior of the fluid contacting vessels, e.g. stirred tanks, bubble columns, is the residence times of fluid particles in that particular system. The knowledge of residence time distribution (RTD) has been well established and this has been conducted in many types of chemical contactors/reactors (Nauman, 1969; Fan et. al., 1979; Schwartz, 1979; Dickens et. al., 1989; Fernandez-Sempere et. al., 1995). RTD is also useful for the development of reliable mathematical models because it provides information about the characteristics of mixing pattern inside the system, e.g. channeling or by-passing, and dead zones. However, the information about RTD in gas-liquid contactors are rare and most of the mathematical models developed for these systems were always based on simple assumptions such as plug flow or completely mixed flow regimes (Merchuk and Stein, 1980; Ruffer et. al., 1994; Gavrilescu and Tudose, 1996). Few reports have shown the investigation of RTD in internal-loop airlift contactors such as the work by Gavrilescu (1999) who studied the RTD of liquid phase in a concentric tube airlift reactor and concluded that the flow in the airlift reactor was more uniform than obtained from the bubble column reactors.

In lights of a complete mathematical development for such gas-liquid contacting systems, there is a clear need for the investigation of residence time distribution in such systems. This work, hence, aimed to fulfill this need and was set out to evaluating the mixing performance of various gas-liquid contactors. An pulse injection technique as explained in Levenspiel (1999) was employed to examine the residence time distribution of the contactor systems.

Experimental procedure

A. Experimental setup

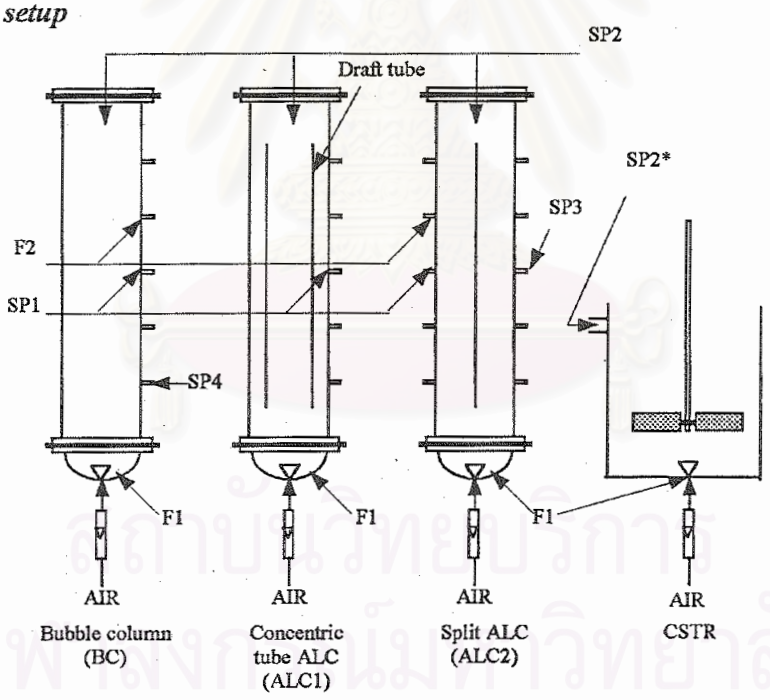

Figure 1. Experimental apparatus (SP = sampling point, F = feed location)

Experiments were carried out in various types of gas-liquid columns including a 15 L bubble column, a 15 L concentric tube internal loop airlift contactor (ALC), and a 15 L split ALC. A schematic diagram of each of the contactors is shown in Figure 1 and their corresponding dimensions are given in Table 1. During the experiment, air at a volumetric flow rate of 2.5 L/s was sparged centrally at the base of each column. Water was fed at 0.02 L/s in a vicinity of the air sparger at the bottom of the contactors. At time zero, 10 mL of an acid tracer (2.0 N hydrochloric acid) was rapidly injected at the sampling ports and samples were taken from the contactors at every ten second interval until no further change in pH was observed (pH was measured using a pH meter from METTLER TOLEDO Model MP220/225). Figure 1 illustrates the injection and sampling points for each

contactor. The residence time distribution function (E) was calculated from the measured hydrogen ion concentration as described in Levenspiel (1999).

Table 1 Dimension of contactors used in this work.

Contactor type[1]	Height[2] (cm)	Diameter (cm)
BC	100	14
ALC1 (column)	120	14
(draft tube)	100	9.3
ALC2	120	14

[1]BC = Bubble column.
ALC1 = Concentric tube ALC
ALC2 = Split ALC
[2]Unaerated liquid height.

B. Experimental verification

To verify the method of residence time distribution (RTD) measurement, a verifying test was carried out in an 11 L laboratory scale aerated stirred tank where air and water (at the above mentioned volumetric flow rates) were supplied at the base of the tank. The resulting E curve obtained from this verifying experiment is shown in Figure 2 together with a theoretical E curve for a completely mixed stirred tank. It can be seen that this pulse tracer injection technique gave a rather good fit for the E curve with theory. The early deviation is thought to occur due to the existence of non-ideal conditions in the tank.

However, the calculated ratio between dispersion and convection (D/uL) is greater than 0.01 which indicates that a perfectly mixed condition can still be assumed for this tank(Levenspiel, 1999). It is worth noting that dead zones were expected to exist as the area of the E curve from this experiment was slightly less than unity. The locations of these dead zones were anticipated to be at the bottom of the tank as shown in Figure 6a.

Results and discussion

A. RTD for Bubble column

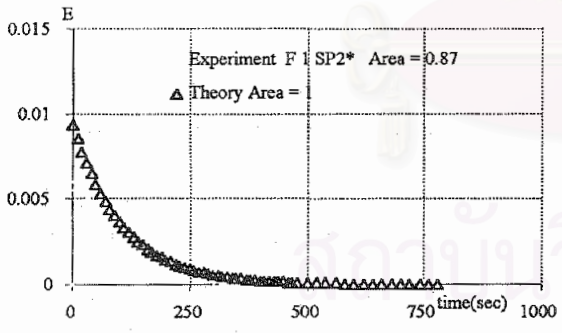

Figure 2. E curve of CSTR

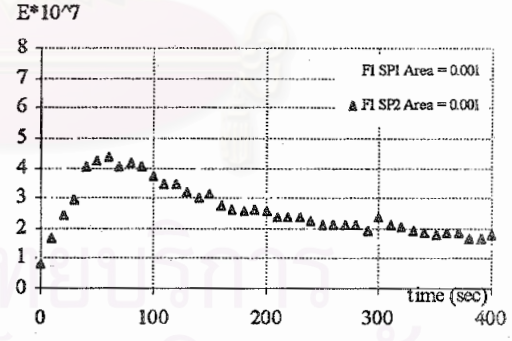

Figure 3a. E curve of bubble column when tracer was injected at F1 and samples were collected at SP1 and SP2

In this experiment, the tracer was injected both at points F1 and F2 (see Figure 1). Results from Figure 3a show that if the tracer was fed at the bottom part of the column (F1), a significantly small quantity of tracer (less than 1%) could be detected at sampling points SP1 and SP2. This is because most of the tracer was trapped at the feed location, and if the sampling was taken at the bottom of the column (SP4), a much higher quantity of tracer could be found (area = 41% in Figure 3b). This implies that there existed dead zones at this feed location (Figure 6b). This conclusion was emphasised by injecting the tracer at F2 (at the middle part of the column). In this case, the corresponding area underneath the E curve (around = 0.2) indicates a much higher quantity of tracer leaving the contactor at both sampling points (SP1 and SP2). Apart from the dead zone region, the

remaining part of the BC was found to behave like a completely mixed tank where D/uL is calculated to be approximately 0.2.

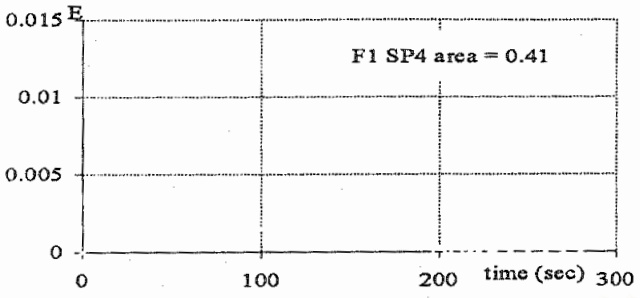

Figure 3b. E curve of bubble column when tracer was injected at F1 and samples were collected at SP4.

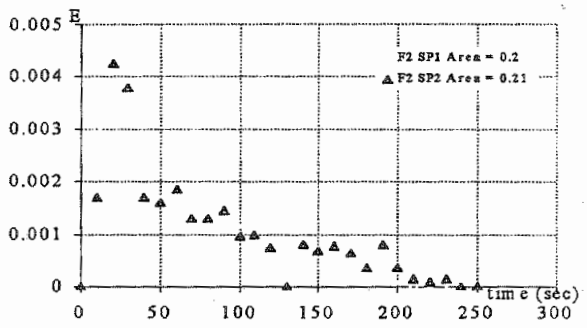

Figure 3c. E curve of bubble column when tracer was injected at F2 and samples were collected at SP1 and SP2.

B. RTD for Concentric tube ALC

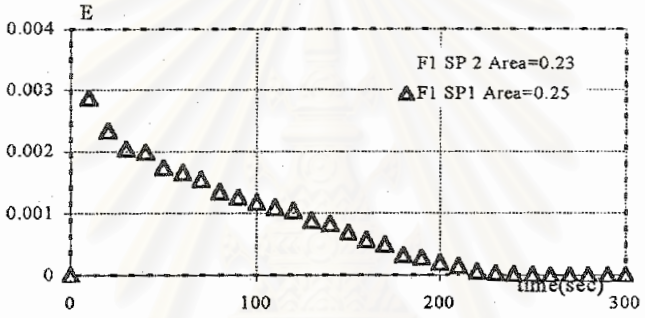

Figure 4. E curve of concentric tube ALC when tracer was injected at F1 and samples were collected at SP1 and SP2.

Figure 4 shows that E curves at different parts of the concentric tube airlift contactor (ALC) behaved in the same manner as that of stirred tank. The calculation of D/uL at each location was found to be in the range of 0.15-0.16 which indicates that the flow patterns in this ALC were perfectly mixed. This finding is in contrast with the literature where riser and downcomer were usually represented by a plug flow region. (Merchuk and Stein, 1980) The reason for this is still unknown but is thought to be due to the scale of the contactor which was rather small in this work. As the contactor becomes larger (or taller), it might have a plug flow characteristic as found by Gavrilescu and Tudose (1996). Area under E curve in Figure 4 was around 0.2 implying that there were also dead zones in this contactor. The location for the dead zone in this contactor is still opened as an area for further investigation, and it is expected to take place at several points as illustrated in shaded areas in Figure 6c.

C. RTD for Split ALC

E curves for this type of ALC (Figures 5a. and 5b.) were found to be approximately the same as those for the concentric tube ALC type (Figure 4) which means that the flow patterns in each part of the ALC were perfectly mixed (D/uL was around 0.12-0.18), and there existed some dead zones in the column. In this experiment, the tracer was not only injected at the base, but it was also given at the middle part of the column. This was to examine whether the dead zone was located at the bottom of the contactor. However, the results did not draw such conclusion as the area under E curve were almost the same for both cases. Further investigation for the exact location of dead zones in this contactor is still needed. For this work, the anticipated locations of dead zones in this contactor are shown in Figure 6d.

Table 2. D/uL obtained from various types of gas-liquid contactors

Contactor Type	Sampling Location	Feed Location	D/uL
CSTR	SP 2*	F 1	0.16
BC	SP 4	F 1	0.25
	SP 2	F 1	0.21
	SP 1	F 1	0.24
	SP 2	F 2	0.09
ALC 1	SP 1	F 2	0.18
	SP 2	F 1	0.15
ALC 2	SP 1	F 1	0.16
	SP 2	F 1	0.18
	SP 1	F 1	0.16
	SP 3	F 2	0.12
	SP 1	F 2	0.15

Point SP 1 = 60 cm from bottom
Point SP 2 = 110 cm from bottom (top location of BC and ALCs)
Point SP 2* = over flow stream of CSTR
Point SP 3 = 60 cm from bottom (riser)
Point SP 4 = 5 cm from bottom
Point F 1 = Feed location at bottom
Point F 2 = Feed location at 60 cm from bottom

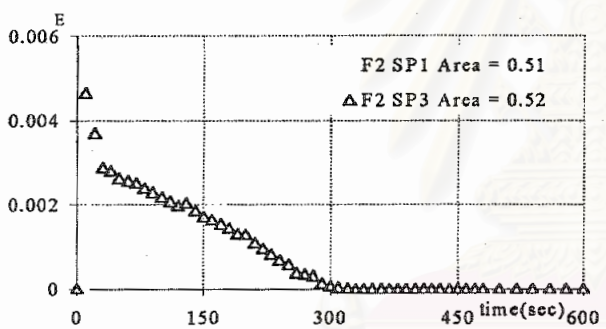

Figure 5a. E curve of Split ALC when tracer was injected at F2 and samples were collected at SP1 and SP3.

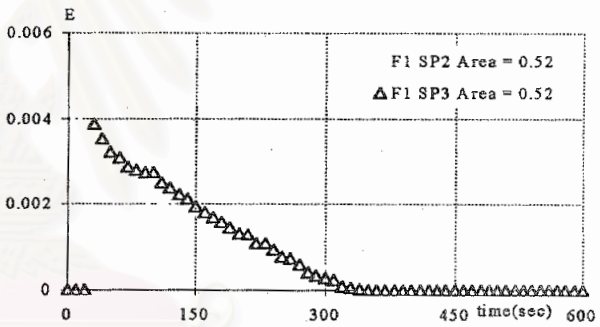

Figure 5b. E curve of Split ALC when tracer was injected at F1 and samples were collected at SP2 and SP3.

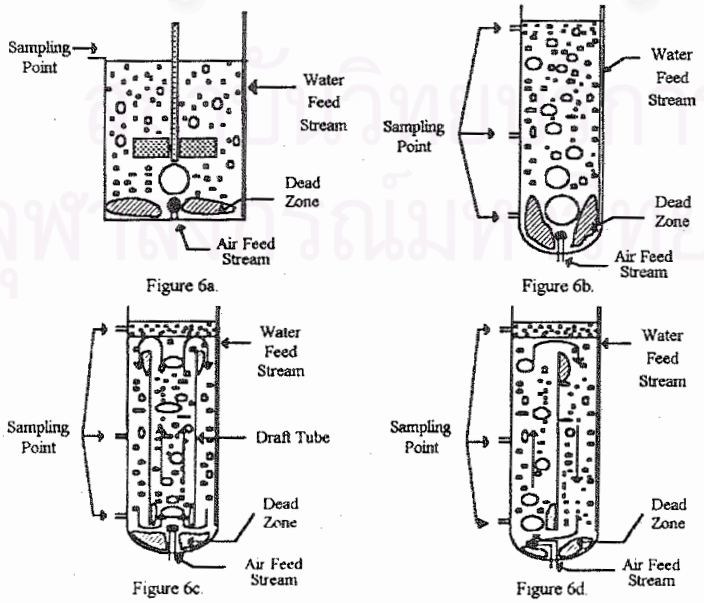

Figure 6. Expected locations of dead zones in gas-liquid contactors employed in this work.

Conclusion

All of the contactors used in this work can be represented by a combination of completely mixed and dead zone regions. However, the exact locations for dead zones in the ALCs are still to be investigated. The knowledge of dead zone plays a significant role in the design of gas-liquid contactors as serious mixing problems can occur particularly if feed is unintentionally supplied into this stagnant region. This work contributes significantly to the future development of a mathematical model for ALCs as it reveals that, with a small scale contactor, a completely mixed model might correctly predict the behavior of the system.

References

Dickens, A. W., Mackley, M. R. and Williams, H. R. 1989. Experimental residence time distribution measurements for unsteady flow in baffled tubes, Chemical Engineering Science, 44: 1471-1479.

Fan, L. T., Fan, L. S. and Nassar, R. F. 1979. A stochastic model of the unsteady state age distribution in a flow system, Chemical Engineering Science, 34: 1172-1174.

Fernandez, S. R. Font-Montesinos and Espejo-Alcaraz. 1995. Residence time distribution for unsteady-state systems, Chemical Engineering Science, 50: 223-230.

Gavrilescu, M. and Tudose, R.Z. 1996. Residence time distribution in external-loop airlift bioreactor, Bioprocess Engineering, 14: 183-193.

Gavrilescu, M. and Tudose, R.Z. 1999. Residence time distribution of the liquid in a concentric-tube airlift reactor, Chemical Engineering and Processing, 38: 225-228.

Levenspiel, O. 1999. Chemical Reaction Engineering, John Wiley & Sons.

Merchuk, J.C. and Stein, Y. 1980. Distribution parameter model of an airlift fermentor, Biotechnology and Bioengineering, 22: 1189-1211.

Nauman, E. B. 1969. Residence time distribution theory for unsteady stirred tank reactors, Chemical Engineering Science, 24: 1461-1470.

Ronald, W. M., Charles, A. M. and Bradley, A. S. 1999. Introduction to Chemical Reaction Engineering and Kinetics, John Willey & Sons.

Ruffer, H.M., Liwei W., Lubbet, A. and Schugerl, K. 1994. Interpretation of gas residence time distributions in large airlift tower loop reactors, Bioprocess Engineering, 11: 153-159.

Schwartz, S. E. 1979. Residence time in reservoirs under non-steady-state condition: application to atmospheric SO_2 and aerosol sulfate, Tellus, 31: 530-547.

สถาบันวิทยบริการ
จุฬาลงกรณ์มหาวิทยาลัย

BIOGRAPHY

Mr. Vichian Suksoir was born on 8th January, 1976 in Udonthanee. He finished his higher secondary course from Taweetapisek School in March, 1995. After that, he studied in the major of Chemical Engineering in Faculty of Engineering at Chulalongkorn University. He continued his further study for Master's degree in Chemical Engineering at Chulalongkorn University. He participated in the Biochemical Engineering research group and achieved his Master's degree in April, 2000.

สถาบันวิทยบริการ
จุฬาลงกรณ์มหาวิทยาลัย